République Algérienne Démocratique et Populaire
Ministère de l'Enseignement Supérieur et de la Recherche Scientifique

Université A. MIRA - Bejaïa

Faculté des Sciences Exactes

Département de Chimie

جامعة بجاية
Tasdawit n Bgayet
Université de Béjaïa

Mémoire de Master

Présenté par :

- BIRUNGI JohnBaptist

En vue de l'obtention du diplôme de Master en Chimie

Spécialité : Chimie analytique

Thème :

Elaboration and characterization of rare earth coordination polymers.

Soutenu le : 29 / 06 / 2025

Devant le jury composé de :

Nom & Prénom	Département d'affiliation	Qualité
ZIDANE Youcef	Chimie	Président
TOUATI Djahida	Chimie	Examinateur
BENMERAD Belkacem	Chimie	Encadrant

2024-2025

Acknowledgment

First and foremost, I thank the Almighty God for the gift of life, health, and wisdom throughout this academic journey. Without His grace, none of this would have been possible.

I extend my deepest gratitude to my supervisor, Pr. B. BENMERAD and Dr. Y. CHEDDANI (assistant supervisor), for their exceptional guidance, encouragement, and unwavering support during the entire course of this research. Your patience and insightful feedback greatly shaped the quality of this work.

I would also like to express my sincere appreciation to all the professors and lecturers of the Department of Chemistry at the University A. MIRA – Béjaïa. Your dedication and commitment to teaching laid the strong academic foundation upon which this work is built. I am equally thankful to the laboratory staff for providing the necessary materials and a conducive environment for experimentation.

To the members of the jury Dr. Y. ZIDANE and Pr. D. TOUATI. I am honored by your willingness to evaluate my work and offer your valuable insights. Your time, effort, and constructive comments are genuinely appreciated.

Lastly, I am grateful to my fellow students and colleagues who shared their knowledge, ideas, and encouragement along the way. You made this journey enriching and memorable.

Dedication

This work is wholeheartedly dedicated to:

My beloved parents, whose love, prayers, sacrifices, and unwavering belief in my potential have been the foundation of all my achievements. Your endless support and encouragement have sustained me through the most challenging times.

My brothers and sisters, thank you for your companionship, motivation, and moral support. Your presence in my life continues to inspire me to strive for excellence.

My close friends, who stood by me with encouragement, advice, and laughter during moments of doubt and fatigue, you made the journey lighter and more enjoyable.

To all who have supported my academic journey, directly or indirectly, your kindness, patience, and belief in me are deeply appreciated. This accomplishment is as much yours as it is mine.

Table of content

List of abbreviations and symbols.

CPs	Coordination Polymers
Ln	Lanthanoid
REEs	Rare Earth Elements
1D	One Dimension
IR	Infrared
PXRD	Powder X-ray Diffraction
MOFs	Metal Organic Frameworks
OLEDs	Organic Light Emitting Diodes
TGA	Thermogravimetric Analysis
FT-IR	Fourier-Transform Infrared Spectroscopy
LPCMC	Laboratoire de Physico-Chimie des Matériaux et Catalyse
MeOH	Methanol
EtOH	Ethanol

List of tables.

List of figures.

General introduction.

In recent decades, coordination chemistry has emerged as a central field in modern chemical science, bridging inorganic, organic, and materials chemistry. Of particular interest are coordination polymers (CPs)-infinite network structures formed by the self-assembly of metal ions and multidentate organic ligands. Among these, rare earth-based coordination polymers are gaining increasing attention due to their unique structural diversity and promising applications in fields such as luminescence, magnetism, catalysis, gas storage, and sensing. The rare earth elements (REEs), comprising the lanthanoids along with scandium and yttrium, possess distinct electronic configurations specifically, partially filled 4f orbitals that confer exceptional optical and magnetic properties to their complexes [1].

Carboxylic acids, particularly those containing multiple carboxylate groups, serve as excellent ligands for constructing coordination polymers due to their ability to adopt various coordination modes monodentate, bidentate (chelating or bridging), and polydentate. These ligands not only fulfill the coordination needs of rare earth ions but also contribute to the rigidity, porosity, and overall topology of the resulting CPs. Moreover, by tuning the ligand design using rigid aromatic versus flexible aliphatic backbones, it is possible to influence the dimensionality (1D, 2D, or 3D) and functionality of the final polymer [2].

This research project focuses on the synthesis and characterization of coordination polymers based on rare earth elements, with a particular emphasis on lanthanum (III) complexes. The work is structured in two major parts: a bibliographic study and an experimental investigation. The bibliographic section outlines the fundamental chemistry of rare earth elements, their coordination behavior, and the principles governing the design and formation of CPs. It also reviews the relevant synthetic methodologies and techniques used for structural and physicochemical characterization.

The experimental section involves the actual elaboration of coordination polymers through hydrothermal and reflux synthesis using various lanthanum precursors and dicarboxylic acid ligands. Both rigid ligands (terephthalic, isophthalic, and phthalic acids) and flexible ligands (malonic, fumaric, succinic, glutaric, and adipic acids) were used in single and mixed-ligand systems. The synthesized compounds were subjected to Infrared spectroscopy (IR) and Powder X-ray diffraction (PXRD) to confirm coordination, determine structural features, and assess purity and crystallinity.

The ultimate goal of this research is to contribute to the understanding of structure–property relationships in rare earth coordination polymers and to identify synthetic parameters that govern their formation, stability, and potential applicability in material science.

PART I: BIBLIOGRAPHIC RESEARCH.

I.1 The rare earth elements.

I.1.1 History and definition.

The category of rare earth elements (REE) consists of the lanthanoids (lanthanides) along with Scandium and Yttrium, making a total of 17 elements **Table I. *1***. These elements possess distinctive characteristics that distinguish them from transition elements[3].

The discovery of the lanthanoids dates back to 1787 in Ytterby, Sweden, where an unusual black mineral called Gadolinite was found. Researchers later managed to extract various lanthanoid elements from this mineral. In 1794, Professor Gadolin successfully obtained yttria, an impure variant of yttrium oxide, from the mineral. Subsequently, Moseley employed X-ray spectroscopy to validate the presence of 14 elements between Lanthanum and Hafnium. Initially labeled as 'rare earth' due to their extraction from a rare mineral, the name Lanthanoids was later adopted, reflecting the first element in the series, Lanthanum, as their abundance became recognised[4].

The lanthanoids are a series of elements located in the f-block of the sixth period of the periodic table **Figure I. *1***. This group includes elements with atomic numbers ranging from 57 to 71. Although lanthanum is categorized as a group 3 metal, its chemical properties closely resemble those of the other lanthanoids, leading to its common classification within this group[5].

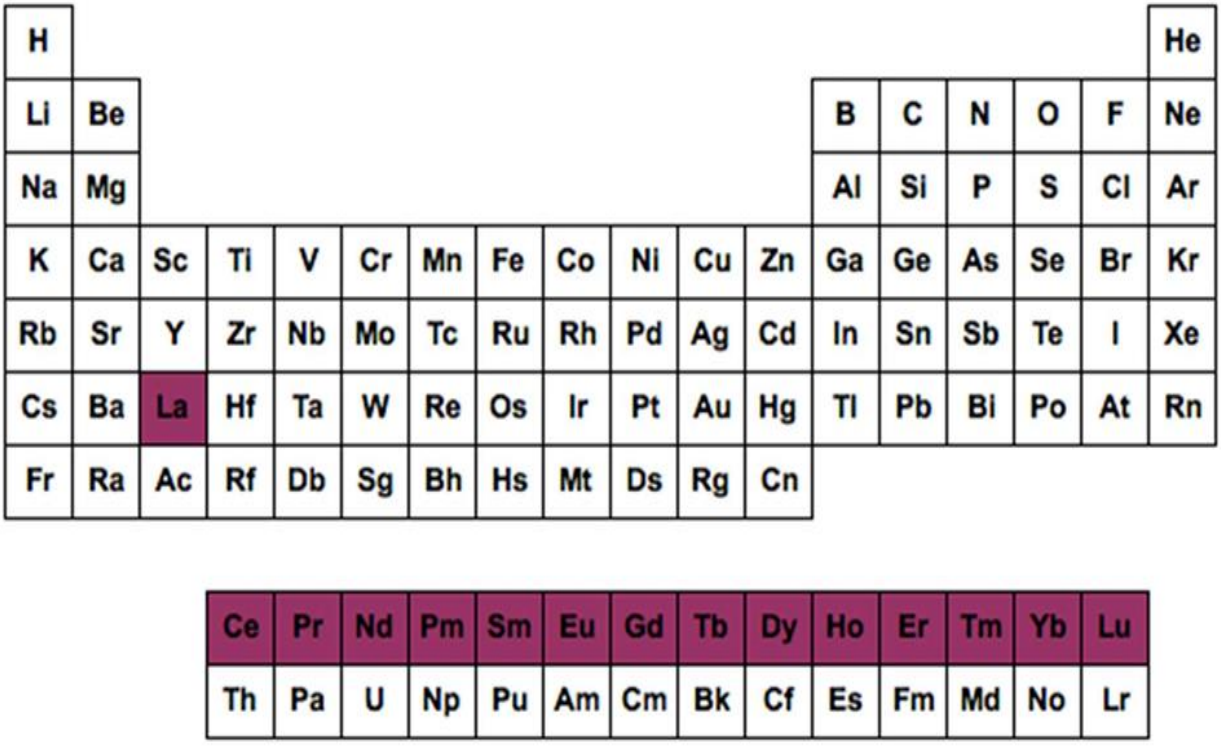

Figure I. 1: Position of lanthanides on the periodic table

Table I. 1 Name, atomic number and symbol of rare earth elements.

Name	Atomic number	Symbol	Name	Atomic number	Symbol
Scandium	21	Sc	Gadolinium	64	Gd
Yttrium	39	Y	Terbium	65	Tb
Lanthanum	57	La	Dysprosium	66	Dy
Cerium	58	Ce	Holmium	67	Ho
Praseodymium	59	Pr	Erbium	68	Er
Neodymium	60	Nd	Thulium	69	Tm
Promethium	61	Pm	Ytterbium	70	Yb
Samarium	62	Sm	Lutetium	71	Lu
Europium	63	Eu			

I.1.2 Sources and abundance of lanthanoids.

With the exception of promethium (Pm), which is radioactive, the remaining lanthanoids are relatively abundant in the Earth's crust **Table I. *2***. The primary sources of these elements are phosphate minerals, including bastnaesite ($LnFCO_3$), monazite ($(Ln, Th)PO_4$), which is richer in the earlier lanthanoids, and xenotime ($(Y, Ln)PO_4$), which tends to be richer in the later lanthanoids[4].

Table I. 2 Abundance of the lanthanoids [5]

	La	Ce	Pr	Nd	Pm	Sm	Eu	Gd	Tb	Dy	Ho	Er	Tm	Yb	Lu	Y
Crust (ppm)	35	66	9.1	40	0.0	7	2.1	6.1	1.2	4.5	1.3	3.5	0.5	3.1	0.8	31
Solar System (with respect to 10^7 atoms Si)	4.5	1.2	1.7	8.5	0.0	2.5	1.0	3.3	0.6	3.9	0.9	2.5	0.4	2.4	0.4	40.0

I.1.3 Oxidation states.

Lanthanoids have a common oxidation state of Ln (III) resulting from the loss of 6s and 5d electrons, some do show a significant chemistry in +II and +IV oxidation states **Table I. *3***. For example, cerium which can be oxidized to Ce (IV) and europium, which can be reduced to Eu(II)[6].

Table I. 3 The distribution of oxidation states of lanthanoids.

Oxidation state	Element														
	La	Ce	Pr	Nd	Pm	Sm	Eu	Gd	Tb	Dy	Ho	Er	Tm	Yb	Lu
+2				+II		+II	+II				+II		+II	+II	
+3	+III	+III	+III	+III	+III	+III	+III	+III	+III	+III	+III	+III	+III	+III	+III
+4		+IV	+IV						+IV	+IV					

I.1.4 Electronic configuration of the lanthanoids.

Lanthanoids exhibit two types of electronic configurations according to the principle of lowest energy; $[Xe]4f^n\ 6s^2$ and $[Xe]4f^{n-1}\ 5d^16s^2$ with [Xe] representing the electronic configuration of Xenon and n= [1, 2, 3, …..., 14]. Lanthanum, cerium, gadolinium, and Lutetium belong to the $[Xe]4f^{n-1}\ 5d^16s^2$ type while the rest of the series elements belong to the $[Xe]4f^n\ 6s^2$ **Table I.** ***4*** Scandium and yttrium lack 4f electrons, but because of their outermost electronic configuration $(n-1)d^1ns^2$, they have similar chemical properties to lanthanoids [7].

Table I. 4 Electronic configuration of lanthanoids.

Z	symbol	Electronic configuration			
		Ln	Ln^{3+}	Ln^{2+}	Ln^{4+}
21	Sc	$[Ar]\ 3d^1\ 4s^2$	[Ar]		
39	Y	$[Kr]\ 4d^1\ 5s^2$	[Kr]		
57	La	$[Xe]\ 5d^1\ 6s^2$	$[Xe]\ 4f^0$		
58	Ce	$[Xe]\ 4f^1\ 5d^1\ 6s^2$	$[Xe]\ 4f^1$		$[Xe]\ 4f^0$
59	Pr	$[Xe]\ 4f^3\ 6s^2$	$[Xe]\ 4f^2$		$[Xe]\ 4f^1$
60	Nd	$[Xe]\ 4f^4\ 6s^2$	$[Xe]\ 4f^3$	$[Xe]\ 4f^4$	$[Xe]\ 4f^2$
61	Pm	$[Xe]\ 4f^5\ 6s^2$	$[Xe]\ 4f^4$		
62	Sm	$[Xe]\ 4f^6\ 6s^2$	$[Xe]\ 4f^5$	$[Xe]\ 4f^6$	
63	Eu	$[Xe]\ 4f^7\ 6s^2$	$[Xe]\ 4f^6$	$[Xe]\ 4f^7$	
64	Gd	$[Xe]\ 4f^7\ 5d^16s^2$	$[Xe]\ 4f^7$		
65	Tb	$[Xe]\ 4f^9\ 6s^2$	$[Xe]\ 4f^8$		$[Xe]\ 4f^7$
66	Dy	$[Xe]\ 4f^{10}\ 6s^2$	$[Xe]\ 4f^9$	$[Xe]\ 4f^{10}$	$[Xe]\ 4f^8$
67	Ho	$[Xe]\ 4f^{11}\ 6s^2$	$[Xe]\ 4f^{10}$		
68	Er	$[Xe]\ 4f^{12}\ 6s^2$	$[Xe]\ 4f^{11}$		
69	Tm	$[Xe]\ 4f^{13}\ 6s^2$	$[Xe]\ 4f^{12}$	$[Xe]\ 4f^{13}$	
70	Yb	$[Xe]\ 4f^{14}\ 6s^2$	$[Xe]\ 4f^{13}$	$[Xe]\ 4f^{14}$	
71	Lu	$[Xe]\ 4f^{14}\ 5d^16s^2$	$[Xe]\ 4f^{14}$		

I.1.5 Lanthanoid contraction.

The atomic**Figure I.** ***2*** and ionic **Figure I.** ***3*** radii of the lanthanoids exhibit a decreasing trend from lanthanum to lutetium **Table I.** ***5***. This phenomenon is primarily attributed to the increase in nuclear charge, coupled with the rising electrostatic repulsion among electrons. As the atomic number ascends, the repulsion among electrons leads to a diminished shielding effect from the inner 4f shell, where additional electrons are introduced[2]. The 4f electrons do not uniformly occupy the inner regions of the 5s and 5p shells due to their diffuse nature, resulting in a partial shielding of the increasing nuclear charge. Consequently, the enhanced attraction experienced by the outer electrons results in a reduction of the atomic or ionic radius[8].

The phenomenon known as lanthanoid contraction results in the trivalent yttrium ion (Y^{3+}) having a radius that lies between those of Ho^{3+} and Er^{3+}. Additionally, the atomic radius of yttrium is situated between that of neodymium and samarium, which leads to yttrium exhibiting chemical properties that closely resemble those of the lanthanoids[9].

In metals, the overlap of the outermost electron clouds allows the free movement of electrons, which contributes to their conductivity. Europium and ytterbium typically maintain $4f^7$ and $4f^{14}$ electronic configurations, respectively, resulting in only two conducting electrons. This reduced overlap of outermost electrons between neighboring atoms leads to an increase in atomic radius. In contrast, cerium, with a single 4f electron, tends to contribute four conducting electrons to achieve a stable electronic configuration, resulting in a larger overlap and a smaller distance between adjacent atoms compared to other lanthanoids [10].

Table I. 5 Atomic and ionic radii of lanthanoids.

Element	Symbol	Atomic Radius (pm)	Ionic Radius (3+)
Lanthanum	La	187.7	106.1
Cerium	Ce	182	103.4
Praseodymium	Pr	182.8	101.3
Neodymium	Nd	182.1	99.5
Promethium	Pm	181	97.9
Samarium	Sm	180.2	96.4
Europium	Eu	204.2	95.0
Gadolinium	Gd	180.2	93.8
Terbium	Tb	178.2	92.3
Dysprosium	Dy	177.3	90.8
Holmium	Ho	176.6	89.4
Erbium	Er	175.7	88.1
Thulium	Tm	174.6	89.4
Ytterbium	Yb	194.0	85.8
Lutetium	Lu	173.4	84.8

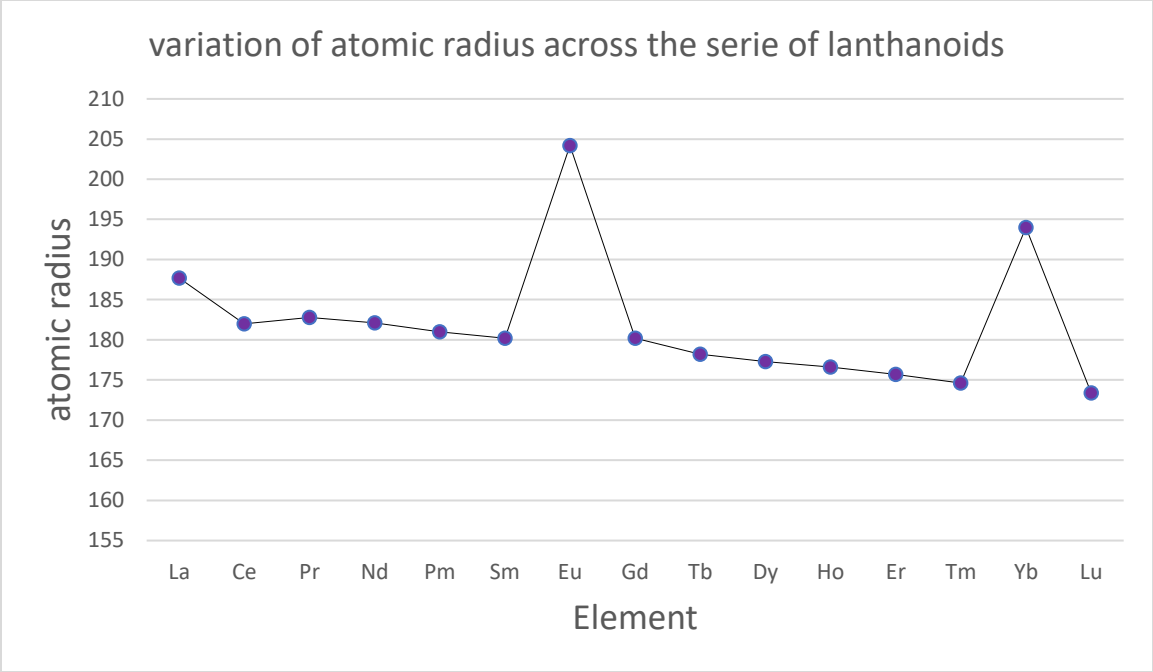

Figure I. 2 Variation of atomic radius of lanthanoids

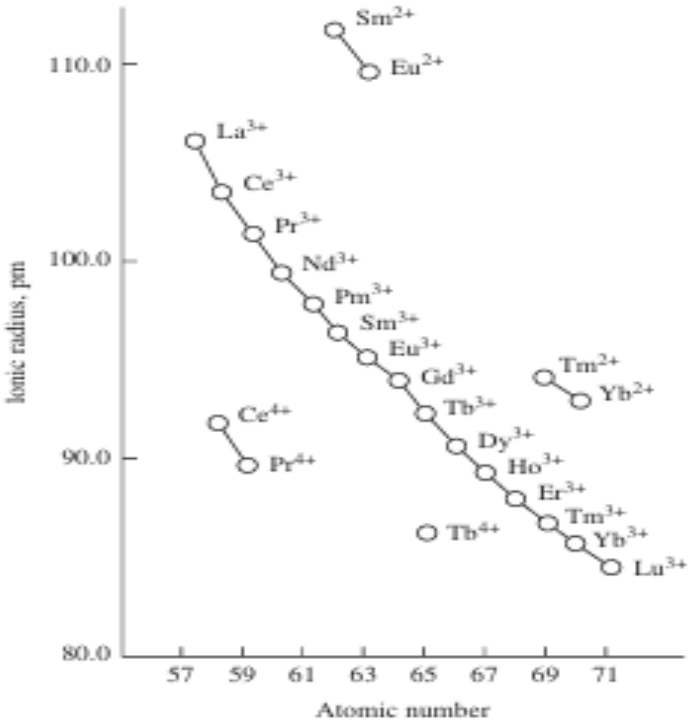

Figure I. 3 Variation of ionic radius of Ln ions.

I.1.6 The optical properties of lanthanoids.

The distinctive optical characteristics of lanthanoids arise from their specific electronic configurations, particularly the transitions of f-electrons within their atomic structure. All lanthanoid ions in the +3-oxidation state exhibit luminescent properties, with the exception of lanthanum and lutetium, as their trivalent forms do not contain f-electrons **Table I. *6***. These f-electron transitions enable the lanthanoids to emit light when stimulated by an external energy source, which is usually ultraviolet (UV) or visible light[11]. The presence of fully filled 5s and 5p orbitals effectively shields the 4f orbital from the electrostatic influences of the crystalline field, resulting in nearly monochromatic absorption and emission spectra for the lanthanoids. Consequently, the emitted color from lanthanoid complexes remains consistent, regardless of the ligands attached[2].

The luminescent properties of lanthanoid ions play a crucial role in modern lighting technologies. Presently, a significant number of fluorescent lamps, light-emitting diodes (LEDs), and display devices utilize phosphors that contain luminescent lanthanoid ions. This preference is largely due to the high purity of the colors emitted, which is particularly evident in the red emissions from europium (III) and the green emissions from terbium (III)[9].

Table I. 6 Colors of Ln^{3+} ions in aqueous solution.

Ion	Unpaired Electrons	Color
La^{3+}	0	Colorless
Ce^{3+}	1	Colorless
Pr^{3+}	2	Green
Nd^{3+}	3	Reddish
Pm^{3+}	4	Pink ; yellow
Sm^{3+}	5	Yellow
Eu^{3+}	6	Pale Pink
Gd^{3+}	7	Colorless
Tb^{3+}	6	Pale Pink
Dy^{3+}	5	Yellow
Ho^{3+}	4	Pink ; yellow
Er^{3+}	3	Reddish
Tm^{3+}	2	Green
Yb^{3+}	1	Colorless
Lu^{3+}	0	Colorless

I.1.7 The magnetic properties of lanthanoids

The magnetic behavior of the lanthanoid elements (rare earth elements, REEs) is predominantly attributed to the presence of unpaired electrons in their 4f orbitals. These orbitals are partially filled in most trivalent lanthanoid ions (Ln^{3+}), leading to characteristic paramagnetic properties. With the exception of La^{3+} and Lu^{3+} which possess empty and fully filled 4f subshells, respectively and Y^{3+}, which lacks 4f electrons, all Ln^{3+} ions exhibit unpaired electrons and are thus paramagnetic **Table I.** *7*. The number of these unpaired electrons directly influences the magnitude of the magnetic moment associated with each ion. However, the precise magnetic behavior can vary across the lanthanoid series due to differences in electronic configuration and the associated total angular momentum quantum numbers (J), which are derived from both spin and orbital contributions[2].

Unlike transition metals, where magnetism is mostly due to the spin of the electrons, lanthanoids show strong orbital contributions to magnetism. This is because their 4f orbitals are well shielded by outer electrons ($5s^2$ and $5p^6$), which means the 4f electrons don't interact much with surrounding atoms or ligands. As a result, the magnetic moment of lanthanoid ions tends to remain consistent regardless of the chemical environment[8].

Table I. 7 Number of unpaired electrons and magnetic moments of Ln^{3+}.

Lanthanoid	Electronic Configuration (Ln^{3+})	Unpaired Electrons	Magnetic Moment (μ_{eff}) (BM)
La^{3+}	[Xe] $4f^0$	0	0 (diamagnetic)
Ce^{3+}	[Xe] $4f^1$	1	2.54
Pr^{3+}	[Xe] $4f^2$	2	3.58
Nd^{3+}	[Xe] $4f^3$	3	3.62
Pm^{3+}	[Xe] $4f^4$	4	2.68
Sm^{3+}	[Xe] $4f^5$	5	0.84
Eu^{3+}	[Xe] $4f^6$	6	3.4
Gd^{3+}	[Xe] $4f^7$	7	7.94 (maximum)
Tb^{3+}	[Xe] $4f^8$	6	9.72
Dy^{3+}	[Xe] $4f^9$	5	10.63
Ho^{3+}	[Xe] $4f^{10}$	4	10.60
Er^{3+}	[Xe] $4f^{11}$	3	9.58
Tm^{3+}	[Xe] $4f^{12}$	2	7.57
Yb^{3+}	[Xe] $4f^{13}$	1	4.54
Lu^{3+}	[Xe] $4f^{14}$	0	0 (diamagnetic)

I.2 Coordination chemistry.

Alfred Werner made foundational contributions to coordination chemistry by proposing the first accurate theory of coordination compounds in 1893. He introduced the concept of coordination numbers and spatial arrangements of ligands around a central metal atom distinguishing between primary valence (ionic) and secondary valence (coordination) and demonstrated that metal ions can form stable complexes with specific geometries, such as octahedral, square planar, or

tetrahedral structures[12]. His work was experimentally confirmed through the synthesis and resolution of optical isomers of cobalt complexes, proving the existence of three-dimensional coordination geometries. Werner's groundbreaking research earned him the Nobel Prize in Chemistry in 1913 and laid the foundation for modern inorganic and coordination chemistry[13].

Coordination compounds are fundamental to both industrial processes and biological systems. Notable examples include the Ziegler–Natta catalyst, which is essential for the polymerization of ethene into polyethylene; chlorophyll, the green pigment crucial for photosynthesis in plants; hemoglobin, responsible for oxygen transport in animals; and vitamin B_{12}, vital for cellular metabolism. These coordination complexes contain central metal ions, titanium and aluminum in Ziegler–Natta catalysts, magnesium in chlorophyll, iron in hemoglobin, and cobalt in vitamin B_{12} surrounded by a set of ligands, which can be ions or molecules[14].

In the lanthanoid coordination chemistry, complexes formed by trivalent lanthanoid ions (Ln^{3+}) exhibit unique characteristics compared to those of transition metal ions. One of the most notable differences is the absence of a fixed coordination number. Instead, the coordination number in lanthanoid complexes is influenced primarily by the steric and spatial demands of the ligands involved. For instance, the number of donor atoms that can pack around a lanthanoid ion depends on the size and flexibility of the ligand as well as potential secondary interactions between distant parts of bulky ligands.

With monodentate ligands, lanthanoid ions commonly adopt coordination numbers of 8 or 9, while the use of multidentate ligands can lead to coordination numbers as high as 12. This variability is a key feature of lanthanoid chemistry and has implications for their behavior in catalysis, materials science, and medicinal applications[15].

Coordination compounds typically adopt a limited number of fundamental geometries, which can be rationalized using models that account for electron pair repulsion. While the Valence Shell Electron Pair Repulsion (VSEPR) model was originally developed to describe the shapes of main group compounds, a modified version (the Kepert model) was been proposed to describe geometries in transition metal complexes[6]. In the Kepert model, the coordination number is the primary determinant of molecular geometry. Several additional factors significantly influence the observed geometry, including :

- Metal–ligand electronic interactions, particularly those involving the d- or f-electrons of the metal center, which can alter bonding preferences and spatial arrangement.
- Metal ion size and its preferred metal–ligand bond lengths, which impact how ligands are spatially accommodated.
- Ligand–ligand repulsions, which can distort idealized geometries due to steric crowding.
- The inherent geometry and rigidity of ligands, which may constrain the complex into specific shapes regardless of the coordination number.

These considerations help explain why coordination compounds of similar coordination numbers can adopt different geometries, and why predictions based solely on simple models like VSEPR or Kepert may not always align with experimental observations[16].

I.2.1 Ligands

I.2.1.1 Definition

A ligand is generally defined as a chemical species that forms a stable complex by binding to a central atom, typically a metal ion. Ligands are remarkably diverse and can include inorganic atoms, ions, and molecules, as well as a wide range of organic species. In coordination chemistry, a ligand is specifically a molecule or ion that possesses donor atoms or functional groups capable of forming coordinate (dative covalent) bonds with a central metal atom or ion. These donor atoms usually have lone pairs of electrons available for bonding[17].

Ligands are commonly denoted by the symbol L. When a ligand contains a single donor atom that contributes one lone pair of electrons to the metal center, it occupies one coordination site and is classified as a monodentate ligand. Polydentate ligands on the other side have more than one donor atom [18].

A species is typically recognized as a ligand if it has atoms with lone electron pairs that can participate in bonding. Heteroatoms such as oxygen (O), nitrogen (N), sulfur (S), and phosphorus (P) frequently serve as donor atoms in organic ligands due to their ability to carry lone pairs[17]. Ligands that possess two or more distinct donor atoms, each capable of coordinating to the metal center, are known as ambidentate ligands, as they offer multiple binding modes depending on the coordination environment[19].

I.2.1.2 Coordination.

In the gas phase, a ligand may encounter a bare (naked) metal atom or ion. However, in the solid or liquid phase, metal ions are typically already coordinated with a variety of surrounding ligands, which may include counterions or solvent molecules. For a new ligand to bind directly to the inner coordination sphere of a metal ion, it generally must displace an existing ligand, a process known as ligand substitution[17].

I.2.1.3 Chelation and bridging.

Chelation occurs when a single ligand coordinates to a metal ion through two or more donor atoms, forming a ring structure known as a chelate ring[20]. This ring includes the metal ion, the two donor atoms, and the ligand framework that connects them[21].

Bridging coordination arises when one or more donor atoms from a single ligand coordinate to different metal centers, thereby forming a bridge between them[18]. A classic example is the carboxylate group ($RCOO^-$) **Figure *I. 4***, which can adopt multiple coordination modes: it may bind to a single metal through one oxygen atom (monodentate), bridge two metal centers with each oxygen coordinating separately (bridging bidentate), or bind to one metal via both oxygen atoms (chelating bidentate).[22]

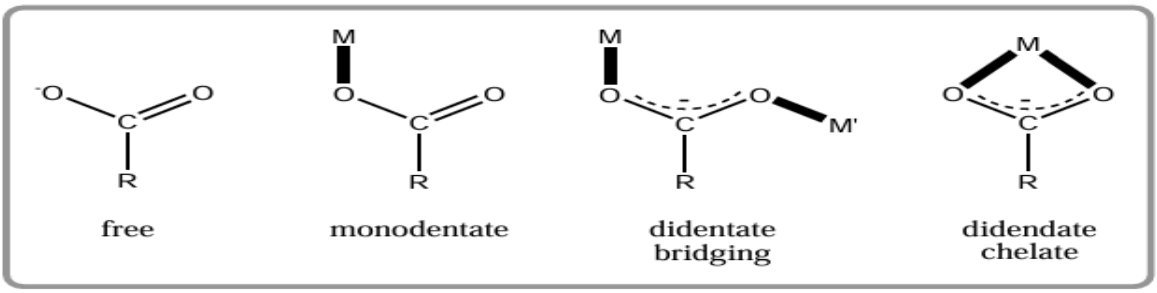

Figure I. 4 Metal ion binding options for a carboxylate group [22].

The size of a chelate ring is defined by the number of atoms forming a continuous covalent chain that starts at the metal center, traverses through the donor atoms and the ligand backbone, and returns to the metal **Figure *I. 5***. As the number of atoms in the linking chain between donor groups increases, the corresponding chelate ring size also increases.

There exists an optimal chelate ring size for complex stability. In general, as the chelate ring grows, the stability of the resulting complex initially increases, reaches a maximum, and then decreases with further ring enlargement. This trend is influenced by several factors, including the nature of the metal ion, the electronic and steric properties of the donor atoms, and the rigidity or flexibility of the ligand framework[18].

Five-membered chelate rings are commonly favored due to their ideal balance of enthalpic and entropic contributions, offering both geometric compatibility with most metal coordination spheres and minimal ring strain.

3-membered < 4-membered < 5-membered > 6-membered > 7-membered.

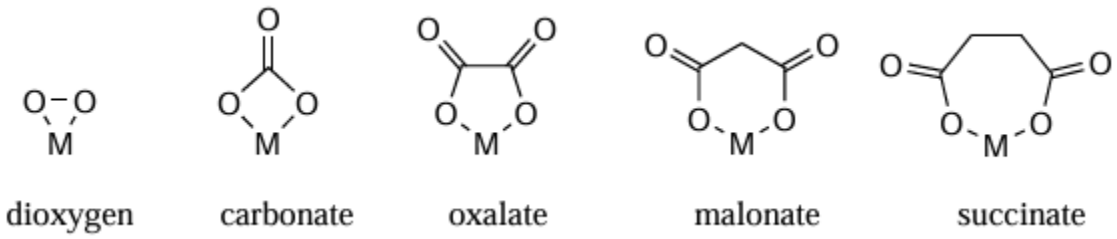

Figure I. 5 Three to seven-membered chelate rings. The ring size affects the L-M-L intra-ligand angle [17].

I.2.1.4 Denticity

Denticity describes the number of donor atoms within a ligand that are simultaneously coordinated to a central metal ion **Figure *I. 6***. When coordination occurs through a single donor atom, the ligand is termed monodentate. If two donor atoms from the same ligand bind to the metal center, it is classified as bidentate; similarly, ligands with three, four, or more coordinated donor atoms are referred to as tridentate, tetradentate, and so on[19].

Ligands that possess multiple coordination sites capable of binding through several donor atoms are collectively referred to as polydentate ligands. The effective coordination of these donor groups depends not only on their number but also on their spatial arrangement within the ligand framework. Factors such as ligand flexibility, backbone length, and the relative positions of the donor atoms strongly influence how many sites can actually engage with the metal center[23].

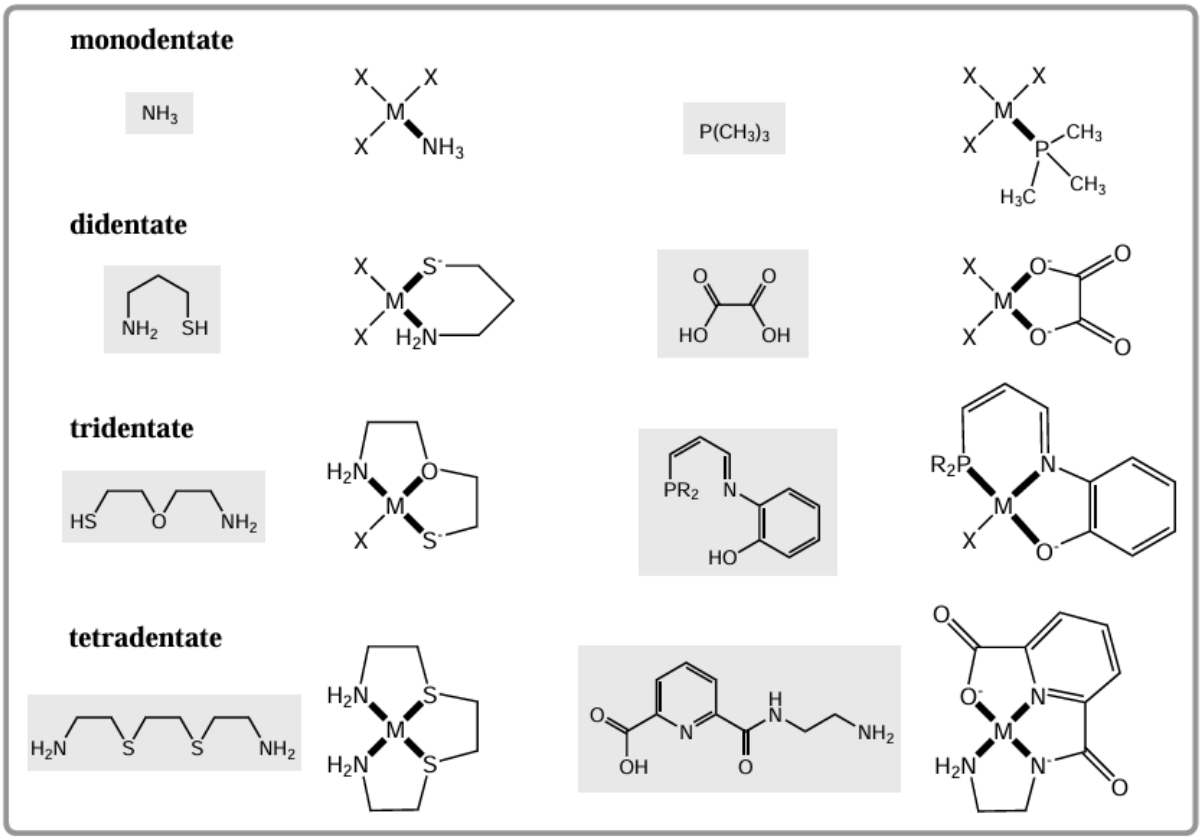

Figure I. 6 Examples of ligands of different denticity.

X-Groups indicate the sites not used by the target ligand[17].

I.2.2 Rare earth complexes with carboxylic acids.

Carboxylic acids are widely used as ligands in the coordination chemistry of rare earth elements due to their oxygen-containing functional groups, which act as effective coordinating atoms. These acids possess diverse structural characteristics that allow them to meet the typically high coordination number requirements of rare earth metal ions. As research in rare earth coordination chemistry has advanced, the utilization of carboxylic acids has significantly increased. One of the key advantages of these ligands is their ability to adopt a variety of binding modes, enhancing the stability and versatility of the resulting complexes [24].

Rare earth–carboxylic acid complexes have found broad applications, especially in fields such as biology and materials science. Notably, they play important roles in the development of metal-organic frameworks (MOFs), the design of organic light-emitting diodes (OLEDs) [25].

I.2.2.1 Preparation of rare earth-carboxylic complexes.

A variety of techniques have been developed for the synthesis of rare earth–carboxylic acid complexes, typically starting from readily available rare earth oxides or salts. The choice of synthetic route often depends on the specific properties of the carboxylic acid ligands, particularly their solubility. These syntheses can be carried out in aqueous media, organic solvents, or mixtures of both. The solvent system is usually selected based on the solubility of the ligands and the target complexes. Furthermore, the reactions can be performed under different conditions, including ambient temperature and pressure, hydrothermal or solvothermal conditions, or via gel-based methods [26].

Among these approaches, hydrothermal and gel synthesis techniques have gained particular attention for their effectiveness in producing high-quality single crystals. These methods offer controlled environments that facilitate slow crystal growth, which is essential for obtaining well-defined structures suitable for detailed characterisation, such as single-crystal X-ray diffraction.

When rare earth oxides are used as starting materials, the synthesis of rare earth–carboxylic acid complexes are typically carried out under atmospheric pressure. The process involves heating or refluxing a mixture of the rare earth oxide with the carboxylic acid in a suitable solvent, such as water or a polar organic solvent commonly methanol (MeOH), ethanol (EtOH), dimethylformamide (DMF), or dimethyl sulfoxide (DMSO). After the reaction is complete, the product is generally isolated by filtration, and the solvent is removed through evaporation to yield the desired complex.

In contrast, when rare earth salts such as chlorides, nitrates, or perchlorates are used, the synthetic route involves a preliminary neutralization step. The carboxylic acid is first neutralized with a base, typically sodium hydroxide (NaOH) or potassium hydroxide (KOH), to form the corresponding carboxylate salt. This is then reacted with the rare earth salt in water or another polar solvent. The reaction can be carried out under mild ambient conditions or under solvothermal conditions, depending on the desired crystal quality or structural features of the final complex.

Gel Synthesis of Rare Earth–Carboxylic Acid Complexes

Gel synthesis is a powerful and widely used method for the preparation of single-crystal coordination compounds, particularly when high-quality crystals suitable for structural analysis are desired. This technique offers a controlled environment that enables slow diffusion and crystal growth, which is crucial for obtaining well-formed crystals. Various types of gels can be employed as the reaction medium, with silica gels, gelatin, and agar being the most commonly used. In a typical procedure, the carboxylic acid ligand is first dissolved in the gel medium, which is then allowed to solidify within a glass tube or similar container. Once the gel has set, a solution containing the rare earth metal salt is carefully added on top of the gel column [27].

Over time, the metal ions slowly diffuse through the gel's porous network, gradually encountering and reacting with the dissolved carboxylic acid molecules. This slow diffusion ensures a gentle and controlled reaction environment, reducing the chances of rapid precipitation and promoting the orderly formation of crystals. Depending on the system and conditions, this process can take several days to a few weeks to yield high-quality single crystals suitable for further characterisation.

I.2.2.2 Structural chemistry of rare earth-carboxylic acid complexes.

Rare earth (RE) complexes with carboxylic acids exhibit rich and diverse structural chemistry, largely influenced by the unique properties of RE(III) ions. Due to their high positive charge and large ionic radii, RE(III) ions typically form complexes with high coordination numbers, generally ranging from 6 to 10. Instead, they tend to adopt coordination environments that maximize the number of ligands around the metal center, often including solvent molecules to satisfy their coordination requirements. The common coordination modes for carboxylates include monodentate, simple chelating, bridging bidentate, and chelating tridentate[12].

In mononuclear complexes, carboxylates generally adopt unidentate or simple chelating modes. In contrast, dimeric and polymeric complexes more commonly feature bridging bidentate and tridentate coordination modes, allowing for the formation of extended structures.

Polymeric complexes (those containing more than one metal center) often formed when carboxylate ligands bridge multiple RE(III) ions. This tendency toward polymerization can, however, be controlled. The introduction of auxiliary ligands such as 1,10-phenanthroline (Phen) or 2,2'-bipyridine (bipy), or the use of bulky carboxylic acids, can inhibit polymer formation by introducing steric hindrance or saturating coordination sites, thereby favoring the formation of mononuclear or dimeric species. Similarly, increasing the carboxylate-to-metal ratio can also help drive the formation of discrete complexes.

Rare earth–carboxylic acid complexes are most commonly formed with monocarboxylic acids, which tend to promote the formation of simpler, monomeric or dimeric structures. In contrast, polycarboxylic acids (containing two or more carboxylic acid groups) facilitate the formation of bridging interactions that promote polymerization, often leading to more complex two-dimensional (2D) or three-dimensional (3D) coordination polymers. While mono- and polycarboxylic acids can adopt similar coordination modes, the extended networks formed by polycarboxylic acids are often sparingly soluble and pose challenges for single-crystal growth, making structural characterisation more difficult.

I.2.3 Coordination polymers.

I.2.3.1 Introduction.

A coordination polymer is a structure made up of an infinite array of metal cation centers linked by organic ligands. These polymers can vary in architecture, from simple 1D chains to large, porous networks. Essentially, a coordination polymer is a coordination compound where repeating coordination units extend in one, two, or three dimensions, with each unit being a coordination

complex. The formation of these structures happens automatically through a self-assembly process [28].

The type and topology of the self-assembled coordination products depend on the functionality of the ligand and the geometric requirements of the metal used. Choosing the right ligand is crucial in designing coordination frameworks. Variations in the flexibility, length, and symmetry of organic ligands can lead to materials with a wide range of architectures and functions. Depending on the metal's valence, different geometries can be obtained, including linear, trigonal planar, tetrahedral, square planar, square pyramidal, trigonal bipyramidal, octahedral, trigonal prismatic, pentagonal bipyramidal, and their distorted forms [29].

The organic ligands used to build coordination polymer networks generally have at least two donor sites to coordinate with metal ions, ensuring the formation of at least a 1D structure. The overall structure of coordination polymers depends on the coordination properties of both the metal ions and the ligands, as well as secondary interactions, like hydrogen bonding.

I.2.3.2 Dimensionality.

Coordination polymers can be classified in various ways based on their structure and composition. One key classification is dimensionality[29]. Coordination polymers can be classified as 1D, 2D, or 3D. A structure is classified as one, two, or three-dimensional depending on how it extends in space[30].

a. **One-dimensional polymers**.

1D coordination polymers are made of metal centers linked into infinite chains by organic ligands. The 1D structure extends in a straight line (along one axis), and can take different forms for example, linear or zig-zag chains, or ladder as shown in **Figure I.** *7*.

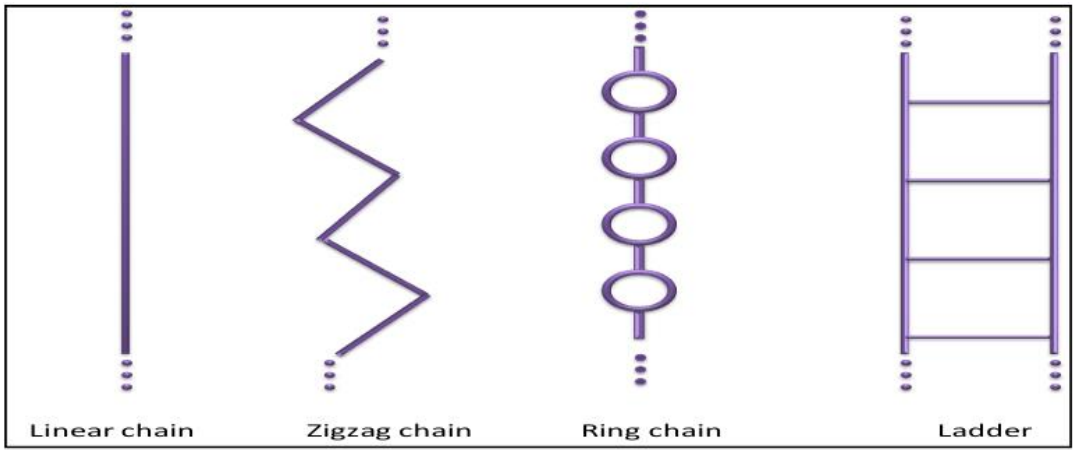

Figure I. 7 Forms of 1D polymers.

b. **Two-dimensional polymers**.

These have structures extending in a plane (across the x and y axes). The metal centers are linked by ligands to form infinite sheets or layers **Figure I. *8***. The layers often stack over each other, held together by weaker forces like π–π stacking, van der Waals forces, or hydrogen bonds[25].

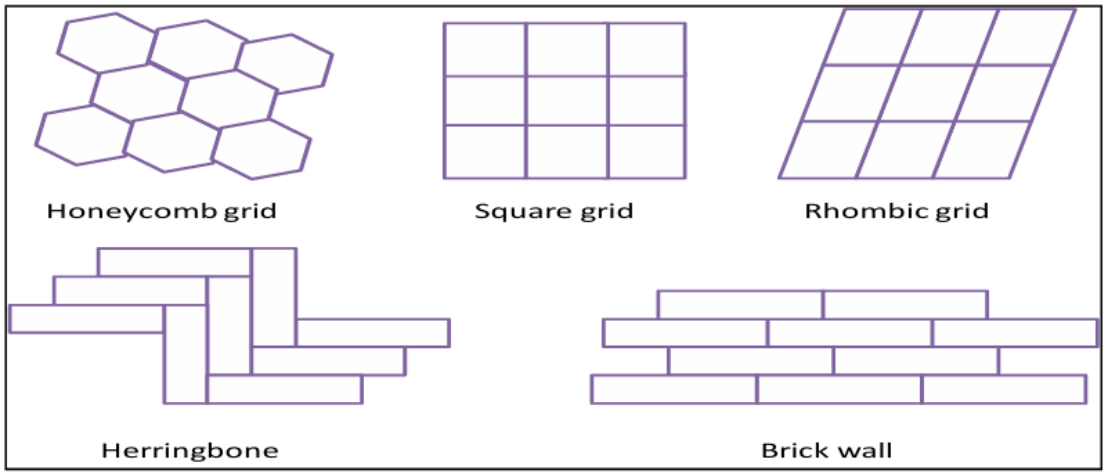

Figure I. 8 Different forms adopted by 2D coordination polymers.

c. Three-dimensional polymers.

The 3D structure extends in all three directions (x, y, and z axes). The connectivity is very complex and can create porous frameworks with big, open spaces (cages, or channels) or dense frameworks with no pores (tightly packed)[14].

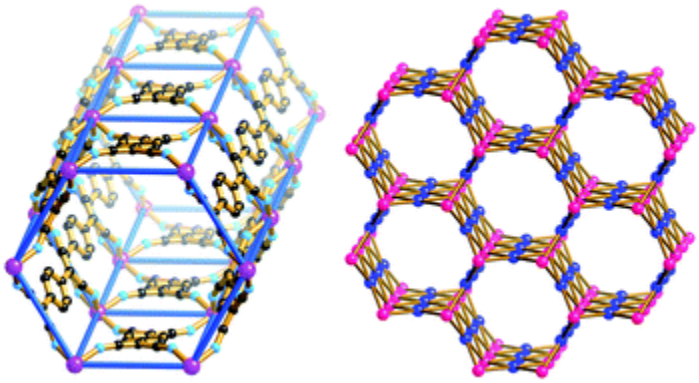

Figure I. 9 Example of 3D structures.[31].

The infinite array of a coordination polymer is defined by coordination bonds linking metal centers and ligands. Structures linked only by hydrogen bonds are not considered coordination polymers. However, if a structure is linked by coordination bonds in one direction and hydrogen bonds in other directions, it is still considered a 1D coordination polymer.

d. Metal-Organic Frameworks (MOFs).

Metal-organic frameworks (MOFs) are a class of porous coordination polymers, which are coordination compounds extending through repeating coordination entities in two or three dimensions. MOFs specifically consist of coordination networks with metal clusters (referred to as Secondary Building Units -SBUs) and organic ligands (linkers) that create potential voids **Figure I.** ***10*** [32].

Generally, the term MOF is used to refer to 3D porous structures. The 2D coordination structures that have permanent voids and crystallinity within a layer might be called 2D MOFs. 2D porous layers can be stacked over each other to make 3D bulky materials **Figure I. 11** [33].

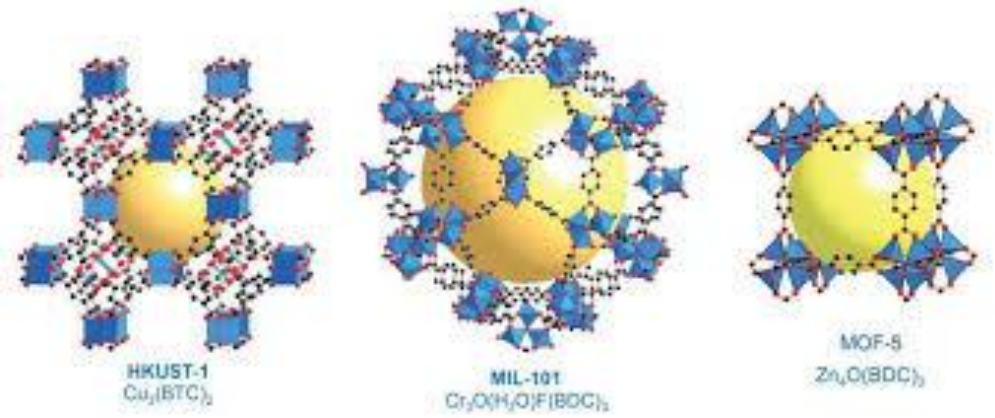

Figure I. 10 Some examples of MOFs.

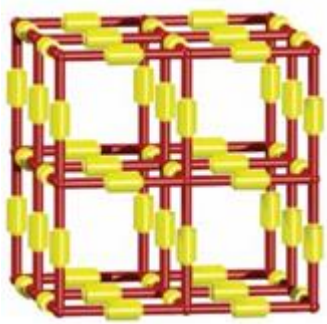

Figure I. 11 *2D porous layers stacked together.*[32].

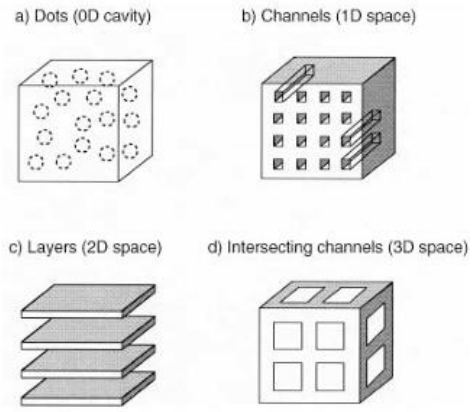

Figure I. 12 Classes of porous structures[33]

I.2.3.3 Synthesis and design of coordination polymers

Coordination polymers are commonly synthesized through a self-assembly process, typically involving the crystallization of a metal salt with an organic ligand[28]. When designing and synthesizing these materials, several key factors must be considered: the metal-to-ligand molar

ratio, the coordinating ability and functionality of the ligands, the type of metal ions used, and the presence of solvent molecules, counterions, or guest organic molecules. Each of these components can significantly influence the structure and properties of the resulting coordination polymer[34].

i. Factors affecting the design of coordination polymers.

- Metal Centers

Metal centers (also referred to as nodes or hubs) are the core points in a coordination polymer that bond to a specific number of ligands at well-defined angles[2]. The number of ligands attached to a metal center is known as its coordination number, and both this number and the angles at which ligands are held determine the overall dimensionality of the structure[35].

- Ligands

Ligands act as electron pair donors, forming coordination complexes with metal cations through a classic Lewis acid-base interaction. A coordination polymer forms when a ligand is capable of binding to more than one metal center, effectively bridging them. Ligands that form only one coordination bond (monodentate/terminal ligands) do not extend the network. In contrast, polydentate ligands can form multiple coordination bonds, making them essential for building extended, infinite structures[15].

The behavior and role of ligands in coordination polymers can be influenced by their Chemical Composition (for example, variety and number of donor atoms) and structural orientation (rigidity and flexibility of the ligand)[36].

- Counterions

Since most metal centers are positively charged and introduced as salts, the choice of counterion can significantly influence the final structure of the coordination polymer.

- Crystallization Environment

Conditions during synthesis such as pH, temperature, or exposure to light can affect the outcome of the crystallization process and lead to different structures. These environmental effects are often system-specific and need to be evaluated on a case-by-case basis.

- Guest Molecules

Many coordination polymers contain pores or channels within their structure, which create thermodynamically unfavorable voids. To stabilize the framework, these spaces are often occupied by guest molecules. While they don't form covalent bonds with the framework, guest molecules can interact through weaker forces like hydrogen bonding or π–π stacking. Common guests include solvent molecules or ambient gases (e.g., O_2, N_2, CO_2). In some cases, the presence of a guest molecule is crucial for maintaining the integrity of a pore or channel that would otherwise collapse.

ii. Synthetic methods for coordination compounds.

The synthetic methods utilized to produce coordination polymers are generally the same methods used to grow a crystal. The **Table I. *8*** below shows the different methods for coordination polymer synthesis[29].

Table I. 8 Synthetic methods for coordination compounds

Method	Description
One pot solution reaction	The ligand and the metal salts are mixed directly in solution and the product is formed by ligand substitution reaction.
Diffusion reaction	Commonly used for single crystal growth. The reactant solutions are separated in a tube by a convenient solvent. The slow diffusion of the reactants into the intermediate solvent layer results into formation of desired crystals.
Mechanical grinding reaction	It is a clean, fast and environmentally friendly technique of synthesizing coordination compounds. It involves direct grinding of metal salts and ligands without using solvents.
Hydrothermal/solvothermal method	Involves the use of aqueous/organic solvents media in sealed Teflon bombs in a temperature range of 100-250 oc.

Hydrothermal method.

The hydrothermal technique is the most popular technique used by scientists and technologists of different disciplines. The word hydrothermal has a geological origin. It was first used by the British Geologist, Sir Roderick Murchison, to describe the action of water at higher temperature and pressure bringing about changes in the earth's crust leading to formation of various rocks and minerals [37].

The first publication on hydrothermal research (in 1845) reports the successful synthesis of tiny quartz crystals by K.F.E.von Schafhautl. The earliest workers, Friedel and Sarasin obtained the first very large crystals of the hydrated potassium silicate by hydrothermal technique. Because of the high-pressure working conditions in their experiments, they termed their hydrothermal autoclave as hydrothermal bomb. The term hydrothermal refers to any heterogenous reaction in the presence of aqueous solvents under high pressure and temperature conditions [38].

Water as a reaction medium.

Water is one of the most important solvents present in nature in abundant amount and has remarkable properties as reaction medium under hydrothermal conditions. It poses environmental benefit and it's cheaper than other solvents. It's nontoxic, nonflammable, thermodynamically stable and volatile, so it can be removed from the product very easily. Water is a polar solvent and its polarity can be controlled by temperature and pressure and this can be of an advantage over other solvents [39].

Autoclave

An autoclave is a specialized reaction vessel designed for crystal growth under hydrothermal conditions and is considered the most critical component of the hydrothermal synthesis system **Figure I.** ***13***. It must maintain a stable and controlled environment capable of withstanding highly corrosive solvents at elevated temperatures and pressures over extended periods. Consequently, the choice of construction material is of paramount importance, with corrosion resistance being a primary criterion. Common materials used include high-strength, corrosion-resistant alloys such as the 316 series stainless steels, which offer an excellent balance of mechanical durability and chemical stability. Additionally, iron-, nickel-, and cobalt-based superalloys are employed for their exceptional resistance to extreme environments, while titanium and its alloys are valued for their outstanding corrosion resistance and favorable strength-to-weight ratio, despite their higher cost [40].

To further enhance the chemical durability of the autoclave, the interior is often lined with a non-reactive polymer such as polytetrafluoroethylene (PTFE), commonly known as Teflon. This liner acts as a protective barrier, preventing the highly corrosive reaction mixture from coming into direct contact with the metal walls. A key property of Teflon that makes it particularly suitable for this application is its high coefficient of thermal expansion, which enables it to expand and contract significantly during heating and cooling cycles without compromising its structural integrity. This thermal adaptability helps maintain the liner's protective function over repeated use, ensuring the longevity and reliability of the autoclave. Thus, the careful selection of both structural materials and internal coatings is essential for the success of hydrothermal synthesis processes. Therefore, an ideal hydrothermal autoclave should [41];

- Be inert to acids, bases and oxidizing agents
- Be easily assembled and dissembled
- Have sufficient length to obtained a desired temperature gradient
- Bear high temperature and pressure for long duration
- Thermodynamically stable in a given range of temperature

According to study reports related to reaction kinetics solubility and material processing under mild hydrothermal conditions (temperature pressure conditions below 300^{o}C and 250bars), Teflon is the most popularly used lining material. The greatest disadvantage of Teflon lining is that beyond 300oC, it cannot be used because Teflon dissociates which affects the pH of neutral solutions.

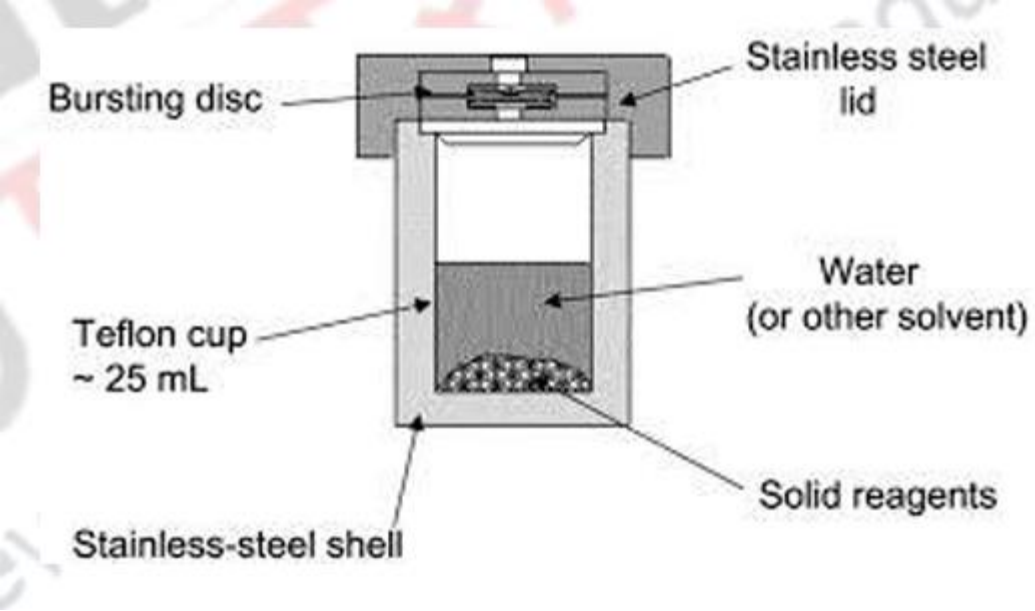

Figure I. 13 Illustration of hydrothermal experiment setup.

Advantages of hydrothermal synthesis.

Hydrothermal synthesis presents many advantages over conventional and nonconventional synthesis methods, among which include;

- ✓ Less cost of instrumentation and energy
- ✓ Hydrothermal methods are more environmentally friendly compared to many other techniques.
- ✓ Varieties of morphologies and particle sizes are possible with hydrothermal processing
- ✓ Hydrothermal synthesis can be hybridized with other processes like microwave, electrochemistry, ultrasound and hot-pressing to gain advantages such as enhancement of reaction kinetics and increase ability to make new materials[42].
- ✓ It's beneficial to industries that rely on powder (e.g. materials, pharmaceuticals, pigments) which benefit from having access to powder of different size and morphology for a wide range of reasons

I.2.3.4 Characterization of coordination polymers.

a. Infrared spectroscopy (IR)

IR is a spectroscopic technique used to characterize compounds and identify the functional groups of organic molecules and can also be used as analytical tool to assess the purity of a compound. It deals with the absorption of radiation in the infrared region of the electromagnetic spectrum **Figure I. *15***. The absorption of infrared radiation by a molecule causes changes in their vibrational and rotational energy levels and hence IR-spectroscopy is also known as vibrational-rotational spectroscopy[19]. The different forms of vibrations are given in **Figure I. *16***

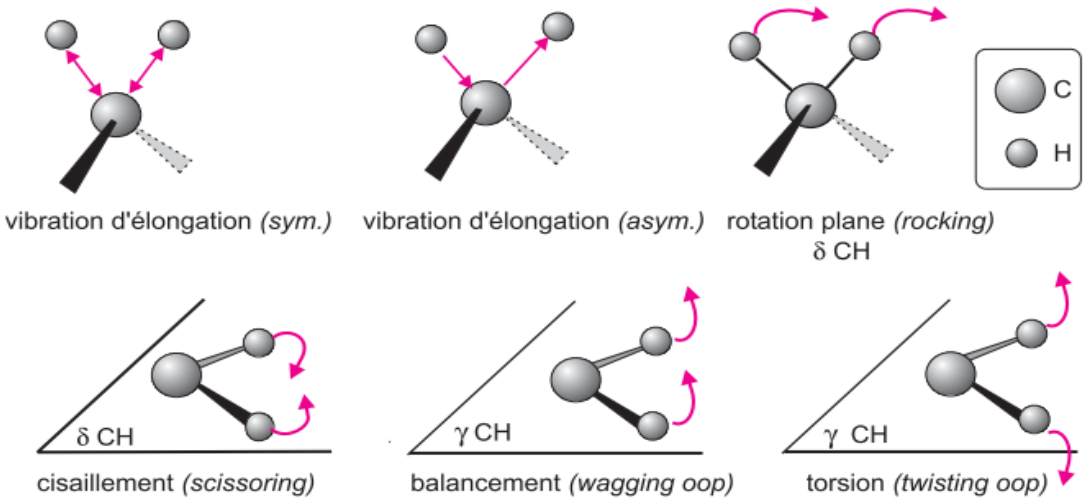

Figure I. 14 The possible vibration modes upon absorption of IR radiations [22].

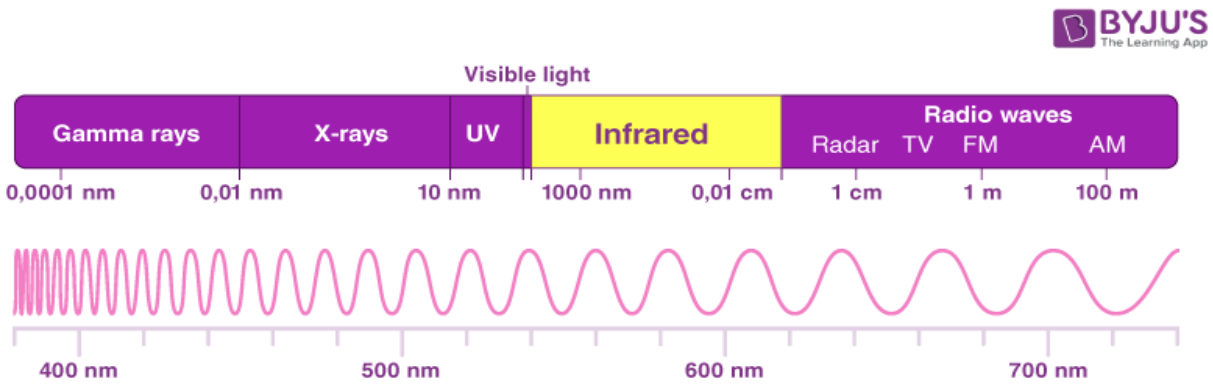

Figure I. 15 The electromagnetic spectrum (source: Wikipedia).

Organic molecules are capable of absorbing infrared radiation in the range of 4000 cm^{-1} to 400 cm^{-1}, domain between visible and microwave region. The corresponding amount of energy initiates transitions between vibrational states within the molecules[43].

The harmonic oscillator model is employed to model molecular vibrations and rotations. The vibration frequency is given by Hooke's law:

$$\nu = \frac{1}{2\Pi}\sqrt{\frac{k}{\mu}}$$

Where μ is the reduced mass of the vibrating atoms, calculated as:

$$\mu = \frac{m1 * m2}{m1 + m2}$$

With m1 and m2 being the masses of the vibrating atoms.

Thus, $\bar{\upsilon} = \frac{1}{2\pi c}\sqrt{\frac{k}{\mu}}$

b. X-ray diffraction.

X-rays were discovered in 1895 by W.C. Röentgen[44], leading to three major uses in, X-ray radiography (for creating images of light-opaque materials), X-ray crystallography (for discovering information about the structure of crystalline materials), and X-ray fluorescence spectrometry (to determine amounts of particular elements in materials)[9].

X-rays are electromagnetic waves with associated waves lengths ranging from 0.01nm to 10nm, corresponding to the energies in the range from 0.125 to 125keV. X-ray diffraction is a widely used analytical technique for characterizing materials. It is a versatile and non-destructive technique for analyzing the properties of a material like phase composition, structure, texture among others. X-ray crystallography and XRPD are the two principal applications of x-ray diffraction[19].

X-ray powder diffraction (XRPD) is a technique using X-ray diffraction that allows characterization the crystalline properties of materials in powder form. The technique is also applied widely for studying particles in liquid suspensions or polycrystalline solids (bulk or thin film materials). The diffraction pattern gives many discrete diffraction peaks, where useful information such as the position, the intensity, the shape of peaks, and the peak intensity distribution can be determined.

Principe of powder X-ray diffraction.

A coherent beam of monochromatic X-rays is produced by Striking a pure anode of a particular metal with high-energy electrons in a sealed vacuum tube. The radiation produced in the tube includes Kα1, Kα2, and Kβ as the highest energy X-rays. The Kβ radiation is removed by use of a filter **Table I. *9*** or a monochromator, and the Kα2 radiation can be removed from the X-ray data electronically during data processing[45].

The parallel beam of X-rays is directed at the powdered sample. Interaction of X-rays with sample creates secondary "diffracted" beams of X-rays, **Figure I. *16*** related to interplanar spacings in the crystalline powder according to a mathematical relation called "Bragg's Law":

$$n\lambda = 2\mathrm{d}(hkl)\sin\theta$$

where n is an integer

λ is the wavelength of the X-rays

d is the interplanar spacing generating the diffraction and

θ is the diffraction angle.

By recording the detected intensity as a function of the angle between the incident ray and the diffracted beam, a powder diffractogram is obtained[46].

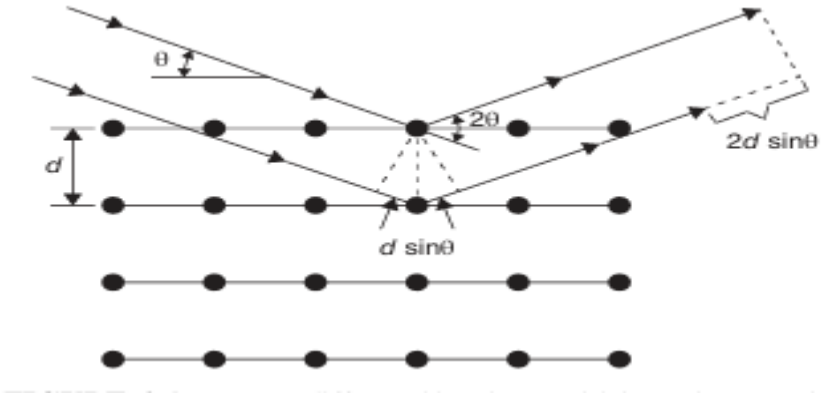

Figure I. 16 Reflection of X-rays by reticular planes

Table I. 9 XRD wavelengths and attenuation filters for Kβ radiations (source: ICDD)

Anode	Wavelength (Å)			Kβ-filter
	Kα1	Kα2	Kβ	
Cr	2.28970	2.29361	2.08487	V
Fe	1.93604	1.93998	1.75661	Mn
Co	1.78897	1.79285	1.62079	Fe
Cu	1.54056	1.54439	1.39222	Ni
Mo	0.70930	0.71359	0.63229	Zr

The Powder diffractogram

The powder diffractogram displays scattered intensities versus the Bragg angle (2θ) with a number of peaks characterized by their position, intensity and profile. These three fundamental parameters are the source of all information in powder XRD. The peak position gives information on lattice parameters and qualitative phase analysis, the intensity for quantitative analysis and crystal structure, and peak profile gives information about crystallites sizes[47].

The diffraction intensity is determined by the position of atoms on the lattice plane and sample presentation (particle size and orientation). Spinning the sample may help increase the number of crystallites that contribute to the measured diffraction pattern. The shapes of diffraction peaks are usually by sample quality and instrumental parameters. Small particle size and poor crystallinity may result in broad peak shape and non-monochromatic radiation exhibit asymmetrical shapes[48].

c. Thermal analysis

For decades, thermal analysis has been widely used in the scientific community to characterize materials or substances. Thermal analysis covers a group of techniques in which the physical or

chemical property of a substance is continuously measured as a function of temperature(or time) while subjected to a controlled temperature program[49].

When matter is heated, it undergoes physical and chemical changes over a wide range of temperature. Physical changes include, phase change (melting, vaporization, crystallization and transition between crystal structures), volume changes (expansion and contraction) and changes in mechanical behavior, while chemical changes include oxidation, corrosion, decomposition, dehydration among others.

Thermal analysis is used for qualitative and quantitative analysis and can be applied to various sorts of substances, be solid, liquid, or gel. It is necessary to determine the suitability of materials for specific applications and what temperature ranges they can withstand without changing[50].

Thermogravimetric analysis.

Thermogravimetric analysis is used to detect any physical or chemical transitions accompanied by a change in weight (gain/loss) as the sample is subjected to controlled heating.

Principle of TGA

In TGA, the sample is heated in the furnace at a controlled rate in a given environment (air, N_2, CO_2, He, Ar, etc.). For a known initial weight of the sample, the temperature is increased at a constant rate and the changes in weight of the sample are recorded as a function of temperature at different time intervals. This function defined the thermogravimetric curve. The change in weight gives information on, changes in sample composition, thermal stability and kinetic parameters for chemical reactions in the sample. The phenomena causing weight changes include gas adsorption/desorption, phase transition, decomposition, gas reactions among others[51].

Applications of TGA

- TGA allows evaluation of boiling, condensation, melting, crystallization, vaporization, decomposition, dehydration, oxidation/reduction and crystal lattice destruction phenomena in artificial and natural organic and inorganic compounds.
- Characterization of thermal stability, material purity and determination of humidity.
- Examination of corrosion studies, kinetic and gasification processes.

PART II: EXPERIMENTAL SECTION.

II.1 Introduction.

This part is about the experiments we performed with the aim of synthesizing coordination polymers from rare earth metals and organic dicarboxylic acids. All experiments were carried out from the university research laboratory LPCMC (Laboratoire de Physico-Chimie des Matériaux et Catalyse). The laboratory materials and chemicals used are given in this section. It also includes the results and discussions.

All IR spectra were recorded with PerkinElmer Spectrum Two FT-IR spectrometer in 4000 to 400cm^{-1} domain and the diffractograms were recorded with Rigaku MiniFlex diffractometer from 5^{o} to 60^{o} with copper anticathode as source of X-rays. The thermostability of one compound was investigated using LabsysEvo-gas option-TG-DSC 1600°C (SETARAM) in Argon environment from 27^{o}C to 700^{o}C.

The phase purity of the samples was determined by comparing the powder XRD patterns with the simulated ones obtained from single crystal X-ray diffraction data using the Mercury software.

II.2 Materials and reactants used for synthesis and characterization.

I. Laboratory materials.

The equipment used for synthesis and characterization of our compounds are shown in the figures below.

Analytical balance
Used to measure the mass of the reagents (±0,0001 precision).

Magnetic stirrer
Used for homogenization of mixtures. Also used during synthesis at room temperature.

The pH meter ((±0.01 precision).

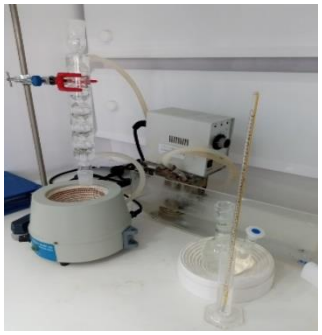

Set-up for reflux synthesis.

The oven used for hydro/solvothermal synthesis.

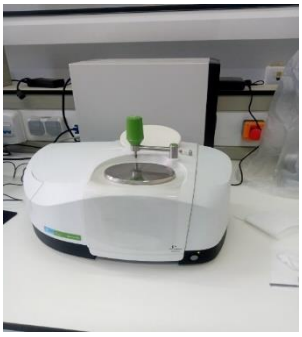

PerkinElmer Spectrum Two Spectrometer for IR spectroscopy analysis.

Thermogravimetric analyzer: LabsysEvo-gas option-TG-DSC 1600 °C (SETARAM),

Rigaku MiniFlex Powder XRD diffractometer.

II. Laboratory chemicals.

❖ Precursor.

Different lanthanoid precursors were used to provide metal ions necessary to prepare coordination polymers. We took interest in the coordination polymers of lanthanum (III) ions. These were obtained from lanthanoid compounds (oxide, chloride, and nitrates).

Compound	Molar mass ($gmol^{-1}$)	Solubility in water
La_2O_3	325.81	Insoluble
$LaCl_3.6H_2O$	353.36	957 g/L (25 °C)
$La(NO_3)_3.6H_2O$	433.01	Highly soluble
$Y(NO_3)_3.6H_2O$	182.22	Highly soluble

❖ Ligands.

a) Aliphatic ligands

Five aliphatic dicarboxylic acids were used in different experiments for synthesis of coordination polymers with mixed ligands **Table II. *1***. These dicarboxylic ligands have carboxylic groups at extreme ends of the aliphatic carbon chain with variation in the length of the chain. The presences of two carboxylic groups allows coordination entities to extend in both directions giving rise to

compounds with infinite structure length and with repeated units (also known as coordination polymers).

Table II. 1 Aliphatic dicarboxylic acids.

Flexible ligands			
Name	**Empirical formula**	**Molar mass ($g \cdot mol^{-1}$)**	**structure**. (source: Wikipedia)
Malonic acid denoted (mal)	$C_3H_4O_4$	104.061	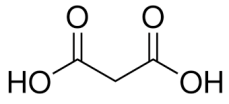
Succinic acid denoted (suc)	$C_4H_6O_4$	118.088	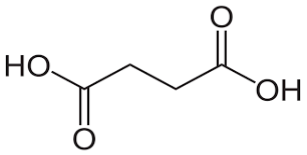
Glutaric acid denoted (glu)	$C_5H_8O_4$	132.12	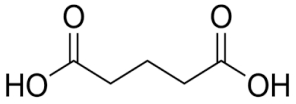
Adipic acid denoted (adi)	$C_6H_{10}O_4$	146.142	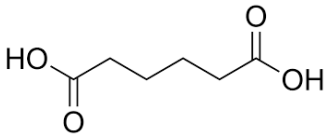
Rigid ligand			
Name	**Empirical formula**	**Molar mass ($g \cdot mol^{-1}$)**	**structure**. (source: Wikipedia)
Fumaric acid denoted (fum)	$C_4H_4O_4$	116.072	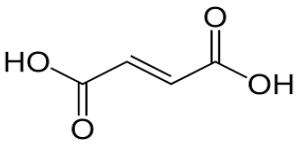

The IR spectra of aliphatic ligands.

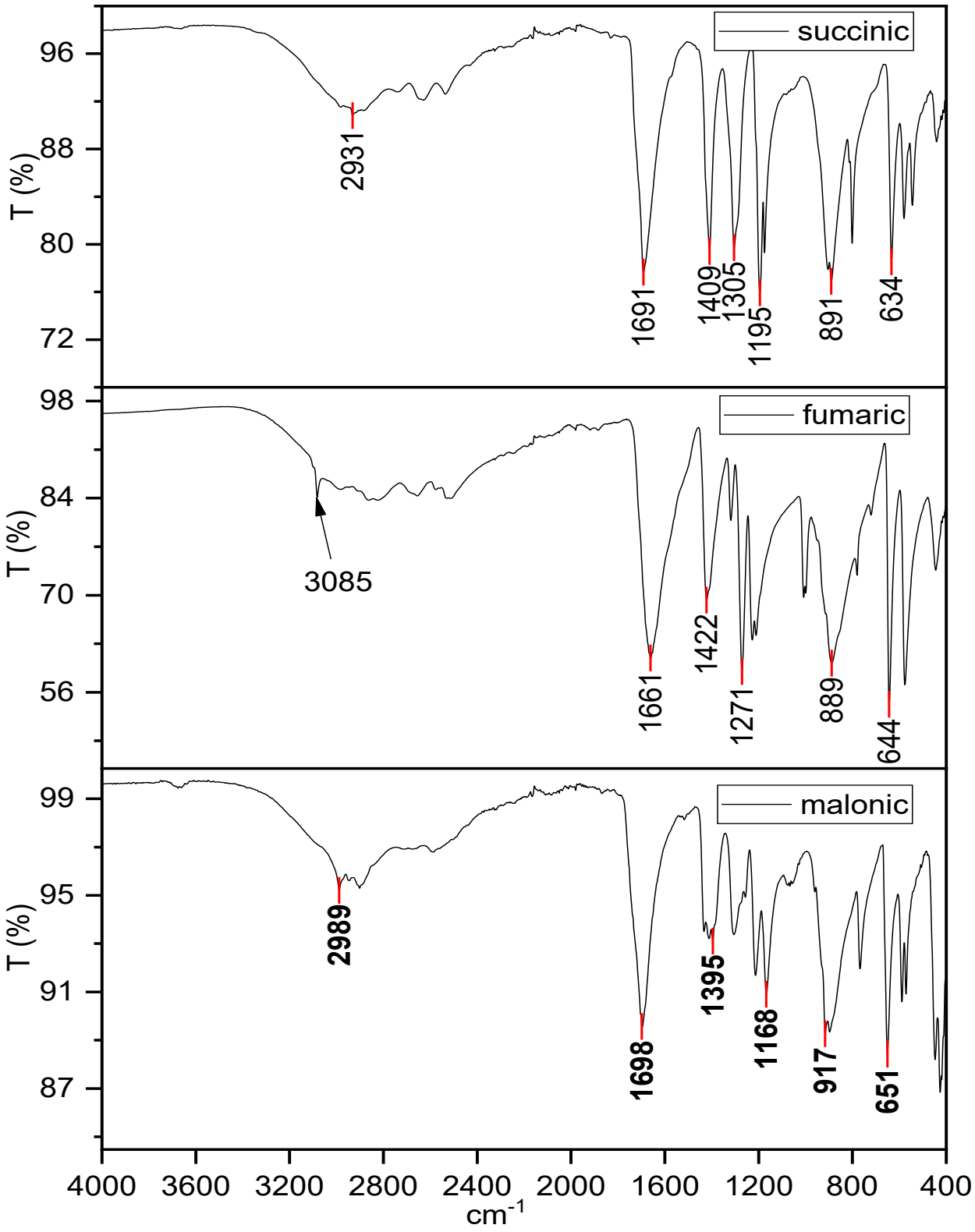

Figure II. 1 The IR spectra of succinic, fumaric and malonic acids.

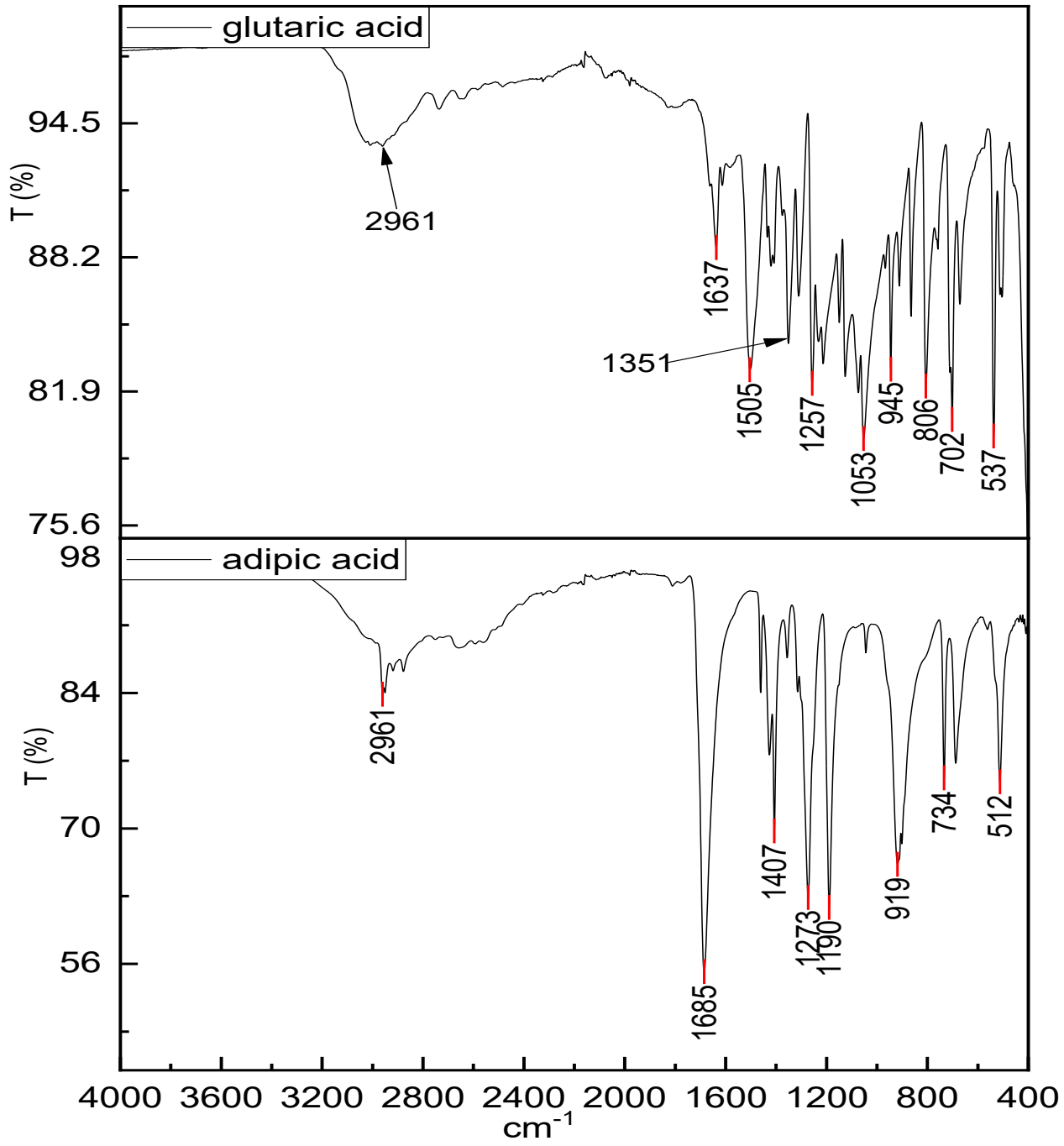

Figure II. 2 The IR spectra of glutaric acid and adipic acid.

The IR spectra of the aliphatic ligands show common bands for carboxylic acids. Large broad bands in the region 3100-2500cm^{-1} characteristic of O-H vibrations of protonated carboxylic acid. Intense vibration bands for C=O groups around 1680cm^{-1} and C-O around 1270cm^{-1}. Bands around 1400cm^{-1} are attributed to O-H in-plane bending and around 900cm^{-1} for O-H out-of-plane distortions [52, 53].

b) Rigid aromatic ligands

Benzene dicarboxylic acids have been used to synthesize coordination polymers. Their structures and rigidity exhibit interesting features in coordination chemistry. The existence of two carboxylic groups allows structure growth, and rigidity for stability.

Table II. 2 Benzene dicarboxylic acids.

Name	**Chemical formula**	**Molar mass (g/mol)**	**Structure**. (source: Wikipedia)
Phthalic acid (Benzene-1,2-dicarboxylic acid) denoted as ligand (**ph**)	$C_8H_6O_4$	166.132	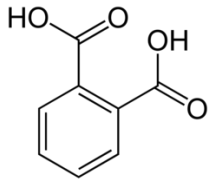
Isophthalic acid (Benzene-1,3-dicarboxylic acid) denoted as ligand (**iph**)	$C_8H_6O_4$	166.132	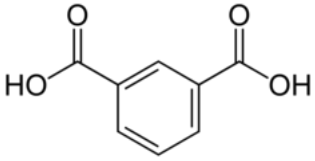
Terephthalic acid (Benzene-1,4-dicarboxylic acid) denoted as ligand (**tph**)	$C_8H_6O_4$	166.132	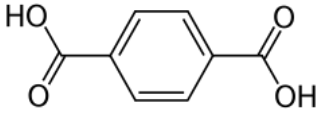

IR spectra of rigid aromatic ligands.

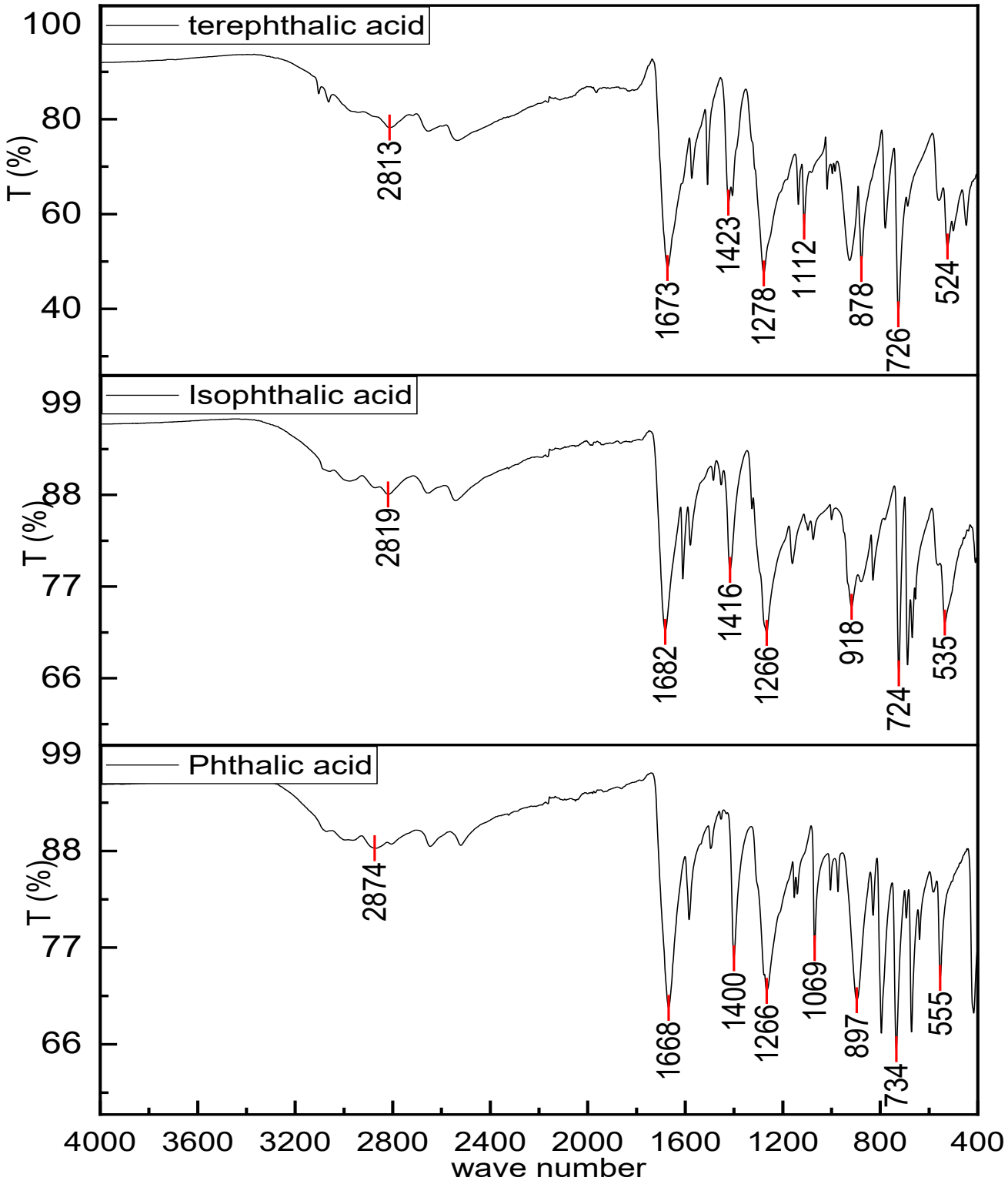

Figure II. 3 IR spectra for rigid aromatic ligands (ph, iph, and tph).

The three acids have almost similar IR spectra with differences in the region around 720cm^{-1}. The peaks in this region are characteristic of the nature of substitution of the carboxyl groups on the aromantic ring [54]. Hence, these acids (ph, iph, and tph) are referred to as position isomers.

- The broad peak in the region 3000cm^{-1} - 2500cm^{-1} is characteristic of the O-H stretch of the COOH group.
- The intense peaks in the region 1720cm^{-1} to 1660cm^{-1} are characteristic of the carbonyl (C=O) group of the acid.
- The peaks around 1580cm^{-1} correspond to aromatic C=C vibrations (stretching).
- The peaks around 1400cm^{-1} correspond to in-plane O-H vibrations and peaks around 900cm^{-1} are characteristic of the O-H out-of-plane vibrations.
- The intense peaks around 1265cm^{-1} correspond to carboxylic C-O stretching vibrations.
- Fine and intense peaks around 720cm^{-1} are typical for C-H out-of-plane bending and define the nature of ring substitution.
- The peak in the region 520cm^{-1} - 560cm^{-1} correspond to C-C vibrations of the ring (ring deformation).

II.3 Synthesis, characterization and discussions.

a. Manipulation I.

In this manipulation, we are interested in synthesizing lanthanoid coordination polymers with a single ligand.

Synthesis protocol.

- System Ln/tph. Reaction mole ratio: Ln/tph: 1/1.5

We mixed 0.1g of $LaCl_3.6H_2O$ and 0.0705g of tph in 10ml of bi-distilled water and stirred constantly for 30 minutes. The pH of the solution is adjusted to 5.18 with NaOH (1M) and the solution is transferred to the autoclave and heat at 170^{0}C for 48hrs. The oven is then cooled at 10^{0}C/hr. to 40^{0}C and the solution is removed and filtered. The filtrate is place in the oven at 40^{o}C to facilitate the evaporation process.

- System Ln/iph. Reaction mole ratio: Ln/iph: 1/1.5.

The protocol is the same as for Ln/tph system above, replacing tph with iph and the solvent with a mixture bi-distilled water/methanol (3/7, v/v).

Results and discussion.

a) System Ln/tph:

Characterization by IR spectroscopy

The IR spectrum of the compound was recorded and compared to that of acid terephthalic (tph). The two spectra can be superimposed which indicates precipitation of acid terephthalic. There was no reaction between the metal (La^{3+}) and the ligand (tph).

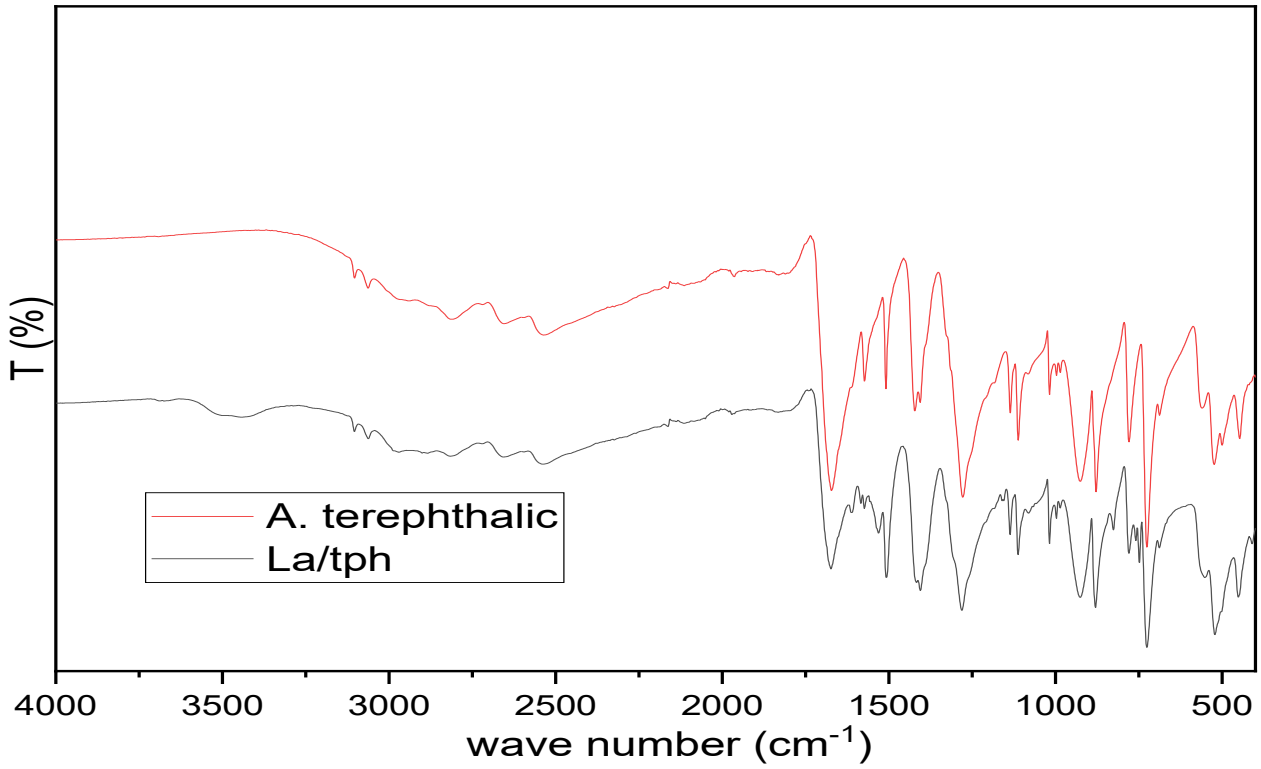

Figure II. 4 The IR spectrum of system Ln/tph.

b) System Ln/iph.

This system yielded two different compounds **cp 1** and **cp 2.** Compound cp 1 was obtained as a residue after hydrothermal heating while cp 2 was obtained as residue after evaporation.

Characterization by IR spectroscopy

The IR spectra of the two compounds obtained (cp 1 and cp 2) are shown in **Figure II. 5**. The two spectra are different from that of acid isophthalic (iph).

The broad-intense band at 3340cm^{-1} for cp 1 and 3344cm^{-1} for cp 2, correspond to O-H stretching of water molecules. The sharp and intense bands at 1604 cm^{-1} and 1541 cm^{-1} for cp 1, 1677 cm^{-1} for cp 2 correspond to asymmetric stretching of OCO and the bands at 1376 cm^{-1} for cp 1 and 1435 cm^{-1} for cp 2 correspond to symmetric OCO stretching [55].

The band at 1296 cm^{-1} for cp 2 is ascribed to C-O stretching of the free COOH group, also characterized by a sharp band at 1731 cm^{-1} due to C=O stretching [56].

The band at 730 cm^{-1} for cp 1 and 724 cm^{-1} for cp 2 are characteristic of aromatic C-H out-of-plane bending. The weak bands at 514cm^{-1} for cp 1 and 483cm^{-1} for cp 2 are attributed to Ln-O bond vibrations. The weak band of cp 1 at 2988cm^{-1} may be assigned to C-H stretching of solvent molecules (methanol).

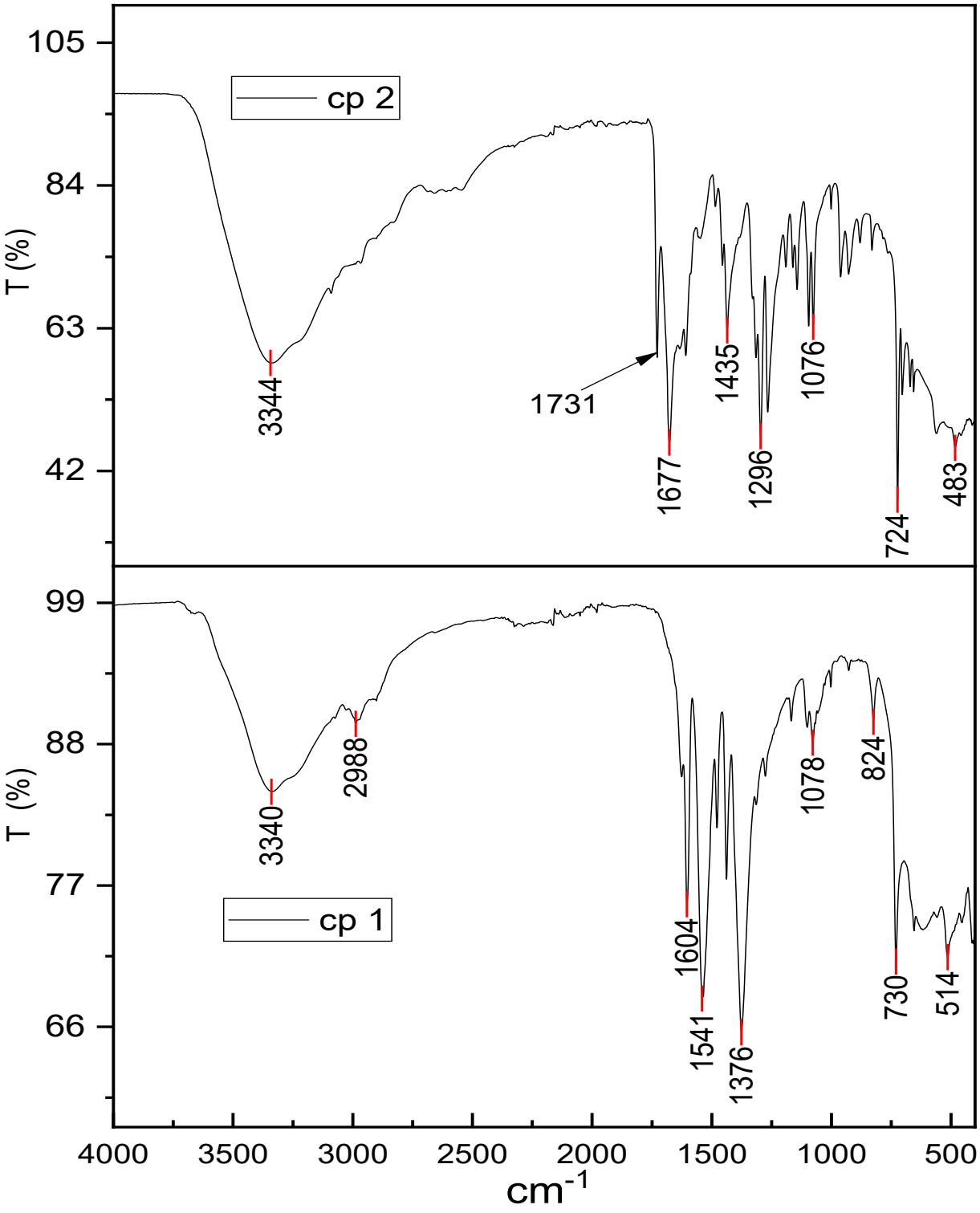

Figure II. 5 IR spectra of compounds of system Ln/iph.

Characterization by powder XRD

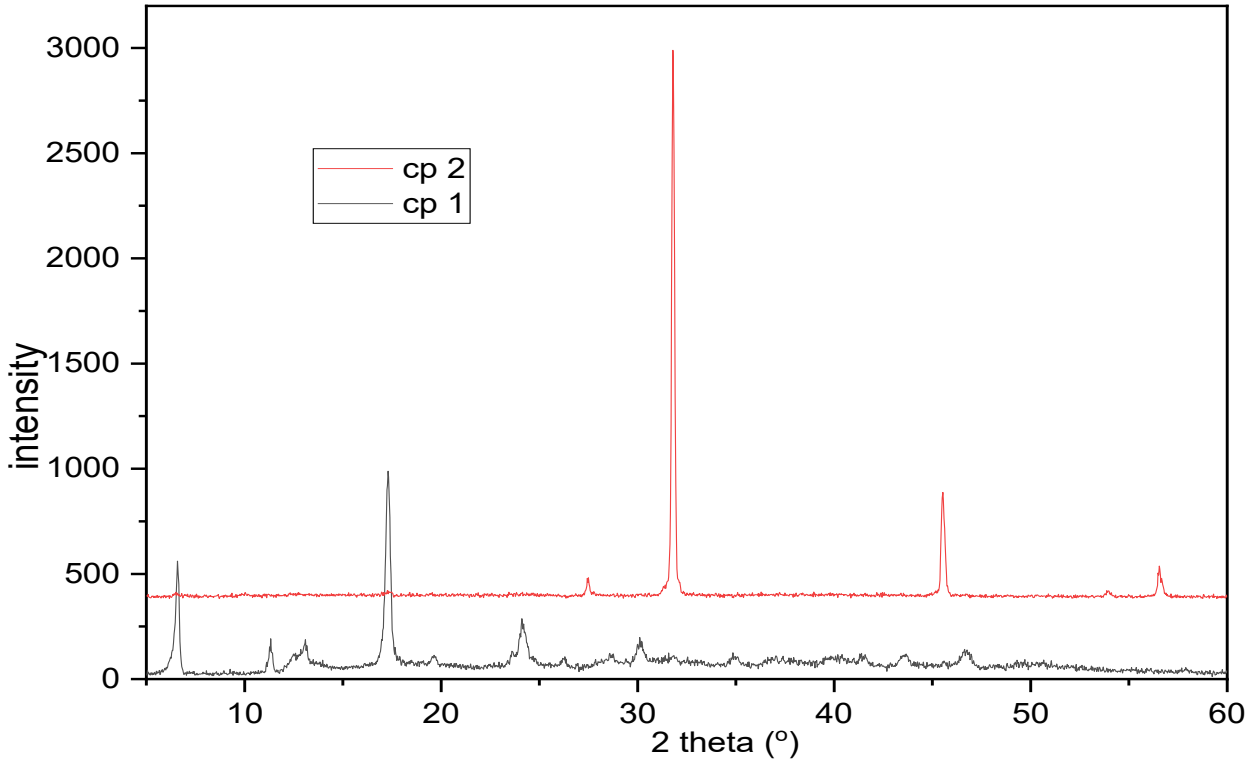

Figure II. 6 powder X-ray diffractograms of compounds of system Ln/iph.

The diffractograms of cp 1 and cp 2 are different as shown above ***Figure II. 6***. This confirms that the two compounds obtained are very different.

The diffractograms were compared with those generated from lanthanoid/isophthalate structures from the CCDC database [57-71], and we did not find a match. This means our compounds could have not been reported before and therefore new.

Conclusion

The IR bands characteristic of COOH group observed for cp 2 indicates that iph is partially deprotonated and we therefore think that our compound is of type $[Ln_x(Hiph)_y(H_2O)_z].p(H_2O)$. The difference ν_{as}-ν_s is 242cm^{-1} which is greater than 200, this suggests monodentate coordination mode.

The absence of bands in the region 1720-1680cm^{-1} for cp 1 indicates that iph is completely deprotonated. The difference between asymmetric and symmetric COO^- vibrations is 228cm^{-1} and 165cm^{-1} which indicates both monodentate and bridging coordination modes [71]. We think, this compound could be of type $[Ln_x(iph)_y(H_2O)_z]_n.pCH_3OH$.

The exact structure can be obtained by optimizing synthesis parameters to obtain single crystals for single crystal XRD technique.

b. Manipulation II

Synthesis protocol.

A number of experiments were carried out with the aim of synthesizing coordination polymers with lanthanum and mixed ligands (rigid + flexible). Three series of experiments, with each series involving lanthanum salt, a fixed ligand (ph, iph or tph) and flexible ligand (mal, fum, suc, glu or adi) were performed with the reaction mole ratio of 2/1.5/1.5 respectively. Taking the mass of lanthanum salt ($LaCl_3.6H_2O$) equal to 0.2g. The composition and reaction conditions are tabled below.

Reaction conditions for various experiments, w (water), w/m (water/methanol)

Serie	Rigid ligand	Flexible ligand	Solvent (ml)	pH	Method	Time (hours)	T (°C)
A	Acid phthalic	mal	w (25)	3.33	Under stirring	02	Ambient
		fum	w (50)	4.00	Reflux	03	70-80
		suc	w(30)	3.88	Under stirring	19	Ambient
		glu	w (30)	4.02	Under stirring	20	Ambient
		adi	w (30)	4.00	Under stirring	20	Ambient
B	Acid terephthalic	mal	w (50)	5.20	Reflux	03	70-80
		fum	w(50)	2.87	Reflux	03	70-80
		suc	w (50)	4.17	Reflux	03	70-80
		glu	w (50)	4.33	Reflux	03	70-80
		adi	w (50)	4.12	Reflux	03	70-80
C	Acid isophthalic	mal	w/m (25/25)	3.08	Reflux	03	70-80
		fum	w/m (25/25)	2.93	Reflux	03	70-80
		suc	w/m (25/25)	3.84	Reflux	03	70-80
		glu	w/m (25/25)	3.53	Reflux	03	70-80
		adi	w/m (25/25)	3.72	Reflux	03	70-80

The under stirring method involved mixing metal salts and the ligands in a solvent and continuously stirring the mixture (in a beaker covered with paraffin film) with a magnetic stirrer at room temperature. Then leaving the solution undisturbed in the oven set at 40°C, allowing the

solvent to slowly evaporate, leading to gradual crystal formation or precipitation of the coordination polymer.

Reflux synthesis involves heating a reaction mixture while continually condensing the vapor back into the liquid form. This is done using a condenser mounted vertically above the reaction flask. The condensed vapors return to the reaction vessel, allowing the reaction to proceed at a constant temperature without loss of material.

Results and discussion.

a) Serie A.

i. System Ln-ph-mal.

We obtained two compounds with this system which gave different IR spectra as shown in **Figure II.** *7*. Ln-ph-mal_1 was obtained from a precipitate formed during stirring process at room temperature while Ln-ph-mal_2 was obtained as residue from the filtrate after evaporation.

For Ln-ph-mal_1, the broad short peak at 3331cm^{-1} is ascribed to ν(O-H) of water molecules. The bands for $\nu_{as}(COO^-)$ at 1585cm^{-1}, 1533cm^{-1} and $\nu_s(COO^-)$ at 1369cm^{-1}. The sharp peak at 712 cm^{-1} is attributed to aromatic out-of-plane C-H vibrations.

The IR spectrum of Ln-ph-mal_2 shows a very strong band at 3289cm^{-1} which is attributed to ν(OH) of water molecules. The bands for asymmetric and symmetric vibrations are located at 1526cm^{-1} and 1362cm^{-1} respectively. The bands around 550cm^{-1} can be assigned to Ln-O bond vibrations.

Conclusion

The presence of asymmetric and symmetric COO^- bands confirms coordination of the ligands to metal center (Ln). The Δν values for Ln-ph-mal_1 (216, 164 cm^{-1}) indicates co-existence of monodentate and bridging coordination modes and for Ln-ph-mal_2 (164 cm^{-1}) refers bridging mode.

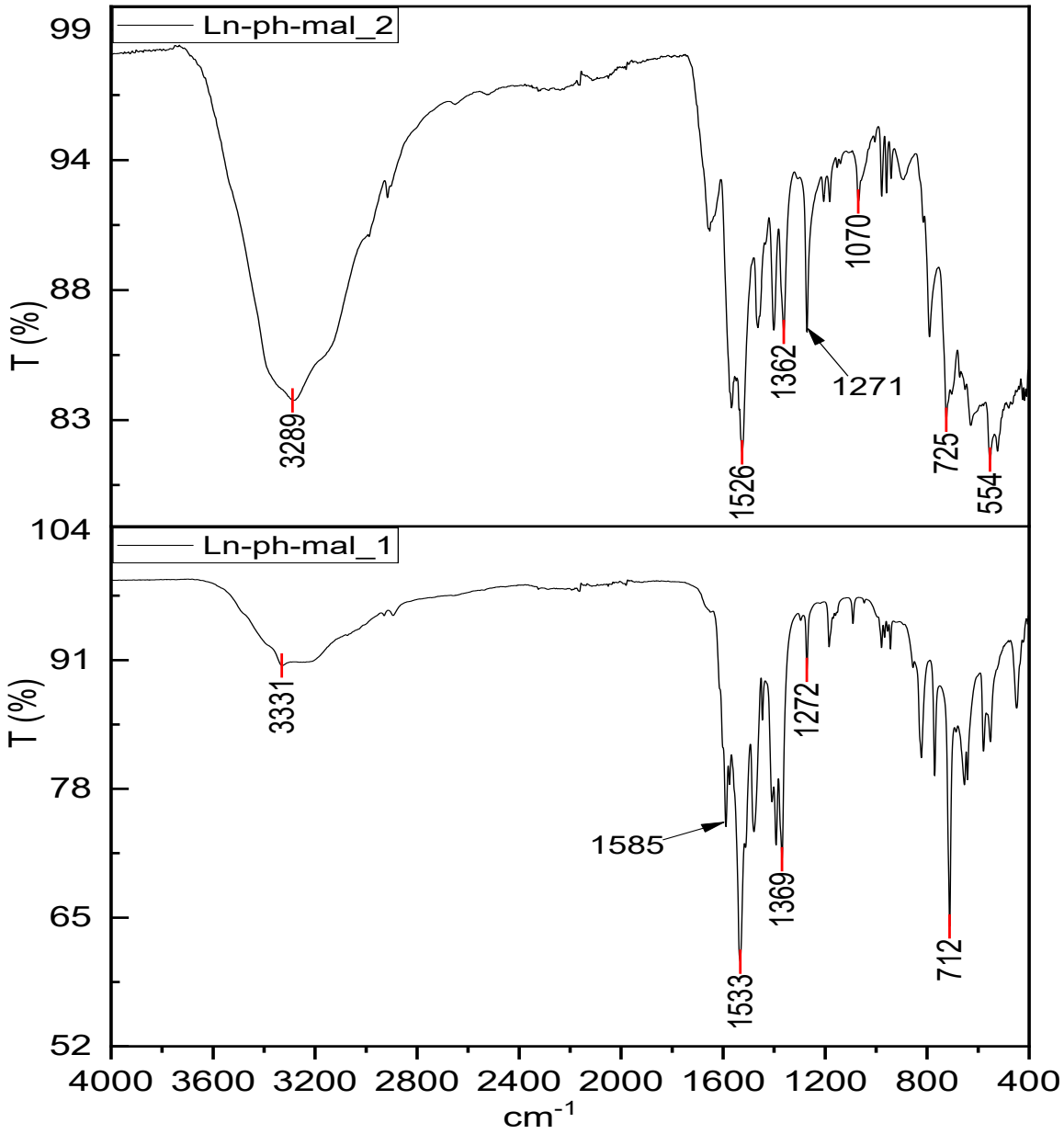

Figure II. 7 IR spectra of compounds of Ln-ph-mal system.

The X-ray diffractograms for the compounds of Ln-ph-mal system are shown in **Figure II. *8***. The diffractograms are different which confirms two different compounds.

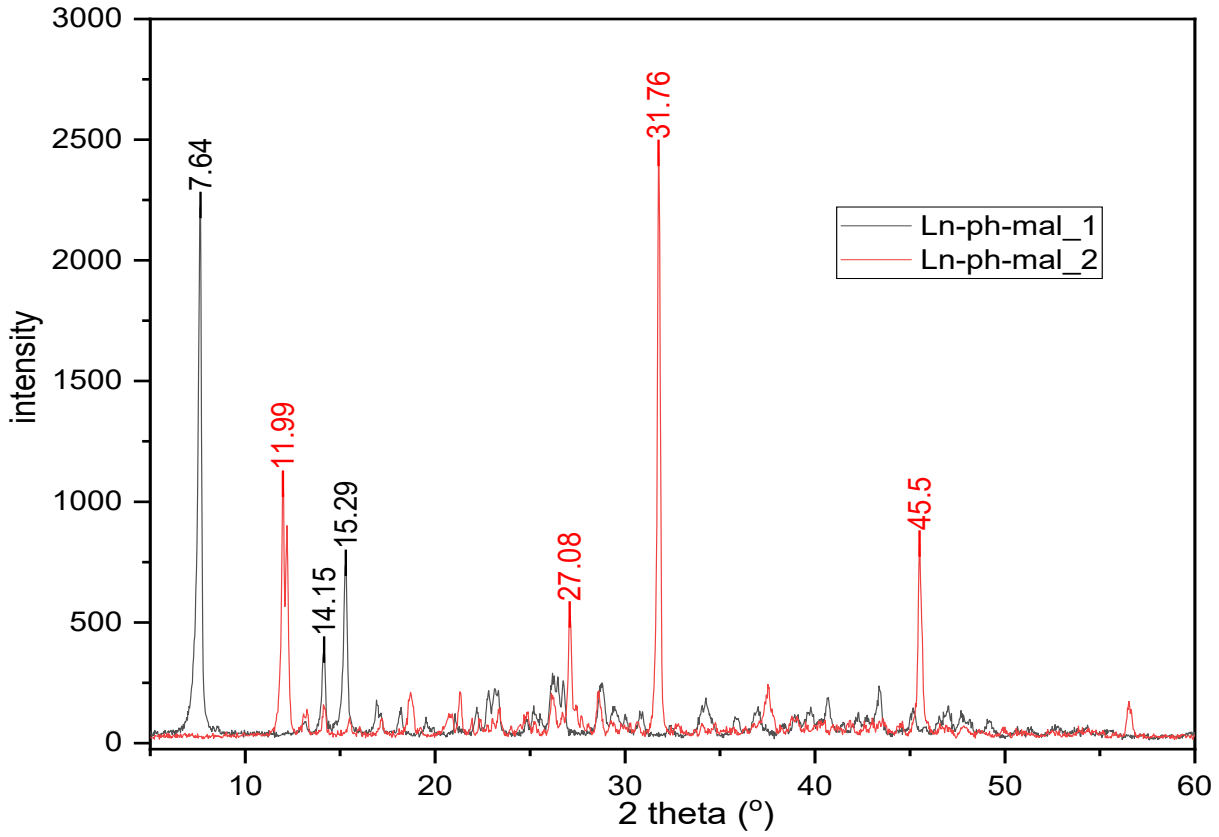

Figure II. 8 The X-ray diffractograms of Ln-ph-mal compounds.

These diffractograms were compared to diffractograms of structure reported with Ln/ph [73-80], and Ln/mal [54, 81-98] systems. No structures of Ln/ph/mal system were found from the CCDC database. By comparison, no matching diffractograms were found which indicates that our compounds could have not been published before.

ii. System Ln-ph-suc

With this system, we could not obtain sufficient quantity for characterization. Very tiny crystals were left upon evaporation.

iii. System Ln-ph-fum.

The IR spectrum of the compound obtained ***Figure II. 9***, exhibits a broad short band at 3347cm^{-1} which corresponds to O-H stretching vibrations of water molecules. The strong bands at 1520 cm^{-1} and 1404cm^{-1} are assigned to asymmetric and symmetric COO^- vibrations respectively. The strong sharp band at 689cm^{-1} is assigned to C-H out-of-plane bending vibrations of ligand fum. Absence of bands in the region 1720 to 1680cm^{-1} signifies complete deprotonation of the ligand.

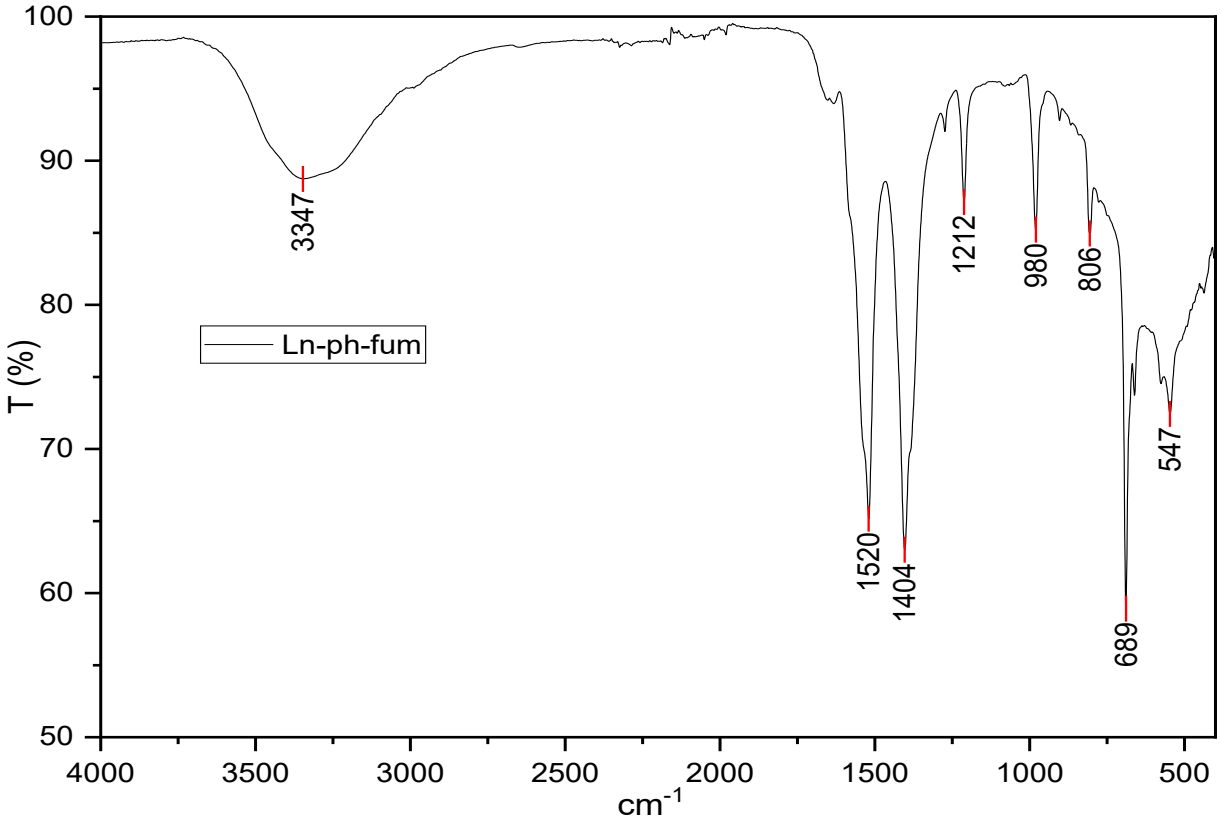

Figure II. 9 IR spectrum of a compound obtained with Ln-ph-fum system.

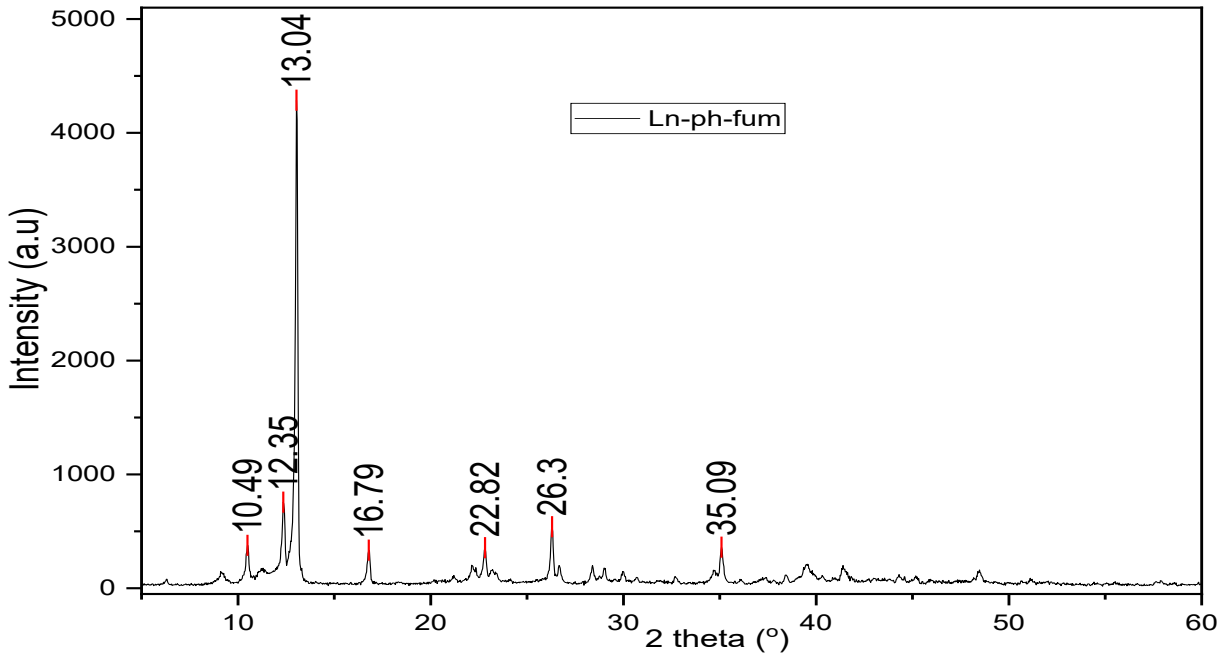

Figure II. 10 X-ray diffractogram of a compound obtained with Ln-ph-fum system.

The PXRD diffractogram of the compound is shown in ***Figure II. 10***. Comparing our diffractogram with those generated from articles with the same ligand (fum) [38, 99-122], we did not find a match. This suggests that our product could have not been synthesized or published before.

iv. Systems Ln-ph-glu and Ln-ph-adi.

The two systems Ln-ph-glut and Ln-ph-adi gave compounds with similar IR spectra **Figure II. *11*.** This indicates inclusion of a common ligand (ph) and absence of other ligands (glut and adi). The presence of ph in our compounds is confirmed by strong bands around 700cm^{-1} corresponding to out-of-plane aromatic C-H bending vibrations. The broad band at 3391cm^{-1} correspond to O-H stretching of water molecules. The bands for asymmetric and symmetric OCO vibrations are located at 1511cm^{-1} and 1418cm^{-1} respectively. The band at 442cm^{-1} is attributed to Ln-O bond vibrations.

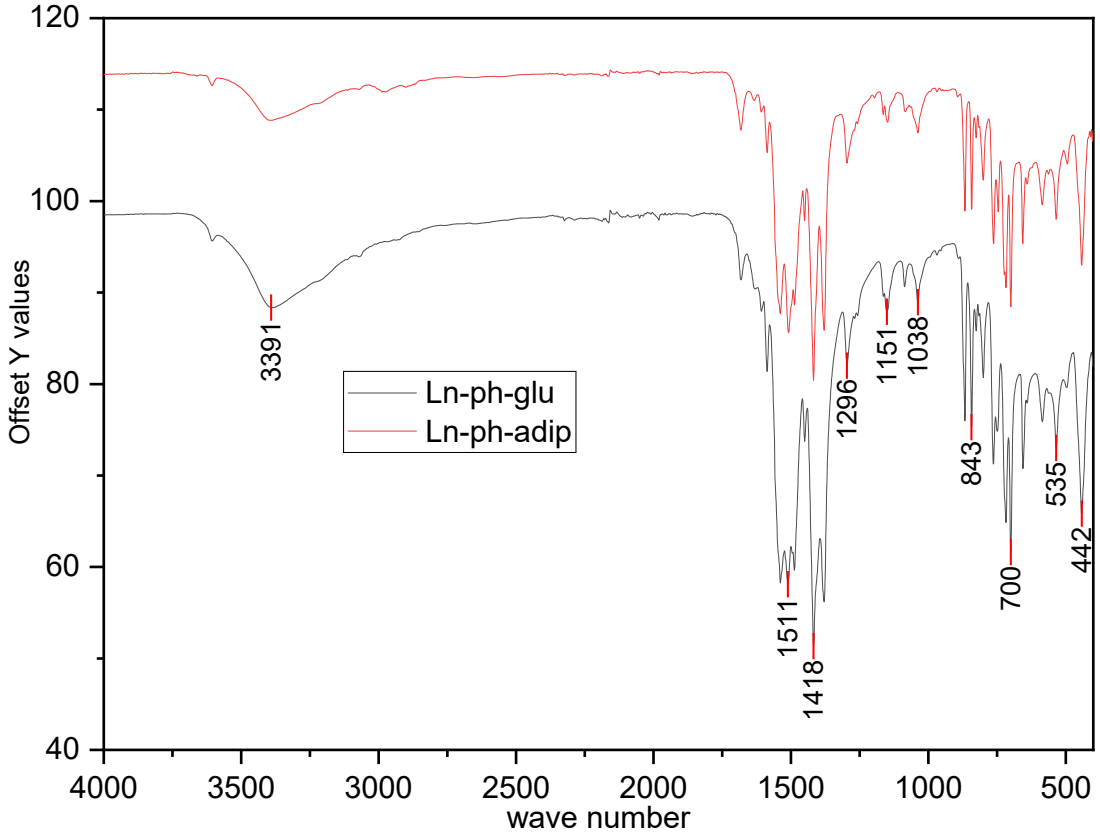

Figure II. 11 IR spectra of systems Ln-ph-glut and Ln-ph-adi.

The **Figure II. *12*** below show the X-ray diffractogram of Ln-ph-adi compound. The diffractogram does not match any of the published lanthanoid/phthalate structures [73-80] from the CCDC database. This indicates that the synthesized product is new.

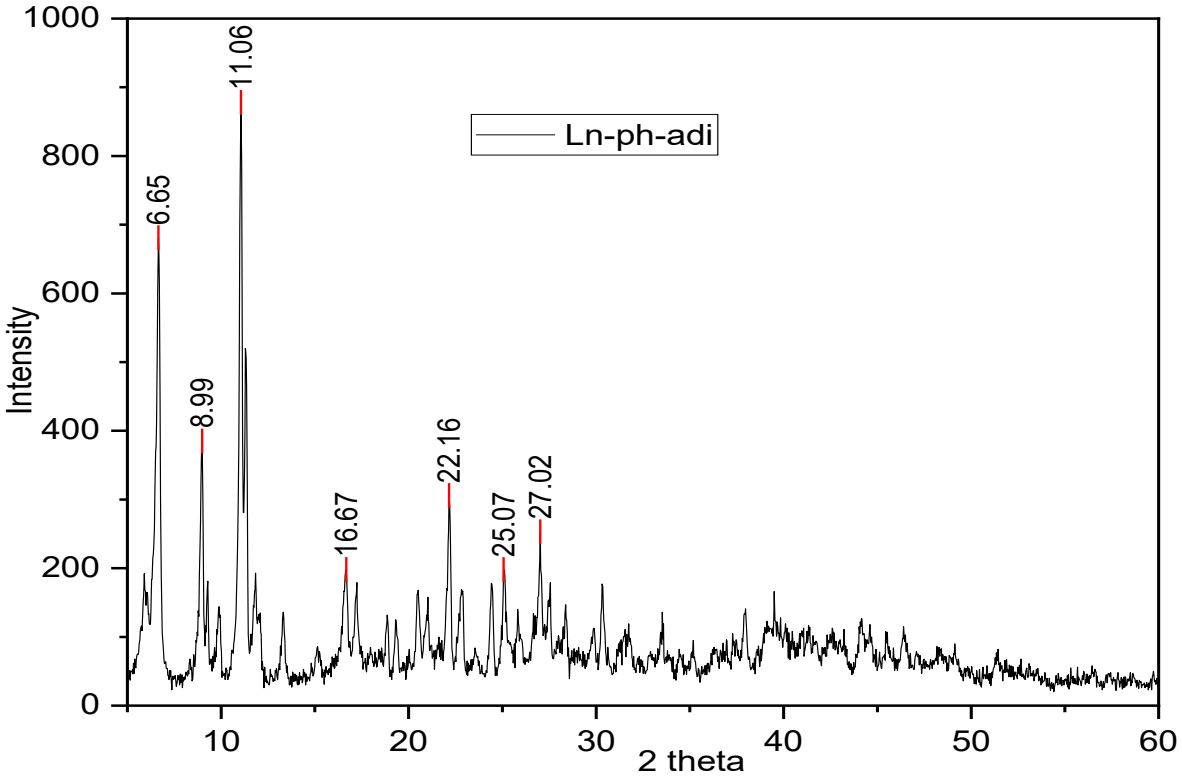

Figure II. 12 Ln-ph-adi Powder XRD diffractogram

b) Serie B.

i. System Ln-tph-mal

This system yielded two compounds Ln-tph-mal_1 and Ln-tph-mal_2.

Ln-tph-mal_1 was obtained as residue by filtration after heating under reflux while Ln-tph-mal_2 was obtained as a residue from the filtrate after evaporation. The IR spectra of the two compounds are shown in **Figure II.** ***13*** .

The characteristic bands of the two compounds are shown in the table below.

Table II. 3 Characteristic bands of Ln-tph-mal compounds.

Type of vibration	Peaks (cm^{-1})	
	Ln-tph-mal_1	Ln-tph-mal_2
ν(O-H) of water	3345	3279
ν(C-H)	none	2916
ν_{as}(OCO)	1602, 1545	1523
ν_{s}(OCO)	1361	1359
ν(C=C)	1474	1466
γ(C-H)	814, 707	700

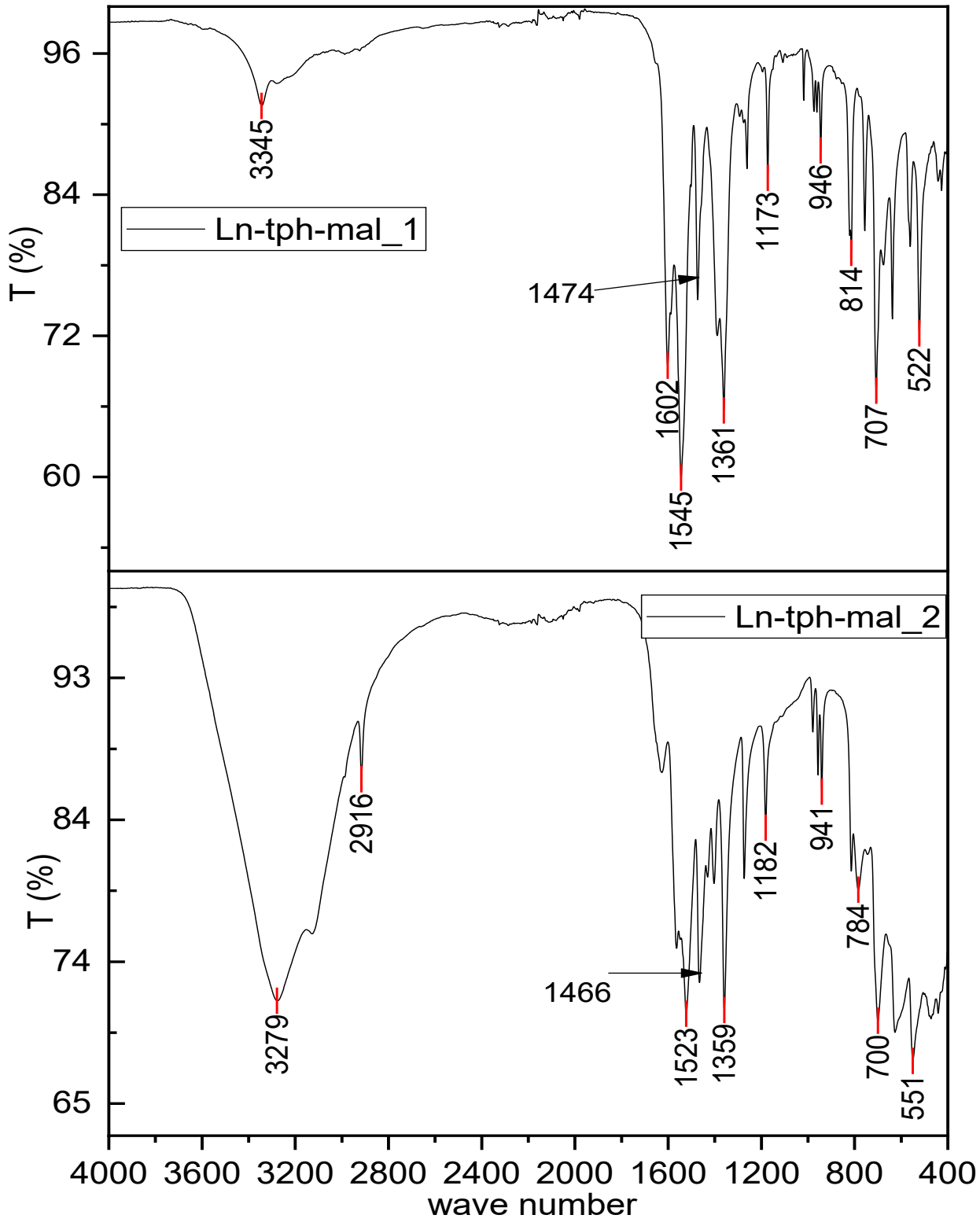

Figure II. 13 IR spectra of Ln-tph-mal compounds.

The ν(C-H) band at 2916cm^{-1} in the spectrum of Ln-tph-mal_2 corresponds to aliphatic -CH_2- which indicates the presence of ligand mal. We therefore think depending on IR spectroscopy that Ln-tph-mal_1 contains the Ln, tph, and water molecules while Ln-tph-mal_2 contains both ligands plus water molecules.

The powder XRD further confirms that the two compounds are different. **Figure II.** ***14***

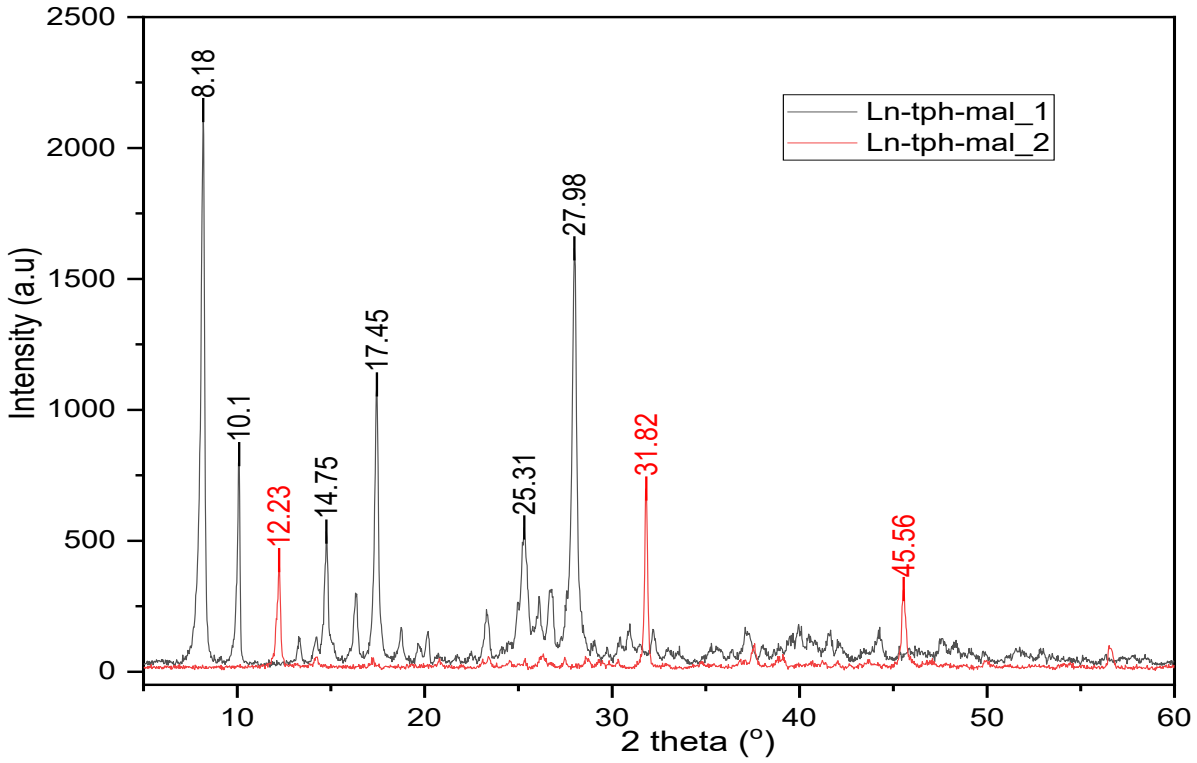

Figure II. 14 X-ray diffractograms of Ln-tph-mal compounds.

The diffractograms were compare to those simulated from reported structure with terephthalic acid [123-129] and malonic acid [54, 81-98] ligands and no match was found.

ii. System Ln-tph-fum

The IR spectrum of the compound obtained shows a broad band at 3435cm^{-1} assigned to O-H stretching vibrations of water molecules. The band at 2529cm^{-1} is attributed to O-H vibrations of hydrogen bonded -COOH groups.

The vibration bands for asymmetric COO^- are located at 1628cm^{-1} and 1515cm^{-1} while the symmetric COO^- bands are located at 1394cm^{-1} and 1294cm^{-1}. The sharp band at 983cm^{-1} can be assigned to the C–H wagging or C=C skeletal mode of fumarate.

The strong band at 688cm^{-1} is indicative of C-H out-of-plane bending. The band at 553cm^{-1} is assigned to Ln-O vibrations.

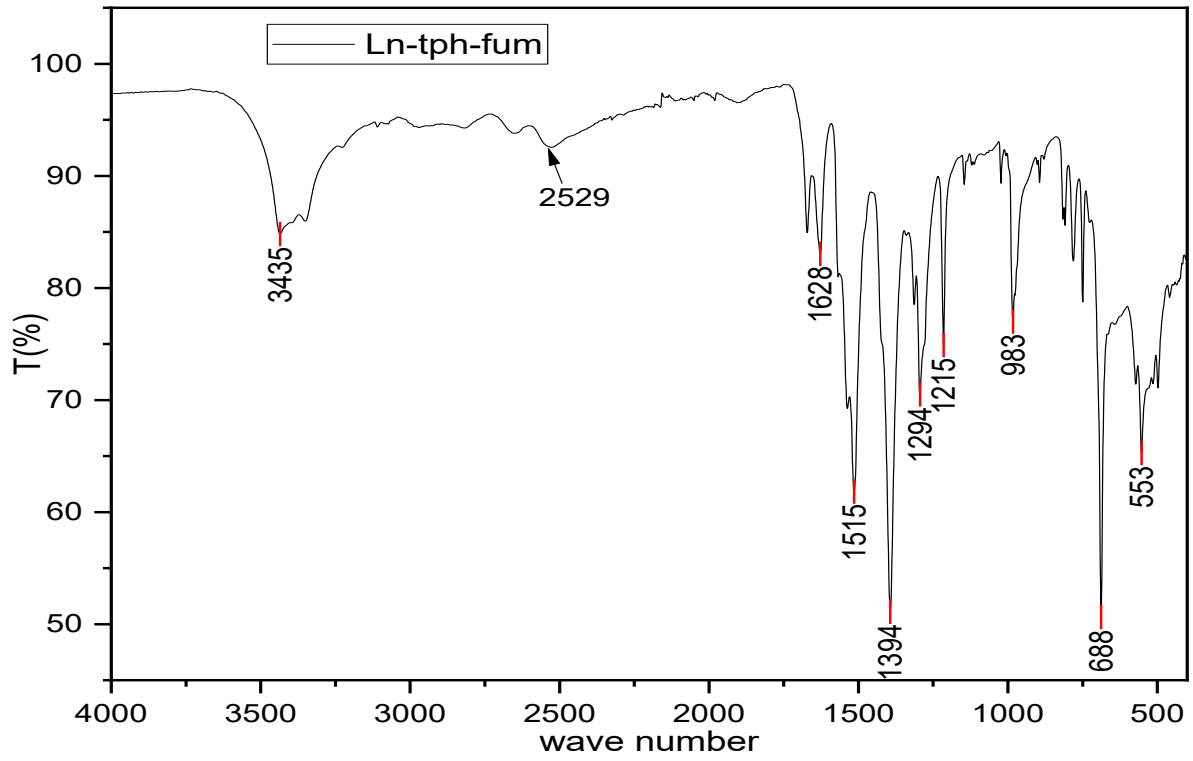

Figure II. 15 IR spectrum of Ln-tph-fum compound.

The PXRD diffractogram of Ln-tph-fum is given in **Figure II. *16***.

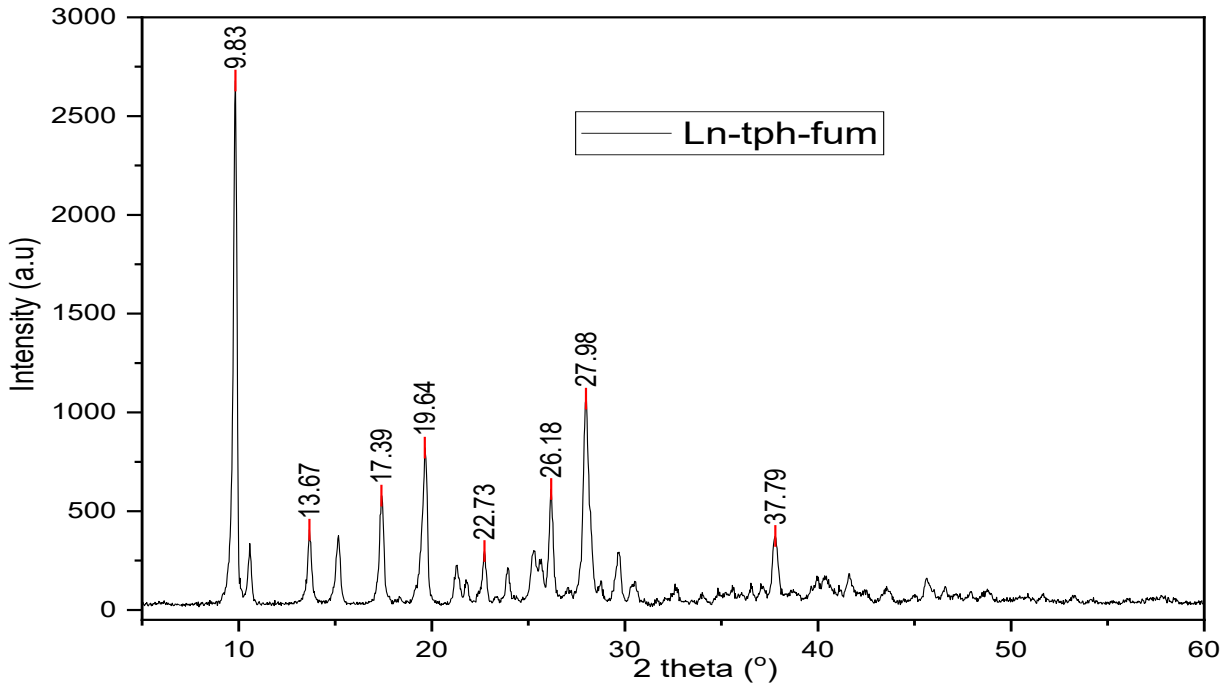

Figure II. 16 powder diffractogram of Ln-tph-fum compound

The diffractogram was compared to simulated diffractograms of reported Ln-tph-fum structures [102]. The positions of the peaks match closely with the ones simulated from $[Sm(fum)_{1.5}(H_2O)_2]\cdot 0.5(H_2tph)\cdot H_2O$ structure **Figure II. *17***. The difference observed maybe due to presence of different phases.

Conclusion

Basing on the IR data, there are no characteristic bands for aromatic CH deformation in the region 850 – 720cm^{-1}. We therefore, think that this compound contains only fum as ligand. The Δν between asymmetric and symmetric stretching vibrations indicate monodentate bridging modes.

The IR data of the reported structure $[Sm(fum)_{1.5}(H_2O)_2]\cdot 0.5(H_2tph)\cdot H_2O$ shows the bands at 3442w, 3112m, 2819m, 2654m, 2528m, 1887m, 1673m, 1633m, 1535s, 1401s, 1292s, 1216s, 987m, 816m, 779m, 749m, 689s, 554m, 526m of which the bands at 816, 779 and 749 cm^{-1} indicate presence of tph. The band at 2529cm^{-1} of our compound therefore signifies partial deprotonation of fum and we deduce that our compound is of form $[La(fum)_x(Hfum)_y(H_2O)_z].mH_2O$

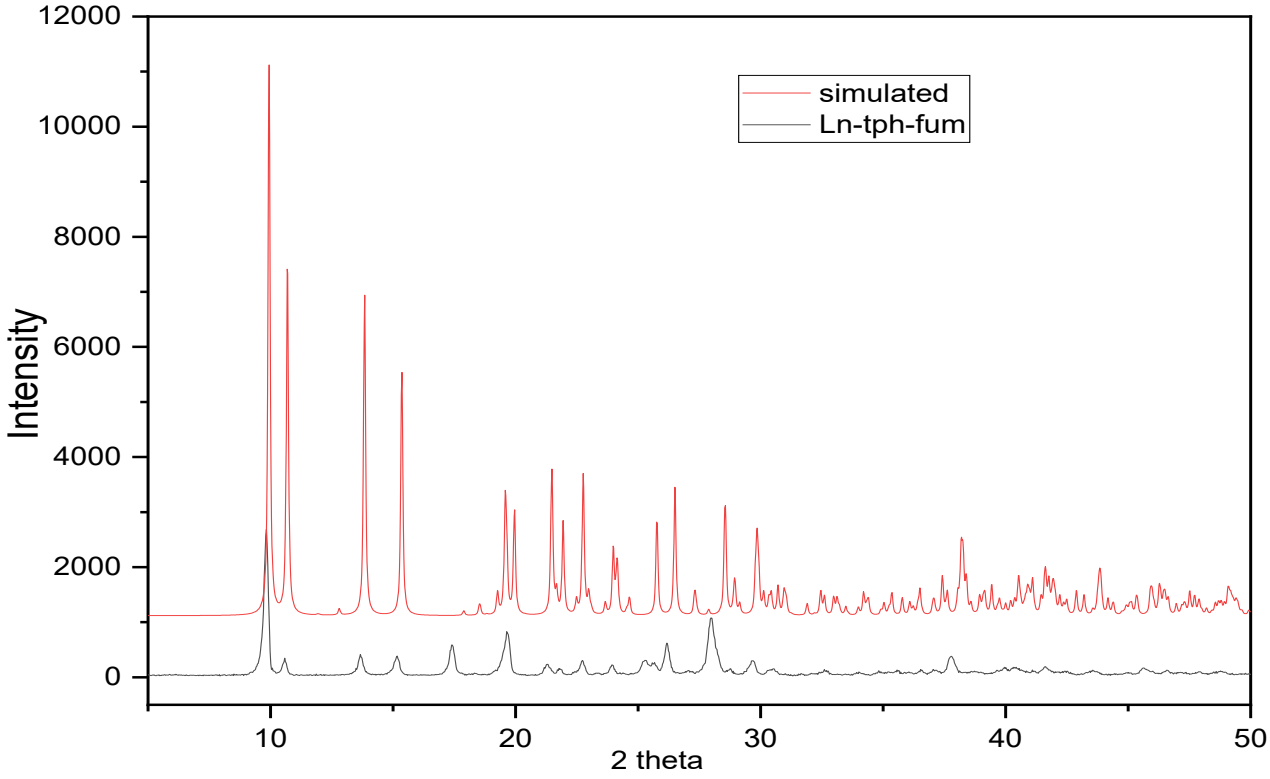

Figure II. 17 Simulated and experimental diffractogram comparison

iii. <u>System Ln-tph-suc</u>

We obtained two compounds Ln-tph-suc_1 and Ln-tph-suc_2. Ln-tph-suc_1 was obtained as residue after heating while Ln-tph-suc_2 was obtained from the filtrate upon evaporation.

From the IR spectrum of Ln-tph-suc_1, a broad short band about 3450 cm^{-1} is due to stretching of O-H of the coordinated water molecules. A large band 3100 to 2500cm^{-1} is characteristic to a free COOH group, an indication of partial deprotonation of the acid. The vibration bands at 1673 and 1282cm^{-1} correspond to C=O and C-O stretching of a free COOH group. The bands at 1535cm^{-1} and 1505cm^{-1} are attributed to asymmetric OCO vibrations while the 1403 cm^{-1} band corresponds to symmetric OCO vibrations. The strong band at 748cm^{-1} corresponds to aromatic C-H out-of-plane bending [129], confirming presence of tph and the peak at 507 cm^{-1} is attributed to metal-ligand bond [130].

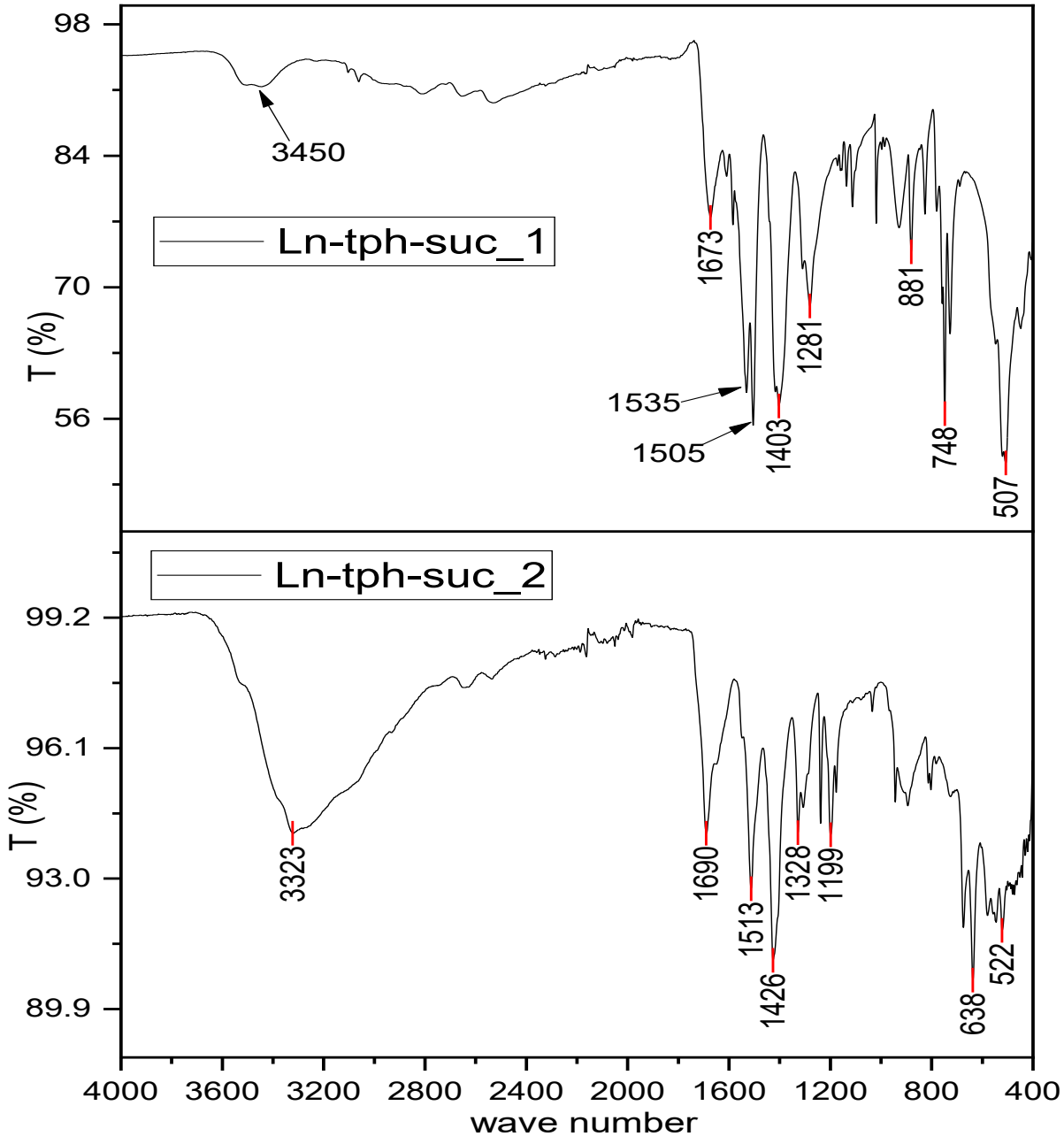

Figure II. 18 IR spectra of Ln-tph-suc compounds

The IR spectrum Ln-tph-suc_2 shows a broad and strong band at 3323cm^{-1} for OH stretching of water molecules; $\nu_{as}(COO^-)$ at 1513cm^{-1}; $\nu_s(COO^-)$ at 1426 cm^{-1} [131]. The bands at 1328 and 1199 cm^{-1} are due to succinic C-C vibrations. The band at 1690 cm^{-1} is assigned to ν(C=O) vibrations of a free COOH group. The spectrum lacks characteristic bands for aromatic CH deformations, suggesting the presence of suc.

Powder XRD analysis.

The powder XRD diagrams of Ln-tph-suc_1 and Ln-tph-suc_2 are different which confirms that, the two compounds of Ln-tph-suc system are different **Figure II. *19***.

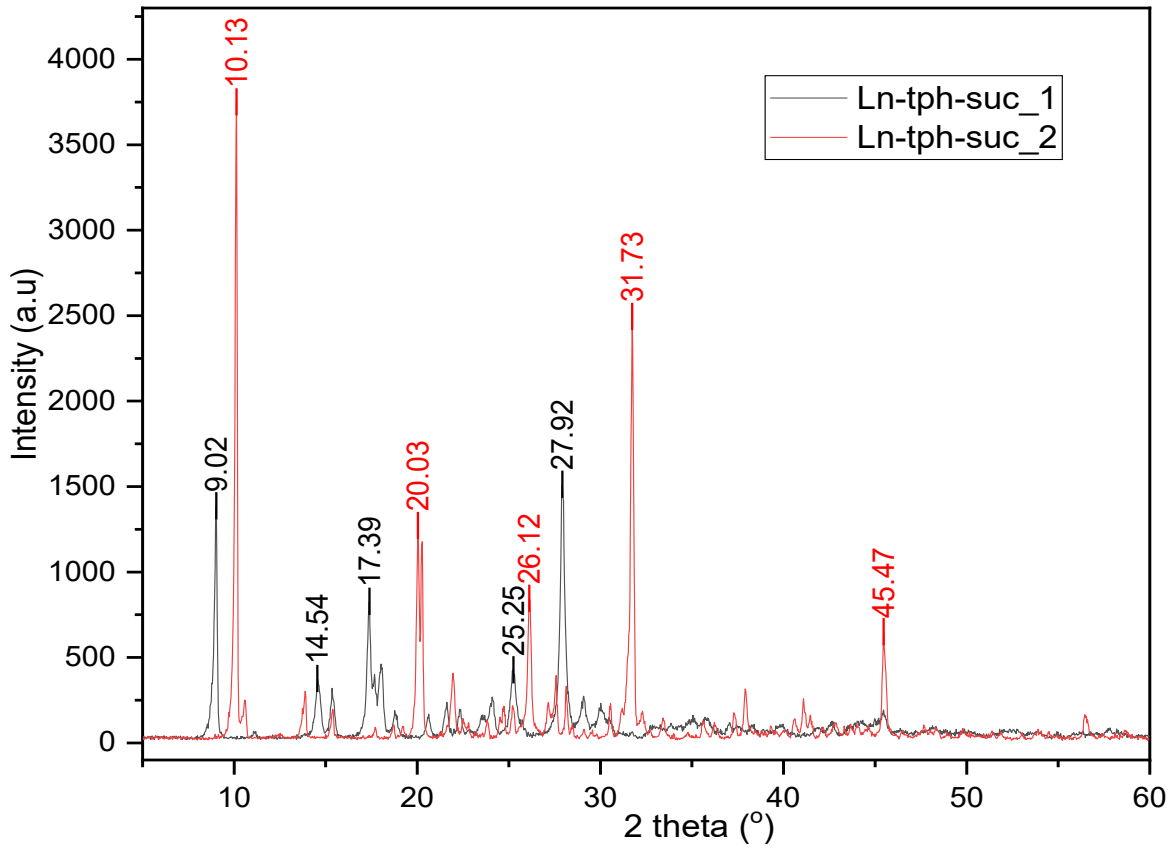

Figure II. 19 XRD diffractograms of Ln-tph-suc compounds.

The diffractograms were compare to those simulated from reported structure with terephthalic acid [123-136] and succinic acid [137-161] and mixed terephthalate-succinate [130] ligands and no exact matches were found.

However, some comparisons give insight on the possible nature of our compounds **Figure II. *20***. Comparing Ln-tph-suc_1 with $Tb_2(tph)_3(H_2O)_4$ [127] and Ln-tph-suc_2 with $\{La(suc)(H_2O)_4Cl.3H_2O\}_n$ [155] manifest the presence of tph and suc in Ln-tph-suc_1 and Ln-tph-suc_2 respectively. The differences are due to presence of other phases in our compounds. The IR data of Ln-tph-suc_1 and Ln-tph-suc_2 shows presence of partially deprotonated ligands. We

therefore, think that our compounds are of type $Ln_x(Htph)_y(H_2O)_z$ and $\{Ln_x(Hsuc)_y(H_2O)_zCl.pH_2O\}_n$

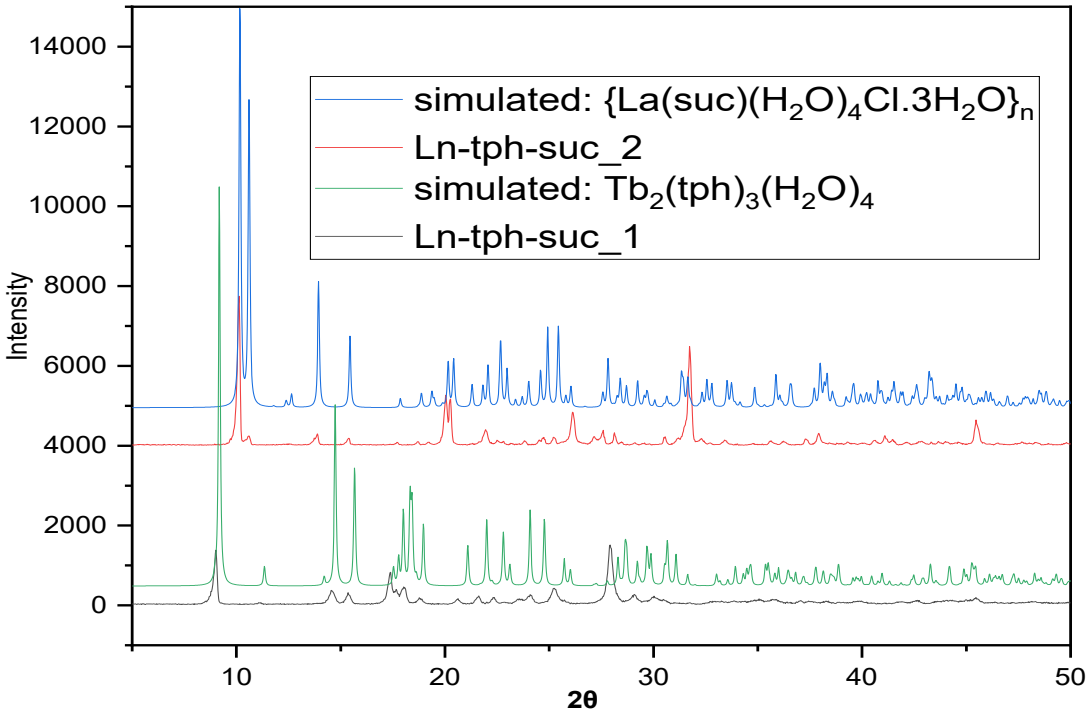

Figure II. 20 Comparison of Ln-tph-suc compounds with reported structures

iv. Systems Ln-tph-glu and Ln-tph-adi.

The compounds of these systems have IR spectra similar to that of Ln-tph-suc_1, **Figure II. *21***. This indicates that these compounds contain components that are common in all systems (i.e. tph).

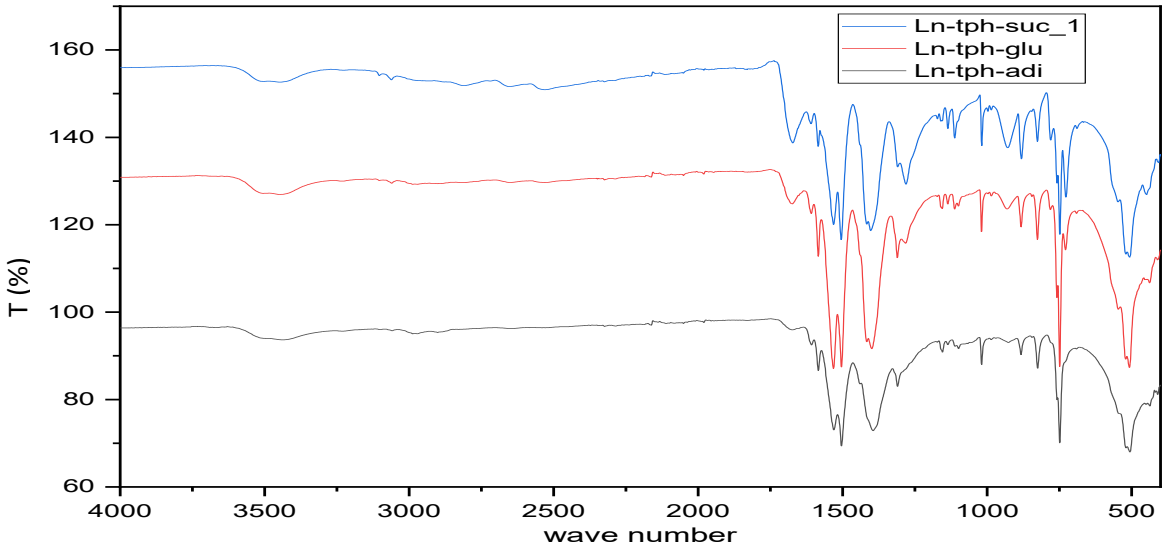

Figure II. 21 IR spectra of Ln-tph-glu and Ln-tph-adi.

The IR spectroscopy data is supported by PXRD which gives similar diffractograms. This confirms that the three compounds are the same, **Figure II. *22***.

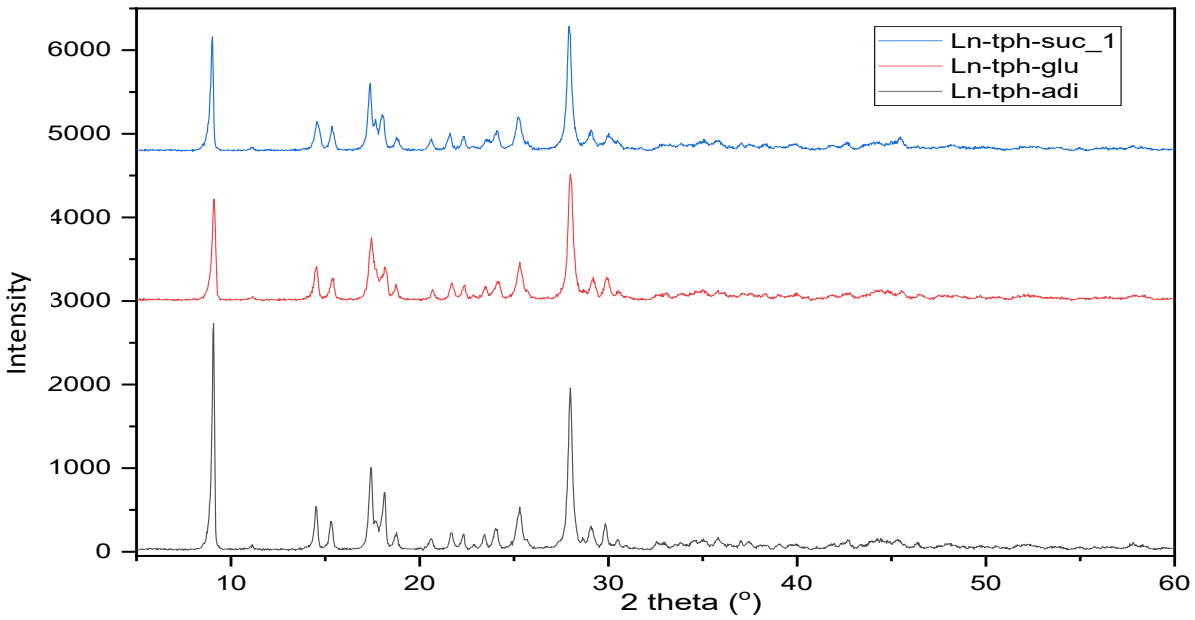

Figure II. 22 PXRD diffractograms of IR spectra of Ln-tph-glu and Ln-tph-adi.

c) Serie C

In this serie of experiments, we were interested in the synthesis of lanthanum-based coordination polymers with mixed ligands, isophthalic and various linear dicarboxylic acids.

The compound obtained from Ln-iph-fum system gave an IR spectrum similar to that of isophthalic acid. This is due to precipitation of isophthalic acid which is insoluble in water.

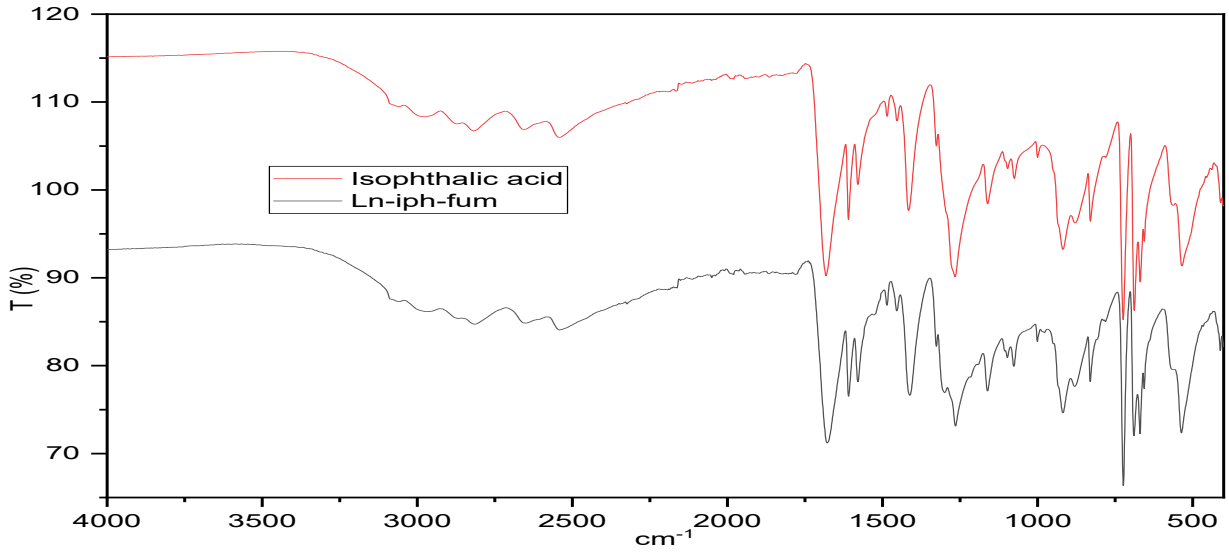

Figure II. 23 IR spectrum of Ln-iph-fum

The compound obtained with Ln-iph-suc gave the IR spectrum shown below. This spectrum lacks characteristic COO^- coordination bands in the region 1650-1370 cm^{-1}.[55] The product could be a result of precipitation of insoluble lanthanum hydroxide compound.

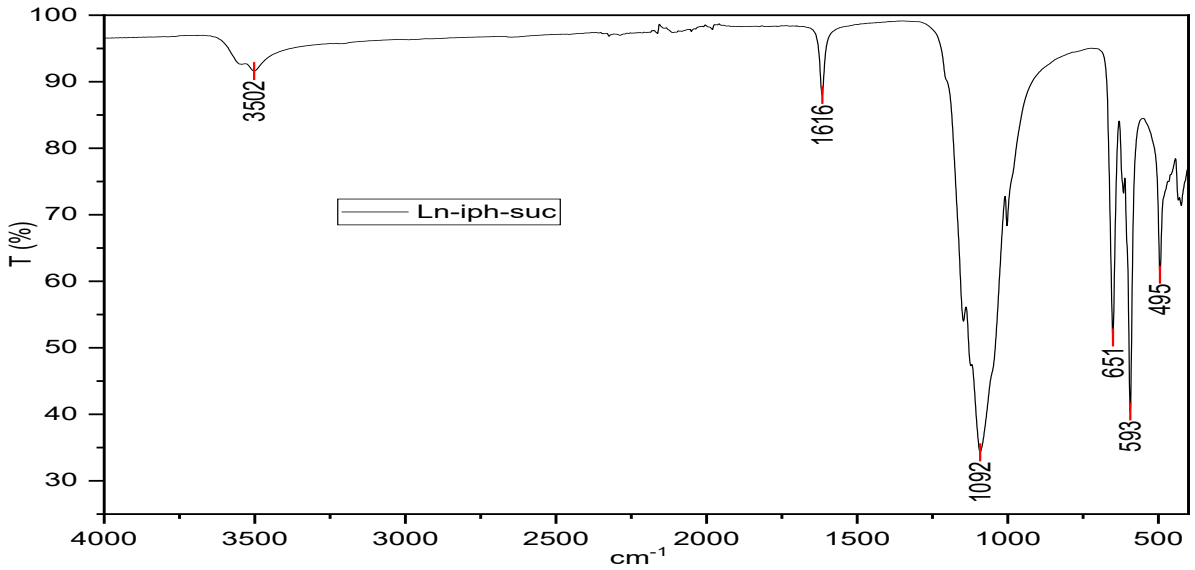

Figure II. 24 IR spectrum of Ln-iph-suc system

The IR spectra of compounds from Ln-iph-mal, Ln-iph-glu, and Ln-iph-adi systems are shown in **Figure II. *25***. The major characteristic bands are attribute as shown in the table below [66] [61].

Type of vibration	IR bands (cm^{-1})		
	Ln-iph-mal	Ln-iph-glu	Ln-iph-adi
ν(O-H)	3332	3348	3289
$\nu_{as}(COO^-)$	1607, 1581, 1542	1605, 1542	1600, 1497
$\nu_s(COO^-)$	1365	1439, 1378	1443, 1372
γ(C-H)	753, 709	825, 731	735, 654

The separations between ν_{as} (COO^-) and ν_s (COO^-) are 242, 216 and 177cm^{-1} for Ln-iph-mal, which are attributable to the co-existence of the monodentate and bidentate bridging modes of the carboxylate groups, 166 and 164cm^{-1} for Ln-iph-glu, and 157 and 125cm^{-1} are attributable to bidentate bridging coordination modes [58, 68].

The powder diffractograms of Ln-iph-mal, Ln-iph-glu, and Ln-iph-adi compounds are different from one another **Figure II. *26***. This supports IR data and confirms synthesis of different compounds. However, the diffractogram of Ln-iph-glu is similar to that of cp 1 for Ln-iph system obtained in manipulation I **Figure II. *6*** confirming that the two compounds are identical. Therefore, the compound obtained from Ln-iph-glu system contains one ligand (iph)

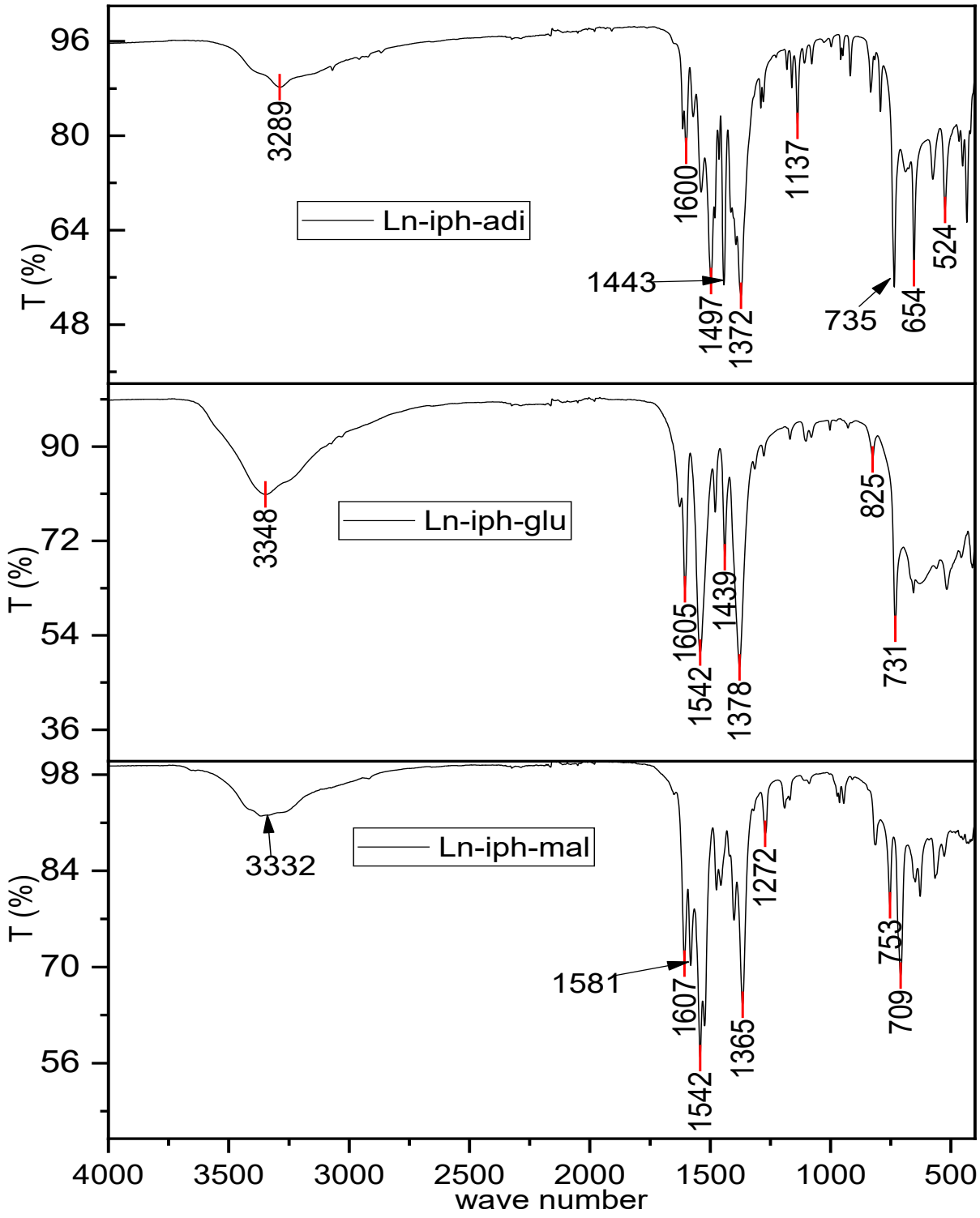

Figure II. 25 IR spectra of Ln-iph-mal, Ln-iph-glu, and Ln-iph-adi systems

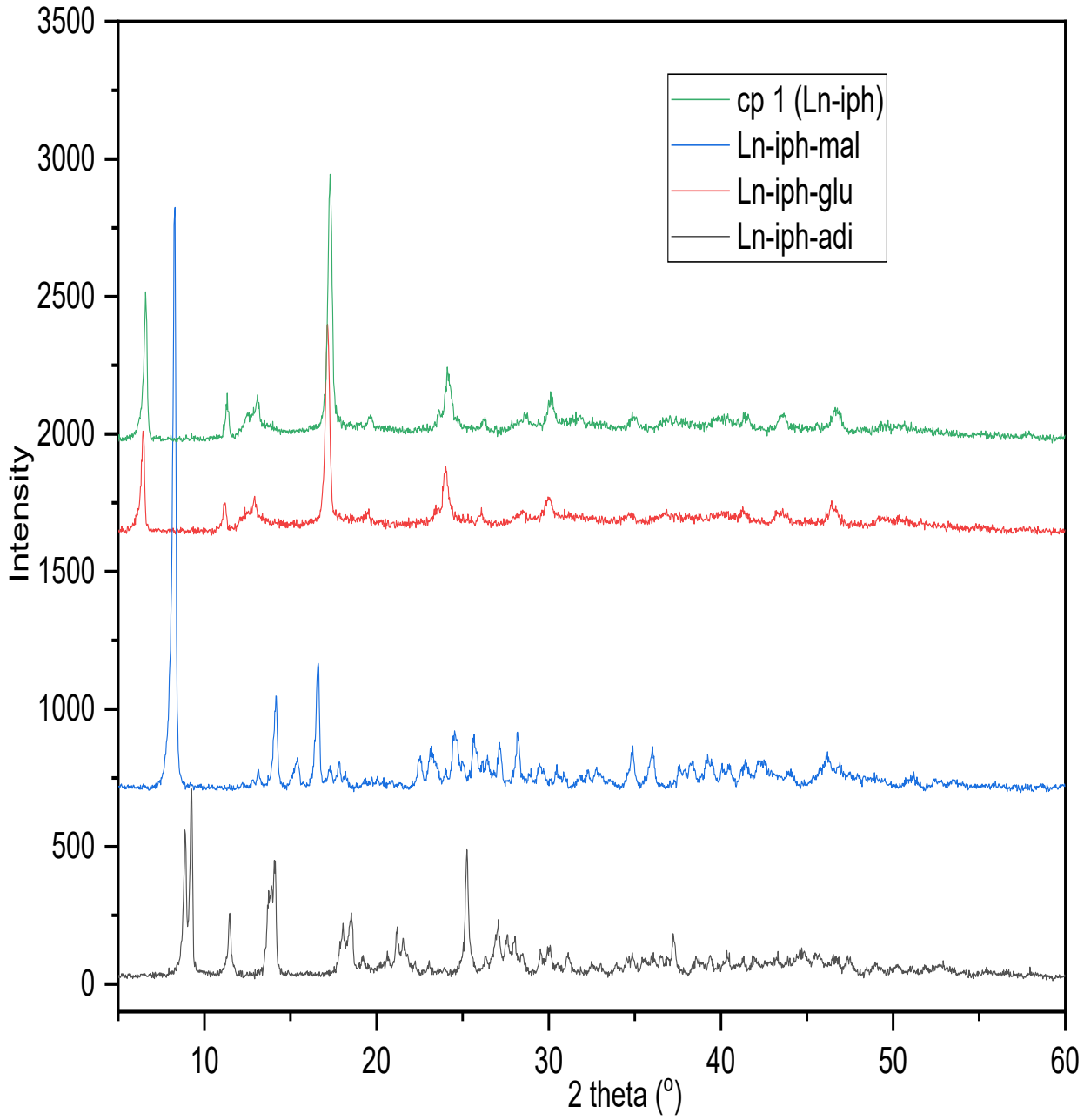

Figure II. 26 X-ray diffractograms for serie C compounds.

The diffractograms of Ln-iph-mal and Ln-iph-adi compounds were compared to XRD diffractograms generated from reported structures of Ln/isophthalate [57-162] , Ln/malonate [81-98] Ln/adipate [163-173] and Ln/isophthalate/adipate [173] coordination compounds. No exact match was found which means our compounds could have not been reported before.

c. Manipulation III.

In this manipulation, we are interested in the synthesis of lanthanum coordination polymers with mixed ligands (acid terephthalic and acid glutaric).

Synthesis protocol.

Table II. 4 Composition of various Ln-tph-glu experiments.

No	Reagents /(g)			Solvent/ ml	pH of the final mixture	T/ °C	Period/ days
	Ln (oxide, nitrate or chloride)	tph	glu				
1	0.1	0.0450	0.0358	w/e (10/5, v/v)	4.60	120	03
2	0.1	0.0675	0.0534		4.04		
3	0.1	0.0900	0.0534		4.85		
4	0.1	0.0680	0.0180		5.02		
5	0.1	0.0300	0.0240		4,14		
6	0.1	0.0448	0.0560	w/a (12/2, v/v)	2.99	160	05
7	0.1	0.0680	0.0545		4.50		
8	0.1	0.0685	0.0360		5.08		
9	0.1	0.0680	0.0540	w/m (9/5, v/v)	4.55		
10	0.1	0.0685	0.0540	w/m (5/10, v/v)	3.35		
11	0.1 La_2O_3	0.0770	0.0610	w/a (8/2, v/v)	4.56	180	04
12	0.1 La_2O_3	0.0770	0.0610	w/a (5/5, v/v)	4.66		
13	0.1 $Y(NO_3)_3.6H_2O$	0.0650	0.0520	w/a (8/2, v/v)	4.45		
14	0.1 $Y(NO_3)_3.6H_2O$	0.650	0.0520	w/a (5/5, v/v)	4.51		
15	0.1	0.0710	0.0560	w/a (5/5, v/v)	4.40		

Ln reagent not specified implies $LaCl_3.6H_2O$. glu (acid glutaric); tph (acid terephthalic); w/e (water/ethanol); w/m (water/methanol); w/a (water/acetonitrile).

The compounds of this manipulation were synthesized using hydro/solvothermal technique from a mixture of lanthanum or yttrium (oxide, nitrate or chloride), acid terephthalic (tph) and acid glutaric (glu). The mixing was done under constant stirring with a magnetic stirrer. The pH was adjusted with NaOH (1M). After the heating period, the oven was cooled at 10^0C per hour up to 40°C. The mixtures are then removed and filtered. The residues are dried at room temperature while the filtrates are kept in the oven at 40°C to facilitate evaporation.

In this manipulation, we varied parameters like precursors, reaction ratios, pH, solvents, temperature and time for the system Ln/ tph/ glu as tabulated above (**Table II. *4***).

Results and discussion.

All the compounds obtained were analyzed by IR spectroscopy and grouped by comparing their spectra. Five different products were obtained, Type I to Type V as shown in **Figure II. 27**

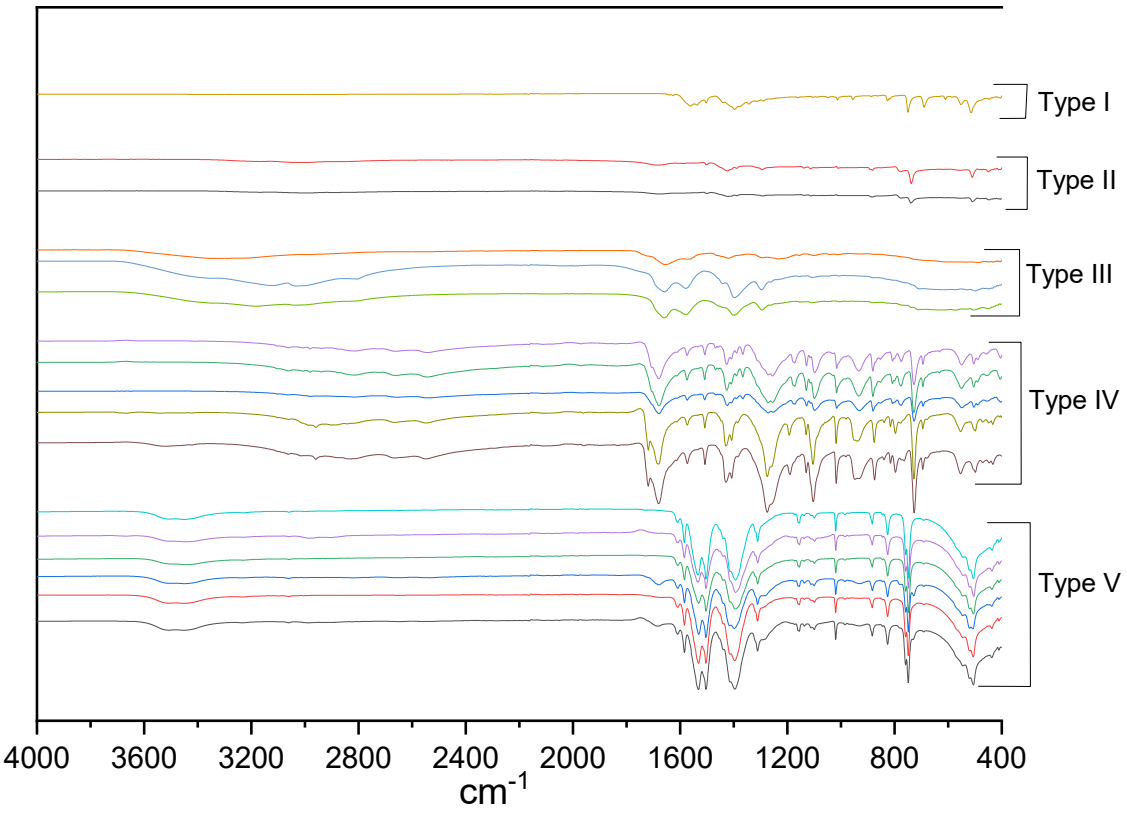

Figure II. 27 Classification of products of manipulation III.

Characterization by IR spectroscopy.

The spectra of the five compounds were compared to the spectra of the ligands (tph and glu). The spectra of Types I, II, III, and V differ from the spectra of isolated ligands. The spectrum of Type IV is comparable to tph spectrum. The compounds of Type IV are therefore as a result of recrystallization/precipitation of tph.

a. Compound Type I. (obtained with $Y(NO_3)_3.6H_2O$)

From the IR spectrum **Figure II. 28**, the bands for asymmetric and symmetric stretching of OCO groups are located at 1561cm^{-1} and 1396cm^{-1} respectively, $\Delta\nu$=165 (bridging coordination mode) [160]. The strong and sharp band at 750 cm^{-1} is characteristic of aromatic C-H out-of-plane bending and a medium fine band at 826 cm^{-1} is characteristic of 1-4 benzene substitution. The intense band at 515 cm^{-1} is assigned to Ln-O stretching. The band at 690 cm^{-1} can be attributed to out-of-plane C-H bending for glu [174].

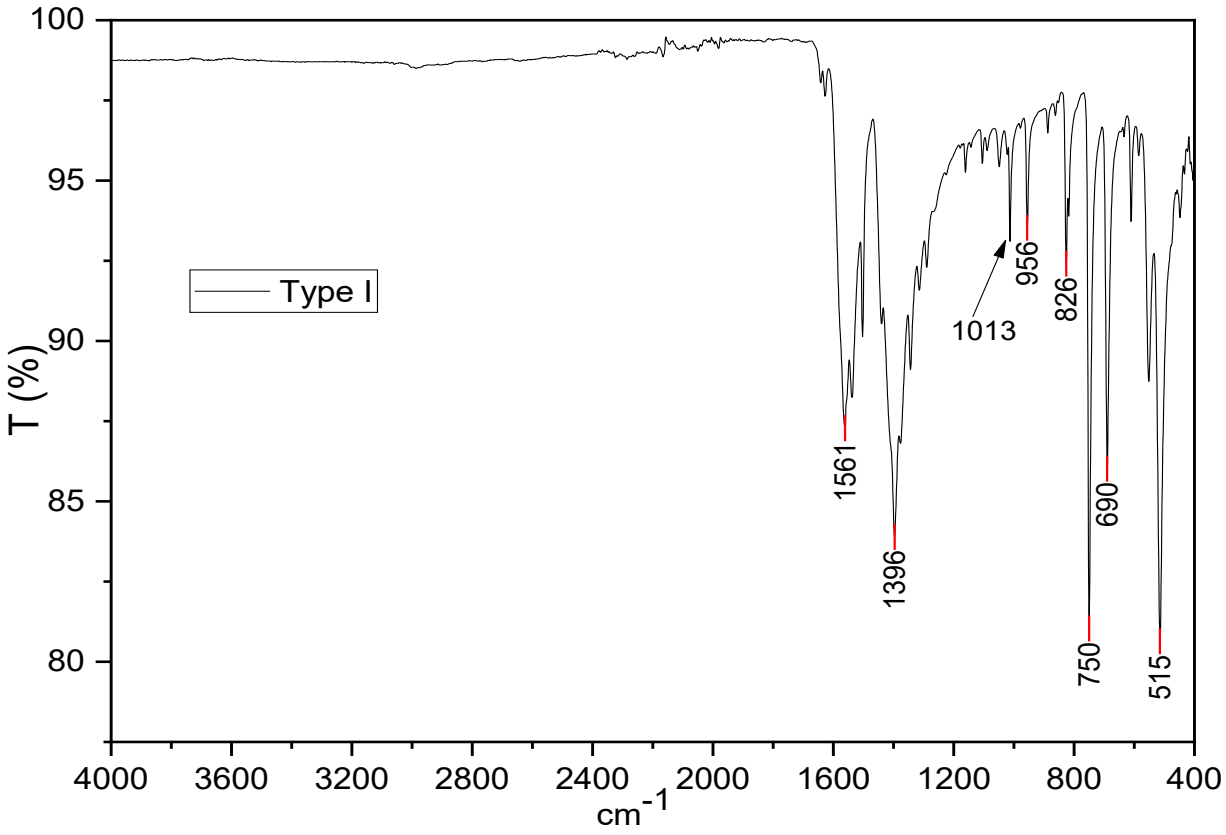

Figure II. 28 IR spectrum of Type I compound.

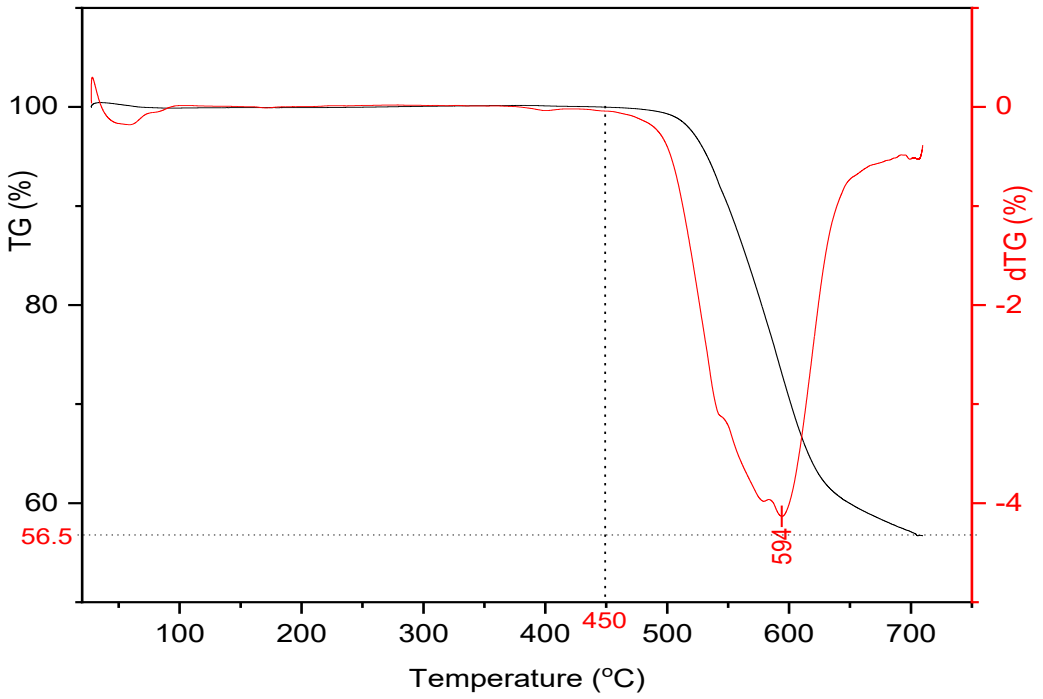

Figure II. 29 TG/dTG curves of compound Type I

The thermogravimetric curve of Type I compound is given in **Figure II. *29***. The TG curve shows one phase of mass loss. The compound is stable up to 450°C, after which a mass loss of 43.5% is registered. This mass loss corresponds to decomposition of the ligands and is associated with an endothermic transition (peak centered at 594°C. The thermogravimetric curve of the compound confirms absence of water molecules.

Conclusion.

Basing on the IR analysis, the absence of bands in the region 1720-1680 cm^{-1} indicates complete deprotonation of the ligand, also evidenced by lack of broad O-H stretching bands in the region 3300-2500 cm^{-1} characteristic of COOH group. There is no characteristic band for OH stretching of water molecules [176, 136], also evidence by the thermogravimetric curve of the compound for temperatures below 400°C. We can deduct that Type I compounds are of form $[Ln_x(tph)_y(glu)_z]_n$.

For electronic charge considerations, two neutral compounds are possible, $Y_2(tph)_2(glu)$ and $Y_2(tph)(glu)_2$. Given that aromatic (tph) is more stable than aliphatic (glu), we expect glu to decompose before tph. The loss of two glu from $Y_2(tph)(glu)_2$ gives a theoretical mass loss of 43.33% which is approximately equal to the 43.5% mass loss observed experimentally.

The weak bands observed in the IR spectrum of the residue **Figure II. *30*** obtained after thermal treatment, 1499 cm^{-1} and 1345 $cm^{-1}$are characteristic of the $\nu(COO^-)$ vibrations. This confirms the presence of tph in the residue.

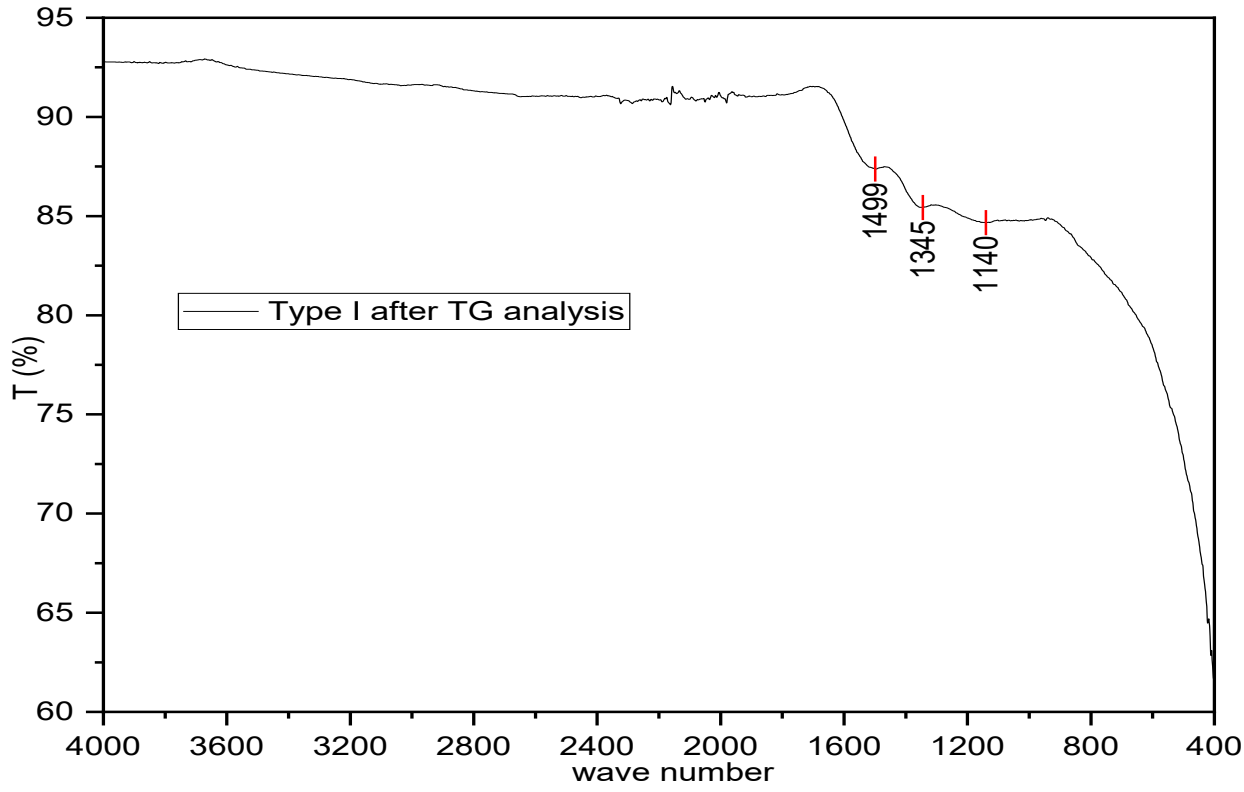

Figure II. 30 IR spectrum of Type I compound residue after TG analysis

b. Compound Type II.

From the IR spectrum of Type II compound **Figure II. 31**;

The broad band in the region 3300-2500 cm^{-1} correspond to O-H stretching of COOH group [134]. The band at 1683 cm^{-1} is assigned to C=O stretching vibrations of the COOH group. The band at 1424 cm^{-1} can be assigned to ν_{as}(OCO) and 1294 cm^{-1} to ν_s(OCO) vibrations. The strong sharp band at 738 cm^{-1} is characteristic of aromatic C-H out-of-plane bending vibrations. The sharp band at 510 cm^{-1} is attributed to Ln-O vibrations.

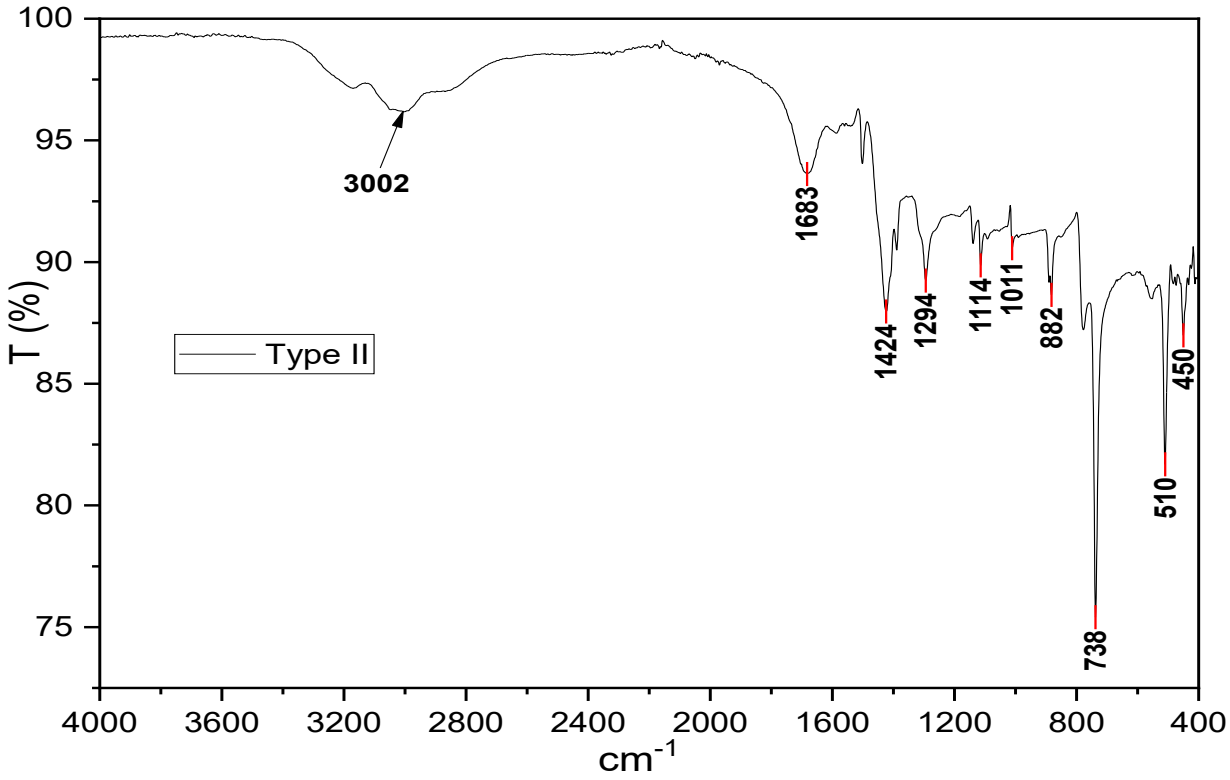

Figure II. 31 IR spectrum of Type II compound.

Conclusion

Basing on IR data, the variation between asymmetric and symmetric bands, $\Delta\nu$=130, indicates that the ligand is linked to the metal in a bridging coordination mode (one carboxyl group links more than one metal center). We therefore, think that Type II compound is of form $[Ln_x(Htph)_y]_n$.

c. Compound Type III.

From Type III compound IR spectrum **Figure II.** ***32***; the bands at 1655 $cm^{-1}$and 1578 cm^{-1} correspond to asymmetric stretching vibrations of the COO^- group. The bands for COO^- symmetric vibrations are located at 1397 cm^{-1} and 1297 cm^{-1}.[176] The band at 499cm^{-1} is assigned to Ln-O bond. The strong bands at 3125 cm^{-1} and 3028cm^{-1} may indicate the presence of water molecules which are coordinated differently. These bands appear at lower wave numbers than usual O-H bands, this may be due to strong hydrogen interactions.

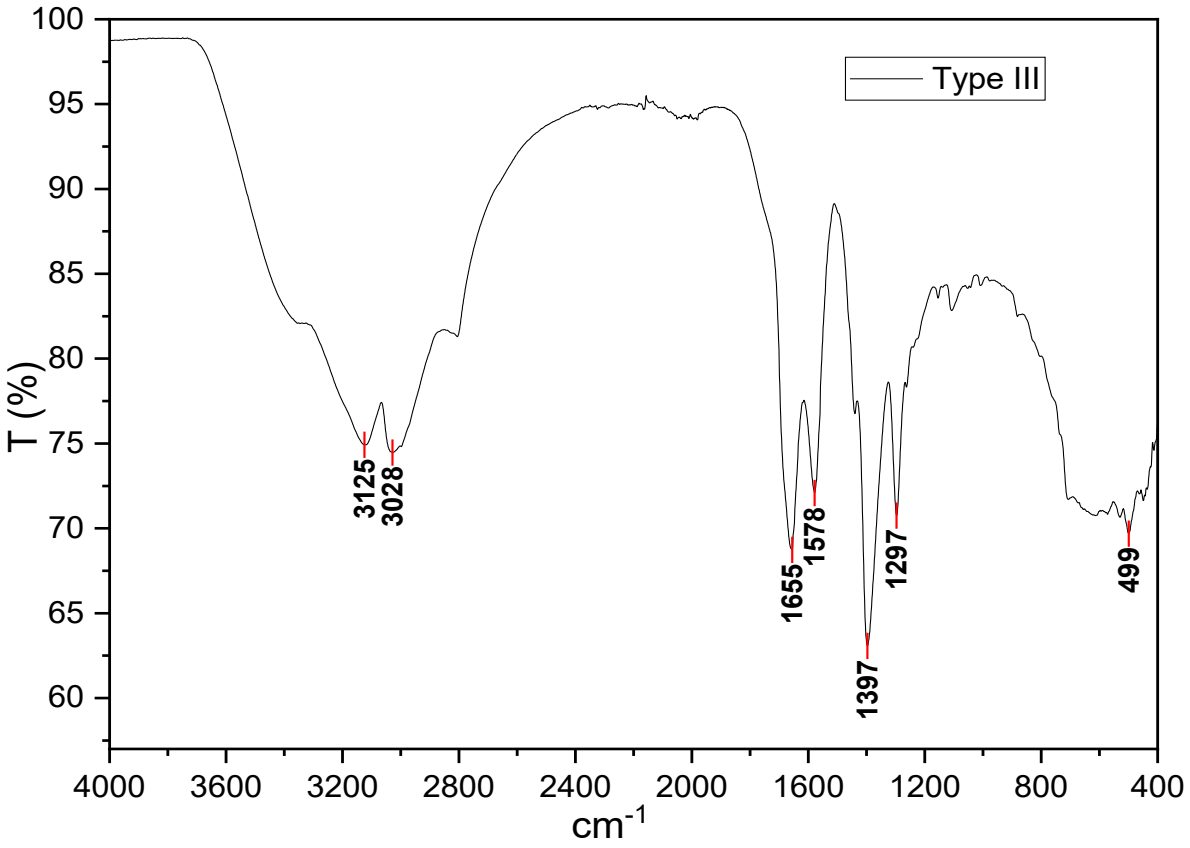

Figure II. 32 IR spectrum of Type III compound.

Conclusion

Lack of characteristic aromatic C-H out-of-plane deformation bands in the region 850-720 cm^{-1} indicates absence of tph in the compound. The strong band in the region 1700-1680 cm−1 attributable to ν(C=O) vibration of carboxylic acid group of the free ligand is absent in the spectrum indicating complete deprotonation and coordination of ligand to the metal through carboxylate group [177]. The difference between asymmetric and symmetric vibrations, $\Delta\nu > 200$ which suggests monodentate coordination mode. We therefore, think that our compound is of form $[Ln_x(glu)_y(H_2O)_z]_n.pH_2O$.

d. Compound Type V.

From the IR spectrum of Type V compound **Figure II. *33***;

The short and broad band at 3454cm^{-1} is assigned to O-H stretching of water molecules. The bands at 1584 cm^{-1}, 1531 cm^{-1}, and 1503 cm^{-1} are attributed to asymmetric OCO vibrations while the bands at 1397 cm^{-1} and 1311 cm^{-1} are assigned to symmetric vibrations of OCO group [133]. The strong sharp band at 749 cm^{-1} corresponds to C-H out-of-plane bending, characteristic of benzene ring. The band at 507 cm^{-1} is ascribed to Ln-O vibrations.

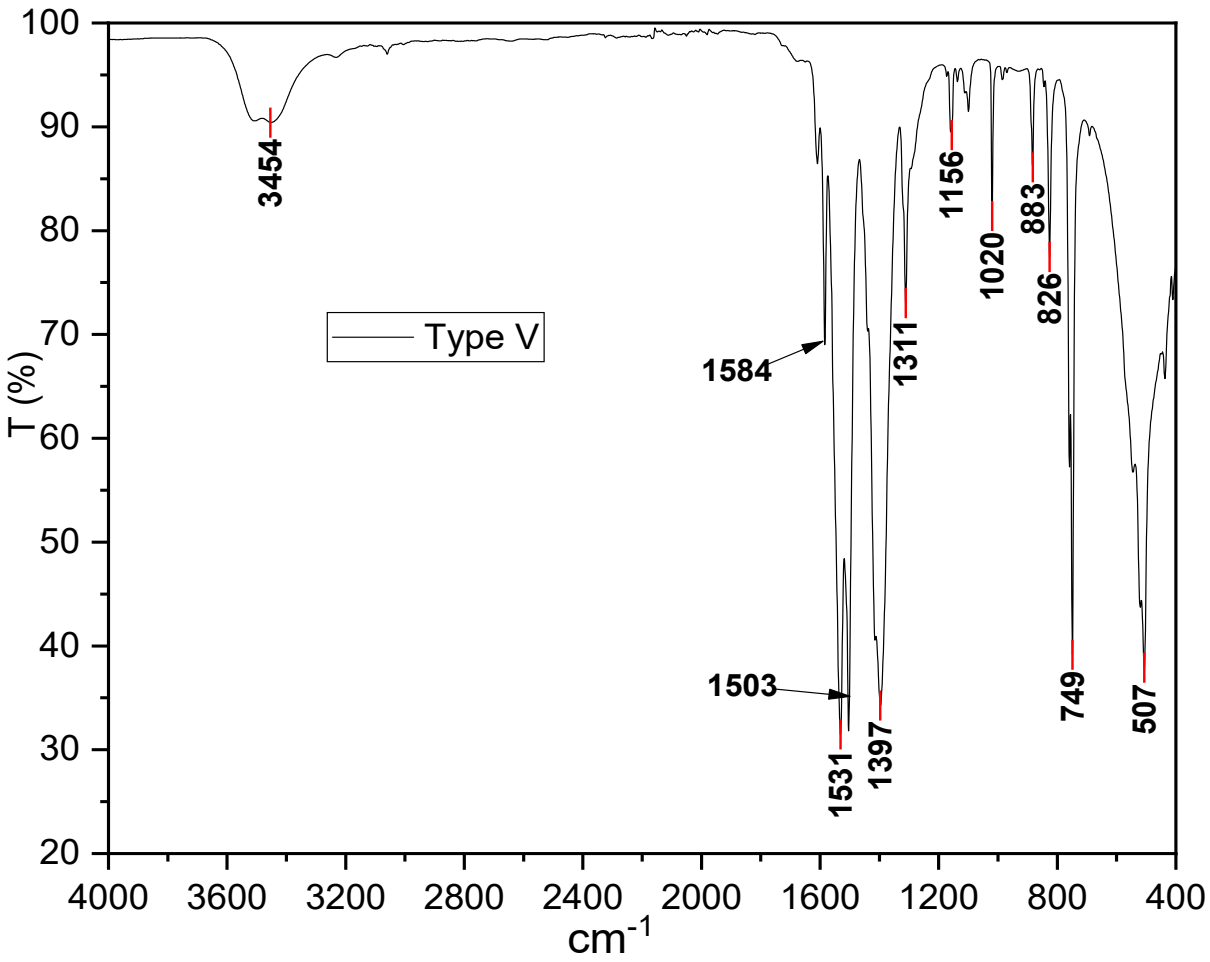

Figure II. 33 IR spectrum of Type V compound.

Conclusion

Lack of absorption band attributable to C=O vibrations of a free COOH group in the region 1715 to 1680 cm-1 is indicative of total deprotonation of the ligand. The variations (Δν) between asymmetric and symmetric bands indicate the co-existence of monodentate and bridging coordination modes.

The IR data strongly confirms the presence of ligand tph with the characteristic bands at 826cm^{-1} and 749cm^{-1} and we think, this compound is of form $[Ln_x(tph)_y]_n.zH_2O$. However, we cannot rule out on the presence or not of ligand glu basing on IR data alone.

Powder XRD analysis.

The XRD diffractograms of compounds Type I, II, III, and V are shown in **Figure II.** ***34***. By comparison, the diffractograms are different from one another which confirms that the compounds obtained are different.

The diffractograms were compared to those simulated from accessible Ln/tph [123-129], Ln/glu [63,90, 135-156] structures reported in CCDC database and we did not find any match. This indicates that these compounds could have not been reported before and are possibly new.

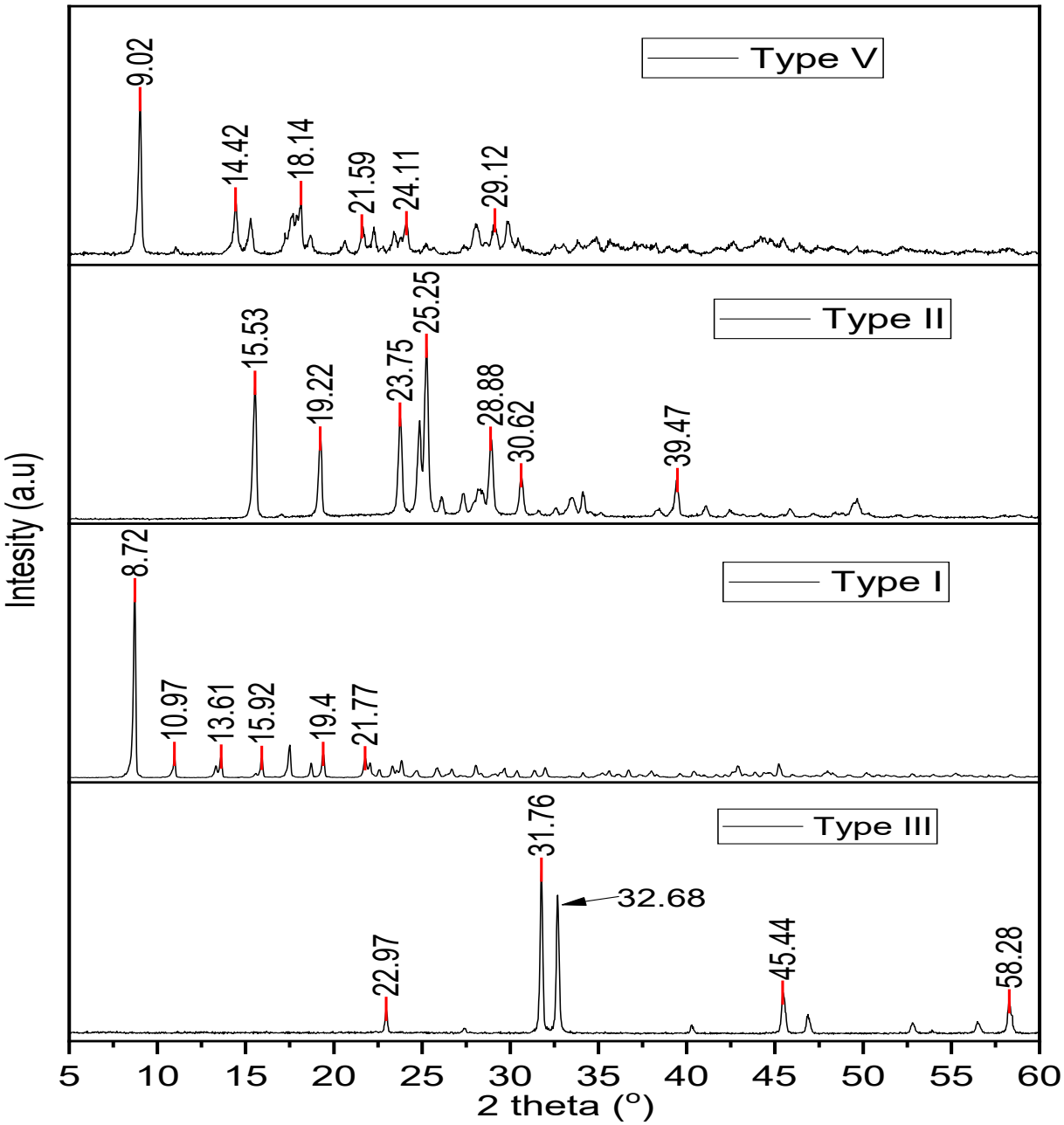

Figure II. 34 Diffractograms of compounds of manipulation III.

General conclusion.

This work aimed to explore and deepen the understanding of rare earth coordination polymers, focusing on their synthesis and characterization using a range of organic ligands. Through an extensive bibliographic review, we established the fundamental principles underpinning rare earth coordination chemistry, highlighting the unique features of lanthanoid ions such as their variable coordination environments, optical and magnetic behavior, and affinity for oxygen-donor ligands, especially carboxylic acids.

The experimental investigation successfully synthesized several new coordination polymers using lanthanum (III) salts in combination with different aliphatic and aromatic dicarboxylic acids. Both single-ligand and mixed-ligand systems were explored under varying conditions namely, hydrothermal, reflux, and ambient temperature methods to study their impact on product formation. Reaction variables such as solvent system, pH, and stoichiometry were carefully controlled to direct the crystallization pathway and influence the final structural outcome.

Infrared (IR) spectroscopy provided crucial insights into the bonding environment within the synthesized polymers. Shifts in the carboxylate stretching frequencies confirmed ligand coordination to the lanthanum centers, with the disappearance of free acid C=O bands and the emergence of symmetric and asymmetric COO^- stretches indicating deprotonation and metal–ligand bonding. Complementing this, Powder X-ray Diffraction (PXRD) analysis revealed distinct crystalline phases, verifying the formation of new materials. In several cases, unmatched diffraction patterns suggested the possible synthesis of novel compounds, highlighting the structural diversity achievable through careful ligand selection and reaction condition optimization in rare earth coordination polymer systems.

Despite these successes, some systems did not yield desired coordination polymers, instead precipitating unreacted ligands. This points to limitations in ligand reactivity or solubility under given reaction conditions and highlights the importance of rational ligand selection and optimisation of synthesis parameters.

The results of this study therefore demonstrate the versatility and complexity of rare earth coordination polymer synthesis. The work advances the field by contributing new data on ligand-metal interactions, structure formation, and phase diversity. These findings can serve as a foundation for future studies targeting applications in areas such as luminescent materials, catalysis, and porous frameworks. Further exploration using single-crystal X-ray diffraction, thermal analysis, and photophysical measurements is recommended to fully characterize these materials and unlock their application potential.

Bibliography

[1] R. H. Petrucci, F. G. Herring, J. D. Madura, and C. Bissonnette, *General Chemistry : principles and modern applications*, 12th ed. 2017.

[2] C. Huang, *Rare Earth Coordination Chemistry Fundamentals and Applications*. China: John Wiley & Sons Ltd, 2010. http://doi.wiley.com/10.1002/9780470824870

[3] African Natural Resources Centre (ANRC), "RARE EARTH ELEMENTS (REE) Value Chain Analysis for Mineral Based Industrialisation in Africa," pp. 1–65, 2021, https://www.afdb.org/fr/documents/rare-earth-elements-ree-value-chain-analysis-mineral-based-industrialization-africa

[4] S. Cotton, "Lanthanide and Actinide Chemistry," *Lanthan. Actin. Chem.*, pp. 1–263, 2006, doi: 10.1002/0470010088.

[5] H. Suwa and S. Todo, "Chapter 23. Geometric Allocation Approach for the Transition Kernel of a Markov Chain," *Monte Carlo Methods Appl.*, December, pp. 213–222, 2012, doi: 10.1515/9783110293586.213.

[6] S. Cotton, "Coordination Chemistry of the Lanthanides," in *Lanthanide and Actinide Chemistry*, John Wiley & Sons, Inc, 2006, ch. 4, pp. 36–60.

[7] A. de Bettencourt-Dias, "Lanthanides: Electronic Structure," *Encycl. Inorg. Bioinorg. Chem.*, 2012, doi: 10.1002/9781119951438.eibc2009.

[8] S. Cotton, *Lanthanide and Actinide Chemistry*. Wiley, 2006. doi: 10.1002/0470010088.

[9] A. Peter, H. Mike, O. Tina, R. Jonathan, W. Mark, and A. Fraser, *Shriver & Atkins' Inorganic Chemistry*, 5th ed. New York: Oxford University Press, 2010.

[10] R. A. Scott, D. A. Atwood, T. P. Hanusa, and A. Messerschmidt, *The rare earth elements, fundamentals and application*. USA: John Wiley & Sons Ltd, 2012.

[11] A. De Bettencourt-Dias, "Introduction to Lanthanide Ion Luminescence," *Lumin. Lanthan. Ions Coord. Compd. Nanomater.*, vol. 9781119950, pp. 1–48, 2014, doi: 10.1002/9781118682760.ch01.

[12] E. C. Constable and C. E. Housecroft, "Coordination chemistry: The scientific legacy of Alfred Werner," *Chem. Soc. Rev.*, vol. 42, no. 4, pp. 1429–1439, 2013, doi: 10.1039/c2cs35428d.

[13] G. B. Kauffman, "Theories of Coordination Compounds," in *In Coordination Chemistry*, Washington, DC: American Chemical Society, 1994, pp. 2–33. doi: 10.1021/bk-1994-0565.ch001.

[14] J. A. McCleverty and T. J. Meyer, *Comprehensive Coordination Chemistry II*, vol. 1. Toronto, Canada: Elsevier, 2004.

[15] T. Kaliyappan and P. Kannan, "Co-ordination polymers," *Prog. Polym. Sci.*, vol. 25, no. 3, pp. 343–370, Apr. 2000, doi: 10.1016/S0079-6700(00)00005-8.

[16] J. P. Birk and J. Foster, "Coordination Compounds," *J. Chem. Educ.*, vol. 70, no. 6, p. 460,

Jun. 1993, doi: 10.1021/ed070p460.2.

[17] G. A. Lawrance, *Introduction to Coordination Chemistry*. Australia: Wiley, 2009. doi: 10.1002/9780470687123.

[18] P. Atkins, T. Overton, J. Rourke, M. Weller, and F. Armstrong, *Shriver and Atkins' Inorganic Chemistry*, Fifth. USA: Oxford University Press, 2009. http://www.amazon.co.uk/Shriver-Atkins-Inorganic-Chemistry-Peter/dp/0199236178

[19] S. F.A. Kettle, *Physical Inorganic Chemistry*. Kingston, Ontario: Spektrum Academic, 1996. doi: 10.1007/978-3-662-25191-1.

[20] K. Hindson, "Coordination chemistry," Elsevier B.V., 2012. doi: 10.1002/ejic.201290090.

[21] M. F. Lappert, "The organometallic chemistry of the transition metals," *J. Organomet. Chem.*, vol. 354, no. 2, p. C26, Oct. 1988, doi: 10.1016/0022-328x(88)87059-1.

[22] R. Janicki, A. Mondry, and P. Starynowicz, "Carboxylates of rare earth elements," *Coord. Chem. Rev.*, vol. 340, pp. 98–133, Jun. 2017, doi: 10.1016/j.ccr.2016.12.001.

[23] E. C. Constable, "Expanded ligands-An assembly principle for supramolecular chemistry," *Coord. Chem. Rev.*, vol. 252, no. 8–9, pp. 842–855, Apr. 2008, doi: 10.1016/j.ccr.2007.10.020.

[24] O. M. Yaghi, M. O'Keeffe, M. Eddaoudi, and H. Li, "Design and synthesis of an exceptionally stable and highly porous metal-organic framework," *Nature*, vol. 402, no. November, pp. 276–279, 1999.

[25] M. Sánchez-Serratos, J. Raziel Álvarez, E. González-Zamora, and I. A. Ibarra, "Porous Coordination Polymers (PCPs): New Platforms for Gas Storage," *J. Mex. Chem. Soc.*, vol. 60, no. 2, pp. 43–57, Oct. 2017, doi: 10.29356/jmcs.v60i2.72.

[26] M. L. Tong and X. M. Chen, *Synthesis of Coordination Compounds and Coordination Polymers*, no. Iii. Elsevier B.V., 2017. doi: 10.1016/B978-0-444-63591-4.00008-2.

[27] A. D. Pomogailo, "Polymer Sol-Gel Synthesis of Hybrid Nanocomposites," *Colloid J.*, vol. 67, no. 6, pp. 658–677, Nov. 2005, doi: 10.1007/s10595-005-0148-7.

[28] A. Morsali and L. Hashemi, "Introduction to Coordination Polymers," in *Main Group Metal Coordination Polymers*, John Wiley & Sons, Inc, 2017, pp. 1–16. doi: 10.1002/9781119370772.ch1.

[29] S. R Batten, S. M Neville, and R. T. David, *Coordination polymers: Design,Analysis and Application*. Victoria, Australia: Royal Society of Chemistry, 2009, www.rsc.org

[30] D. T. De Lill and C. L. Cahill, "Coordination Polymers of the Lanthanide Elements: A Structural Survey," in *Progress in Inorganic Chemistry*, vol. 55, K. Kenneth D, Ed., Washington DC: John Wiley & Sons Ltd, 2007, pp. 143–204. doi: 10.1002/9780470144428.ch3.

[31] B. F. Abrahams, R. W. Elliott, T. A. Hudson, and R. Robson, "A new type of 3D [(M II) 2 (TCNQ −II) 3] 2 − coordination network with spacious channels of hexagonal cross-section generated from TCNQH 2," *CrystEngComm*, vol. 14, no. 2, pp. 351–354, 2012, doi:

10.1039/C1CE06104F.

[32] F. Wang, H. Zhang, and J. Zhang, “Structural Topologies and Interpenetration in the Coordination Polymers,” in *Advanced Structural Chemistry: Tailoring Properties ofInorganic Materials and their Applications*, 1st ed., vol. 1–3, R. Cao, Ed., Fujian, China: WILEY-VCH GmbH, 2021, ch. 8, pp. 425–463. doi: 10.1002/9783527831753.ch8.

[33] S. Kitagawa, R. Kitaura, and S. Noro, “Functional Porous Coordination Polymers,” *Angew. Chemie Int. Ed.*, vol. 43, no. 18, pp. 2334–2375, Apr. 2004, doi: 10.1002/anie.200300610.

[34] C. E. Carraher, C. U. Pittman, and A. S. Abd-El-Aziz, “Introduction to Metal-Coordination Polymers,” in *Macromolecules Containing Metal and Metal-Like Elements*, vol. 5, Wiley, 2005, pp. 1–38. doi: 10.1002/0471727652.ch1.

[35] J. A. McCleverty and T. J. Meyer, *Comprehensive Coordination Chemistry II*, 2nd ed., vol. 2. Elsevier B.V, 2003.

[36] N. Kazou, “Applications in Coordination, Organometallic, and Bioinorganic Chemistry,” in *Infrared and Raman Spectra of Inorganic and Coordination Compounds*, Sixth., John Wiley & Sons, Inc, 2015, ch. 1, pp. 1–273.

[37] G. Zhang, G. Yang, and J. S. Ma, “Hydrothermal syntheses and characterization of novel 3D open-framework and 2D grid lanthanide fumarates: Ln2(fum)3(H 2fum)(H2O)2 (Ln = Ce or Nd), [Sm2(fum)3(H2O)4](H2O) 3, and [Yb2(fum)3(H2O) 4](H2O)2,” *Cryst. Growth Des.*, vol. 6, no. 4, pp. 933–939, 2006, doi: 10.1021/cg050488l.

[38] W. Scherer, B. Penugonda, K. Allen, M. Ruiz, and C. Poveda, “Bonding Amalgam to Tooth Structure: A Scanning Electron Microscope Study,” in *Journal of Esthetic and Restorative Dentistry*, vol. 4, no. 6, G. E. McGuire, S. M. Rossnagel, and R. F. Bunshah, Eds., New York: Noyes publications , william andrew publishing, LLC, 1992, pp. 199–201. doi: 10.1111/j.1708-8240.1992.tb00697.x.

[39] A. Rabenau, “The Role of Hydrothermal Synthesis in Preparative Chemistry,” *Angew. Chemie Int. Ed. English*, vol. 24, no. 12, pp. 1026–1040, Dec. 1985, doi: 10.1002/anie.198510261.

[40] A. Rabenau, “Methods for the study of hydrothermal crystallization,” *Phys. Chem. Earth*, vol. 13–14, no. C, pp. 361–374, Jan. 1981, doi: 10.1016/0079-1946(81)90018-5.

[41] K. Byrappa and T. Adschiri, “Hydrothermal technology for nanotechnology,” *Prog. Cryst. Growth Charact. Mater.*, vol. 53, no. 2, pp. 117–166, Jun. 2007, doi: 10.1016/j.pcrysgrow.2007.04.001.

[42] M. Yoshimura and K. Byrappa, “Hydrothermal processing of materials: Past, present and future,” *J. Mater. Sci.*, vol. 43, no. 7, pp. 2085–2103, Apr. 2008, doi: 10.1007/s10853-007-1853-x.

[43] R. Francis, R. Annick, and C. Daniel, *Analyse Chimique: Méthodes et techniques instrumentales modernes*, 6th ed. Dunod, Paris: Dunod, 1993. https://linkinghub.elsevier.com/retrieve/pii/000326709385368T

[44] J. Epp, “Introduction to X-ray Powder Diffraction X-Ray Analytical Methods Uses of X-

Ray Powder Diffraction Introduction to X-ray Powder Diffraction," *Mater. Charact. Using Nondestruct. Eval. Methods*, vol. 1, pp. 81–124, 2016.

[45] N. E. Widjonarko, "Introduction to advanced X-ray diffraction techniques for polymeric thin films," *Coatings*, vol. 6, no. 4, p. 54, Nov. 2016, doi: 10.3390/coatings6040054.

[46] M. Ermrich and D. Opper, *X-ray Powder Diffraction for the Analyst*. 2011.

[47] B. Principles, "Introduction to Powder X-Ray Diffraction History : Wilhelm Conrad Röntgen," pp. 1–38, 2001.

[48] S. R. Byrn, G. Zografi, and X. S. Chen, "X-ray Powder Diffraction," in *solid-state properties of pharmaceutical Materials*, First edit., G. Z. and X. (Sean) C. Stephen R. Byrn, Ed., John Wiley & Sons, Inc, 2017, ch. 9, pp. 107–123.

[49] D. Dollimore and S. Lerdkanchanaporn, "Thermal Analysis," *Anal. Chem.*, vol. 70, no. 12, 1998, doi: 10.1021/a19800038.

[50] F. W. Wilburn, "Introduction to thermal analysis, techniques and applications," 1989. doi: 10.1016/0040-6031(89)87162-x.

[51] M. M. Chen, *Thermal Analysis*. Tsinghua University Press Limited, 2016. doi: 10.1016/B978-0-12-805256-3.00012-X.

[52] J. L. White, "Interpretation of infrared spectra of soil minerals," *Soil Sci.*, vol. 112, no. 1, pp. 22–31, Jul. 1971, doi: 10.1097/00010694-197107000-00005.

[53] D. U. Q. Uarless, L. E. M. Ay, T. O. M. Isu, S. A. G. S. Obel, M. A. T. Akeda, and E. D. B. Rown, "M OSSBAUER SPECTROSCOPY OF 161 Dy IN DYSPROSIUM DICARBOXYLATES," in *Mössbauer Spectroscopy: Applications in Chemistry, Biology, and Nanotechnology,* First., S. virender K, K. Gostar, and N. Tetsuaki, Eds., John Wiley & Sons Ltd, 2013, pp. 116–122.

[54] C. A. Téllez S., E. Hollauer, M. A. Mondragon, and V. M. Castaño, "Fourier transform infrared and Raman spectra, vibrational assignment and ab initio calculations of terephthalic acid and related compounds," *Spectrochim. Acta - Part A Mol. Biomol. Spectrosc.*, vol. 57, no. 5, pp. 993–1007, Apr. 2001, doi: 10.1016/S1386-1425(00)00428-5.

[55] C. C. R. Sutton, G. V. Franks, and G. Da Silva, "Modeling the antisymmetric and symmetric stretching vibrational modes of aqueous carboxylate anions," *Spectrochim. Acta - Part A Mol. Biomol. Spectrosc.*, vol. 134, pp. 535–542, Jan. 2015, doi: 10.1016/j.saa.2014.06.062.

[56] D. X. Hu, P. kuan Chen, F. Luo, Y. X. Che, and J. M. Zheng, "Hydrothermal synthesis, structure and properties of two lanthanide benzenedicarboxylates, [La2(isophth)2(Hisophth)2(H2O)H2O]n and [Dy4(isophth)4(Ac)4(H2O)82H2O]n, possessing infinite Ln-O-Ln linkages," *J. Mol. Struct.*, vol. 837, no. 1–3, pp. 179–184, 2007, doi: 10.1016/j.molstruc.2006.10.027.

[57] Y. F. Zhou, F. L. Jiang, Y. Xu, R. Cao, and M. C. Hong, "Two-dimensional lanthanide-isophthalate coordination polymers containing right- and left-handed helical chains," *J. Mol. Struct.*, vol. 691, no. 1–3, pp. 191–195, 2004, doi: 10.1016/j.molstruc.2003.12.018.

[58] J. Jin, X. Wang, Y. Li, Y. Chi, and S. Niu, “Synthesis, structure, and photophysical property of series of Ln(III) coordination polymers with different carboxylato ligands (Ln 5 Sm, Eu),” *Struct. Chem.*, vol. 23, no. 5, pp. 1523–1531, Oct. 2012, doi: 10.1007/s11224-012-9957-6.

[59] P. Mahata, K. V. Ramya, and S. Natarajan, “Synthesis, structure and optical properties of rare-earth benzene carboxylates,” *Dalt. Trans.*, vol. 9226, no. 36, pp. 4017–4026, 2007, doi: 10.1039/b706363f.

[60] B. Yan, Y. Bai, and Z. Chen, “Synthesis, structure and luminescence of novel 1D chain coordination polymers [Ln(isophth)(Hisophth)(H2O)4·4H2O]n (Ln=Sm, Dy),” *J. Mol. Struct.*, vol. 741, no. 1–3, pp. 141–147, May 2005, doi: 10.1016/j.molstruc.2005.02.004.

[61] R. S. Zhou, X. B. Cui, J. F. Song, X. Y. Xu, J. Q. Xu, and T. G. Wang, “Syntheses, structures and luminescence properties of lanthanide coordination polymers with helical character,” *J. Solid State Chem.*, vol. 181, no. 8, pp. 2099–2107, 2008, doi: 10.1016/j.jssc.2008.05.011.

[62] X. J. Zheng, T. T. Zheng, and L. P. Jin, “Self-assembly of lanthanide mixed-carboxylates coordination polymers,” *J. Mol. Struct.*, vol. 740, no. 1–3, pp. 31–35, 2005, doi: 10.1016/j.molstruc.2005.01.012.

[63] I. N’Dala-Louika, D. Ananias, C. Latouche, R. Dessapt, L. D. Carlos, and H. Serier-Brault, “Ratiometric mixed Eu-Tb metal-organic framework as a new cryogenic luminescent thermometer,” *J. Mater. Chem. C*, vol. 5, no. 42, pp. 10933–10937, 2017, doi: 10.1039/c7tc03223d.

[64] V. Trannoy, I. N’Dala-Louika, J. Lhoste, T. Devic, and H. Serier-Brault, “Lanthanide Isophthalate Metal-Organic Frameworks: Crystal Structure, Thermal Behavior, and White Luminescence,” *Eur. J. Inorg. Chem.*, vol. 2021, no. 4, pp. 398–404, 2021, doi: 10.1002/ejic.202000906.

[65] A. De Betiencourt-Dias, “Isophthalato-based 2D coordination polymers of Eu(III), Gd(III), and Tb(III): Enhancement of the terbium-centered luminescence through thiophene derivatization,” *Inorg. Chem.*, vol. 44, no. 8, pp. 2734–2741, 2005, doi: 10.1021/ic048499b.

[66] Y. Qu, Y. Ke, S. Lu, R. Fan, G. Pan, and J. Li, “Hydrothermal synthesis, structures and spectroscopy of 2D lanthanide coordination polymers built from helical chains: [Ln2(BDC)3(H2O)2]n (Ln=Sm, 1; Ln=Eu, 2; BDC=1,3-benzenedicarboxylate),” *J. Mol. Struct.*, vol. 734, no. 1–3, pp. 7–13, 2005, doi: 10.1016/j.molstruc.2004.03.035.

[67] L. P. Zhang, Y. H. Wan, and L. P. Jin, “Hydrothermal synthesis and crystal structure of neodymium(III) coordination polymers with isophthalic acid and 1,10-phenanthroline,” *Polyhedron*, vol. 22, no. 7, pp. 981–987, 2003, doi: 10.1016/S0277-5387(03)00021-4.

[68] C. G. Zheng, J. Zhang, Z. F. Chen, Z. J. Guo, R. G. Xiong, and X. Z. You, “A novel three-dimensional network isophthalato-bridged lanthanide complex: {Ln[C6H4(COO-)2-1,3](CH3COO-)(H2O)2}H2O,” *J. Coord. Chem.*, vol. 55, no. 7, pp. 835–842, 2002, doi: 10.1080/00958970220000001584.

[69] C. Daiguebonne, N. Kerbellec, Y. Gérault, and O. Guillou, “A new family of luminescent lanthanide based coordination polymers,” *J. Alloys Compd.*, vol. 451, no. 1–2, pp. 372–376,

2008, doi: 10.1016/j.jallcom.2007.04.200.

[70] Y. X. Zhou, X. Q. Shen, C. X. Du, B. L. Wu, and H. Y. Zhang, "1D, 2D and 3D coordination polymers of aromatic carboxylate Tb III: Structure, thermolysis kinetics and fluorescence," *Eur. J. Inorg. Chem.*, vol. 3, no. 27, pp. 4280–4289, 2008, doi: 10.1002/ejic.200800434.

[71] S. Hussain *et al.*, "Synthesis, Crystal Structures and Photoluminescent Properties of One-Dimensional Europium(III)- and Terbium(III)-Glutarate Coordination Polymers, and Their Applications for the Sensing of Fe3+ and Nitroaromatics," *Front. Chem.*, vol. 7, no. November, pp. 1–14, Nov. 2019, doi: 10.3389/fchem.2019.00728.

[72] X. L. L. Ying Wang, T. W. Wang, Y. Song, and X. Z. You, "Slow relaxation processes and single-ion magnetic behaviors in dysprosium-Containing complexes," *Inorg. Chem.*, vol. 49, no. 3, pp. 969–976, 2010, doi: 10.1021/ic901720a.

[73] Y. H. Wan, L. P. Jin, and K. Z. Wang, "Ytterbium Coordination Polymer with Four Different Coordination Numbers: The First Structural Characterization of Lanthanide Phthalate Complex," *Chinese J. Chem.*, vol. 20, no. 9, pp. 813–815, 2002, doi: 10.1002/cjoc.20020200902.

[74] Y. Wan, L. Jin, K. Wang, L. Zhang, X. Zheng, and S. Lu, "Hydrothermal synthesis and structural studies of novel 2-D lanthanide coordination polymers with phthalic acid," *New J. Chem.*, vol. 26, no. 11, pp. 1590–1596, 2002, doi: 10.1039/b206280c.

[75] S. F. Lush and F. M. Shen, "Poly[[aquatris-(μ4-benzene-1,2-dicarboxylato)dilanthanum(III)] hemihydrate]," *Acta Crystallogr. Sect. E Struct. Reports Online*, vol. 67, no. 10, 2011, doi: 10.1107/S1600536811036282.

[76] J. Ma, Y. Jia, Y. Jing, J. Sun, Y. Yao, and X. Wang, "Preparation and luminescence properties of lanthanide (Eu3+, Sm3+) complexes and their hectorite-based composites," *Spectrochim. Acta - Part A Mol. Biomol. Spectrosc.*, vol. 75, no. 2, pp. 855–858, 2010, doi: 10.1016/j.saa.2009.12.017.

[77] M. Enculescu, N. Preda, E. Matei, and I. Enculescu, "Luminescent micro- and nanofibers based on novel europium phthalate complex," *Mater. Chem. Phys.*, vol. 136, no. 1, pp. 51–58, 2012, doi: 10.1016/j.matchemphys.2012.06.018.

[78] W. D. Song, J. Bin Yan, H. Wang, L. L. Ji, D. Y. Ma, and S. W. Ng, "Hydro(solvo)thermal synthesis and structural characterization of three lanthanide-carboxylate coordination polymers based on BDC and/or EDTA," *J. Coord. Chem.*, vol. 63, no. 4, pp. 625–633, 2010, doi: 10.1080/00958970903560056.

[79] D. Pizon, N. Henry, T. Loiseau, P. Roussel, and F. Abraham, "Synthesis, crystal structure and thermal behavior of two hydrated forms of lanthanide phthalates Ln2(O2C6H 4CO2)3(H2O) (Ln=Ce, Nd) and Nd2(O2CC6H4CO2)3(H2O)3," *J. Solid State Chem.*, vol. 183, no. 9, pp. 1943–1948, 2010, doi: 10.1016/j.jssc.2010.06.021.

[80] S. Aime, M. Bettinelli, M. Ferrari, E. Razzano, and E. Terreno, "NMR and luminescence studies on the formation of ternary adducts between HSA and Ln(III)-malonate complexes (Ln=Eu, Gd, Tb)," *Biochim. Biophys. Acta - Protein Struct. Mol. Enzymol.*, vol. 1385, no. 1, pp. 7–16, 1998, doi: 10.1016/S0167-4838(98)00024-7.

[81] B. H. Doreswamy, M. Mahendra, J. S. Prasad, P. A. Varughese, and G. Varghese, “Samarium Coordinated Polymer: Structural, Vibrational and Thermal Studies of [Sm2(C 3H2O4)3(H2O)6]n,” *J. Inorg. Organomet. Polym. Mater.*, vol. 21, no. 2, pp. 376–383, 2011, doi: 10.1007/s10904-010-9445-7.

[82] L. Cañadillas-Delgado *et al.*, “Two- and three-dimensional networks of gadolinium(III) with dicarboxylate ligands: Synthesis, crystal structure, and magnetic properties,” *Inorg. Chem.*, vol. 45, no. 26, pp. 10585–10594, 2006, doi: 10.1021/ic061173d.

[83] V. Mathew, S. Jacob, L. Xavier, and K. E. Abraham, “Spectroscopic studies of gel-grown lanthanum malonate crystals,” *J. Rare Earths*, vol. 30, no. 3, pp. 245–249, 2012, doi: 10.1016/S1002-0721(12)60039-8.

[84] X. Wenmei, W. Qiguang, Y. Lan, and Y. Rudong, “Synthesis, characterization and crystal structure of tri-aquo bimalonate malonate samarium(III) monohydrate,” *Polyhedron*, vol. 11, no. 16, pp. 2051–2054, Jan. 1992, doi: 10.1016/S0277-5387(00)83161-7.

[85] E. V. Brusau, J. C. Pedregosa, G. E. Narda, E. P. Ayala, and E. A. Oliveira, “Vibrational and thermal study of hexaaquatris(malonato)dieuropium(III) dihydrate,” *An. des la Asoc. Quim. Argentina*, vol. 92, no. 1–3, pp. 43–52, 2004.

[86] M. Hernández-Molina, P. A. Lorenzo-Luis, T. López, C. Ruiz-Pérez, F. Lloret, and M. Julve, “Generation of lanthanide coordination polymers with dicarboxylate ligands: Synthesis, structure, thermal decomposition and magnetic properties of the two-dimensional triaquatris(malonato)dipraseodymium(III) dihydrate {[Pr2(C3H2O4)3(H2O)3];·2H2O},” *CrystEngComm*, vol. 2, no. 31, pp. 169–173, 2000, doi: 10.1039/b006256l.

[87] P. Silva, J. A. Fernandes, and F. A. Almeida Paz, “Catena-Poly[[triaquachlorido-μ3-malonato-cerium(III)] hemihydrate],” *Acta Crystallogr. Sect. E Struct. Reports Online*, vol. 66, no. 12, 2010, doi: 10.1107/S1600536810044727.

[88] B. H. Doreswamy *et al.*, “A novel three-dimensional polymeric structure of crystalline neodymium malonate hydrate,” *Mater. Lett.*, vol. 59, no. 10, pp. 1206–1213, Apr. 2005, doi: 10.1016/j.matlet.2004.12.029.

[89] F. Marrot and J.C. Trombe, “Synthesis, Characterization and Structure of a Diaqua Lanthanum Bimalonate Malonate Monohydrate,” vol. 13, no. 12, pp. 1931–1935, 1994.

[90] T. J. Kemp, P. A. Read, and R. Neal Beatty, “Ligated lanthanide clusters in the fast atom bombardment of lanthanide carboxylates,” *Inorganica Chim. Acta*, vol. 238, no. 1–2, pp. 109–114, 1995, doi: 10.1016/0020-1693(95)04699-A.

[91] K. E. Chrysomallidou, S. P. Perlepes, A. Terzis, and C. P. Raptopoulou, “Synthesis, crystal structures and spectroscopic studies of praseodymium(III) malonate complexes,” *Polyhedron*, vol. 29, no. 16, pp. 3118–3124, Oct. 2010, doi: 10.1016/j.poly.2010.08.020.

[92] M. Hernández-Molina *et al.*, “A phase transition in the novel three-dimensional compound [Eu2(mal)3(H2O)6] (H2mal = malonic acid),” *J. Chem. Soc. Dalt. Trans.*, vol. 2, no. 18, pp. 3462–3470, 2002, doi: 10.1039/b202649j.

[93] F. S. Delgado *et al.*, “Crystal growth and structural remarks on malonate-based lanthanide

coordination polymers," *CrystEngComm*, vol. 18, no. 40, pp. 7831–7842, 2016, doi: 10.1039/c6ce01360k.

[94] F. S. Delgado *et al.*, "Crystal growth and structural remarks on malonate-based lanthanide coordination polymers," *CrystEngComm*, vol. 18, no. 40, pp. 7831–7842, 2016, doi: 10.1039/c6ce01360k.

[95] M. Hernández-Molina, C. Ruiz-Pérez, T. López, F. Lloret, and M. Julve, "Ferromagnetic coupling in the three-dimensional malonato-bridged gadolinium(III) complex [Gd2(mal)3(H2O)6 (H2mal = malonic acid)," *Inorg. Chem.*, vol. 42, no. 18, pp. 5456–5458, 2003, doi: 10.1021/ic034175w.

[96] B. H. Doreswamy *et al.*, "Structural studies on praseodymium malonate hydrate," *J. Mol. Struct.*, vol. 659, no. 1–3, pp. 81–88, 2003, doi: 10.1016/j.molstruc.2003.08.001.

[97] S. Hussain *et al.*, "Synthesis, thermal, structural analyses and photoluminescent properties of a new family of malonate-containing Lanthanide(III) coordination polymers," *Front. Chem.*, vol. 7, no. APR, pp. 1–16, 2019, doi: 10.3389/fchem.2019.00260.

[98] P. L. Liu, W. Cao, J. Wang, R. H. Zeng, and Z. Zeng, "Poly[diaquabis-(μ 4-fumarato-k 4O 1:O 1′:O 4:O 4′)(μ 4- fumarato-k 6 O 1:O 1,O 1′:O 4:O 4,O 4′)(μ 2-fumaric acid-k 2 O 1:O 4)dipraseodymium(III)]," *Acta Crystallogr. Sect. E Struct. Reports Online*, vol. 67, no. 10, 2011, doi: 10.1107/S1600536811038347.

[99] C. K. Oliveira, J. R. De Menezes Vicenti, R. A. Burrow, S. Alves, R. L. Longo, and I. Malvestiti, "Exploring the mechanism of in situ formation of oxalic acid for producing mixed fumarato-oxalato lanthanide (Eu, Tb and Gd) frameworks," *Inorg. Chem. Commun.*, vol. 22, pp. 54–59, 2012, doi: 10.1016/j.inoche.2012.04.036.

[100] B. Benmerad, K. Aliouane, N. Rahahlia, A. Guehria-Laïdoudi, S. Dahaoui, and C. Lecomte, "Studies of two lanthanide coordination polymers built up from dinuclear units," *J. Rare Earths*, vol. 31, no. 1, pp. 85–93, 2013, doi: 10.1016/S1002-0721(12)60240-3.

[101] S. L. Yao *et al.*, "Three Gd-Based Metal-Organic Frameworks Constructed from Similar Dicarboxylate Ligands with Large Magnetic Entropy Changes," *ChemistrySelect*, vol. 2, no. 33, pp. 10673–10677, Nov. 2017, doi: 10.1002/slct.201702223.

[102] K. Chainok *et al.*, "Temperature-dependent 3D structures of lanthanide coordination polymers based on dicarboxylate mixed ligands," *CrystEngComm*, vol. 20, no. 46, pp. 7446–7457, 2018, doi: 10.1039/c8ce01430b.

[103] N. Pawlak, G. Oczko, and P. Starynowicz, "Synthesis, crystal structure, and photoluminescence of lanthanide fumarates (Ln = Sm, Eu, Nd, Er)," *Polyhedron*, vol. 101, pp. 152–159, Nov. 2015, doi: 10.1016/j.poly.2015.08.037.

[104] B. Xu, Q. Chen, H. M. Hu, R. An, X. Wang, and G. Xue, "Hydrothermal syntheses, crystal structures, and luminescence properties of lanthanide-based coordination polymers constructed by sulfonate functionalized imidazophenanthroline derivative ligand," *Cryst. Growth Des.*, vol. 15, no. 5, pp. 2318–2329, 2015, doi: 10.1021/acs.cgd.5b00117.

[105] N. Rahahlia, K. Aliouane, A. Guehria-Laidoudi, S. Dahaoui, and C. Lecomte, "Poly[[tetra-aquadi-μ-5-fumarato-μ-4-fumarato- diholmium(III)] trihydrate]," *Acta Crystallogr. Sect. E*

Struct. Reports Online, vol. 63, no. 5, pp. 1266–1268, 2007, doi: 10.1107/S1600536807016479.

[106] X. Li and Y. Q. Zou, "Hydrothermal synthesis and crystal structure of a new europium fumarate compound," *J. Chem. Crystallogr.*, vol. 35, no. 5, pp. 351–355, 2005, doi: 10.1007/s10870-005-1515-2.

[107] B. Li and L. X. Wu, "Poly[[hexaaqua(μ2-fumarato-κ4O 1,O1′:O4,O4′) bis(μ3-maleato-κ4 O1,O 1′:O4:O4′)disamarium(III)] hexahydrate]," *Acta Crystallogr. Sect. E Struct. Reports Online*, vol. 66, no. 12, pp. 148–155, 2010, doi: 10.1107/S1600536810045204.

[108] X. Li, T. T. Zhang, Z. Y. Zhang, and Y. L. Ju, "Hydrothermal synthesis, crystal structure and luminescence properties of lanthanide fumarate coordination polymers containing 2,2′-bipyridine," *J. Coord. Chem.*, vol. 60, no. 24, pp. 2721–2729, 2007, doi: 10.1080/00958970701308658.

[109] L. Zhao, G. F. Xu, and J. Tang, "Carboxylato-bridged 3D polymeric networks of Pr(III): Synthesis, crystal structure, magnetic property and thermal behavior," *J. Mol. Struct.*, vol. 979, no. 1–3, pp. 160–164, 2010, doi: 10.1016/j.molstruc.2010.06.019.

[110] A. Michaelides, S. Skoulika, E. G. Bakalbassis, and J. Mrozinski, "Cyclic water hexamers and decamers in a porous lanthanide-organic framework: Correlation between some physical properties and crystal structure," *Cryst. Growth Des.*, vol. 3, no. 4, pp. 487–492, 2003, doi: 10.1021/cg034025w.

[111] L. P. Zhang, L. Huang, L. bo Qu, H. Peng, and Y. F. Zhao, "Two novel R- and S-malato-bridged coordination polymers by reacting lanthanide chloride and maleic anhydride, 1,10-phenanthroline at hydrothermal condition," *J. Mol. Struct.*, vol. 787, no. 1–3, pp. 14–17, 2006, doi: 10.1016/j.molstruc.2005.10.026.

[112] X. F. Tan, J. Zhou, L. Fu, H. P. Xiao, H. H. Zou, and Q. Tang, "A series of new lanthanide fumarates displaying three types of 3-D frameworks," *Dalt. Trans.*, vol. 45, no. 12, pp. 5253–5261, 2016, doi: 10.1039/c6dt00205f.

[113] G. Zhang, Q. Wang, Y. Qian, G. Yang, and J. Shi Ma, "Synthesis, characterization and photoluminescence properties of two new europium(III) coordination polymers with 3D open framework," *J. Mol. Struct.*, vol. 796, no. 1–3, pp. 187–194, 2006, doi: 10.1016/j.molstruc.2006.01.048.

[114] S. T. Yang, K. Zhang, B. Zhang, and H. Huang, "Fumaric Acid," *Compr. Biotechnol. Second Ed.*, vol. 3, pp. 163–177, 2011, doi: 10.1016/B978-0-08-088504-9.00456-6.

[115] L. Huang and L. P. Zhang, "Hydrothermal synthesis and structural characterization of three novel lanthanide coordination polymers with fumarate and 1,10-phenanthroline," *J. Mol. Struct.*, vol. 692, no. 1–3, pp. 249–253, 2004, doi: 10.1016/j.molstruc.2004.02.012.

[116] W. H. Zhu, Z. M. Wang, and S. Gao, "Two 3D porous lanthanide-fumarate-oxalate frameworks exhibiting framework dynamics and luminescent change upon reversible de- and rehydration," *Inorg. Chem.*, vol. 46, no. 4, pp. 1337–1342, 2007, doi: 10.1021/ic061833e.

[117] J. Yang and S. W. Ng, "Poly[[tetraaquabis(μ4-fumarato-κ4 O:O′:O″:O‴)(μ2-fumarato- κ4

O,O′:O″,O‴) diterbium(III)] N,N-dimethylformamide solvate]," *Acta Crystallogr. Sect. E Struct. Reports Online*, vol. 63, no. 4, pp. 1168–1170, 2007, doi: 10.1107/S1600536807011282.

[118] W. H. Zhu, Z. M. Wang, and S. Gao, "A 3D porous lanthanide-fumarate framework with water hexamer occupied cavities, exhibiting a reversible dehydration and rehydration procedure," *Dalt. Trans.*, no. 6, pp. 765–768, 2006, doi: 10.1039/b515151a.

[119] B. Sieklucka *et al.*, "Towards high Tc octacyanometalate-based networks," *CrystEngComm*, vol. 11, no. 10, pp. 2032–2039, 2009, doi: 10.1039/b905912a.

[120] H. Anana, C. Trifa, S. Bouacida, C. Boudaren, and H. Merazig, "Hydrothermal synthesis and crystal structure of a new lanthanum(III) coordination polymer with fumaric acid," *Acta Crystallogr. Sect. E Crystallogr. Commun.*, vol. E71, pp. m114–m115, 2015, doi: 10.1107/S2056989015007008.

[121] G. Zhang, G. Yang and J.S. Ma, "Hydrothermal Syntheses and Characterization of Novel 3D Open-Framework and 2D Grid Lanthanide Fumarates: Ln2(fum)3(H2fum)(H2O)2 (Ln=Ce or Nd), [Sm2(fum)3(H2O)4](H2O)3, and [Yb2(fum)3(H2O)4](H2O)2," Crystal Growth and Design, vol. 6, no. 4, pp. 933–939, 2006.

[122] A. Thirumurugan and S. Natarajan, "Inorganic-organic hybrid compounds: Synthesis and structures of new metal organic polymers synthesized in the presence of mixed dicarboxylates," *Eur. J. Inorg. Chem.*, vol. 2004, no. 4, pp. 762–770, Feb. 2004, doi: 10.1002/ejic.200300594.

[123] R. A. Zehnder *et al.*, "Network dimensionality and ligand flexibility in lanthanide terephthalate hydrates," *J. Mol. Struct.*, vol. 985, no. 1, pp. 109–119, Jan. 2011, doi: 10.1016/j.molstruc.2010.10.030.

[124] L. Pan *et al.*, "Synthesis, characterization and structural transformation of a condensed rare earth metal coordination polymer," *Inorg. Chem.*, vol. 40, no. 5, pp. 828–830, Feb. 2001, doi: 10.1021/ic0007254.

[125] P. Wang, Z. F. Li, L. P. Song, C. X. Wang, and Y. Chen, "Catena-poly[[[μ-benzene-1,4-dicarboxylato-bis[tetraaqualutetium(III)]] -di-μ-benzene-1,4-dicarboxylato] dihydrate]," *Acta Crystallogr. Sect. E Struct. Reports Online*, vol. 62, no. 2, pp. m253–m255, Feb. 2006, doi: 10.1107/S1600536806000225.

[126] C. Daiguebonne, N. Kerbellec, K. Bernot, Y. Gérault, A. Deluzet, and O. Guillou, "Synthesis, crystal structure, and porosity estimation of hydrated erbium terephthalate coordination polymers," *Inorg. Chem.*, vol. 45, no. 14, pp. 5399–5406, Jul. 2006, doi: 10.1021/ic060241t.

[127] T. M. Reineke, M. Eddaoudi, M. Fehr, D. Kelley, and O. M. Yaghi, "From condensed lanthanide coordination solids to microporous frameworks having accessible metal sites," *J. Am. Chem. Soc.*, vol. 121, no. 8, pp. 1651–1657, Mar. 1999, doi: 10.1021/ja983577d.

[128] C. Serre, F. Millange, J. Marrot, and G. Férey, "Hydrothermal synthesis, structure determination, and thermal behavior of new three-dimensional europium terephthalates," *Chem. Mater.*, vol. 14, no. 5, pp. 2409–2415, May 2002, doi: 10.1021/cm0211148.

[129] Y. Cheddani *et al.*, “Elaboration, structural characterization, thermal behavior and visible region photoluminescence properties of two series of lanthanide-based coordination polymers,” *J. Mol. Struct.*, vol. 1327, p. 141238, 2025, doi: 10.1016/j.molstruc.2024.141238.

[130] C. G. Wang *et al.*, “Synthesis, crystal structures and properties of a series of three-dimensional lanthanide coordination polymers with the rigid and flexible mixed dicarboxylate ligands of 1,4-benzene dicarboxylic acid and succinic acid,” *J. Mol. Struct.*, vol. 921, no. 1–3, pp. 126–131, 2009, doi: 10.1016/j.molstruc.2008.12.057.

[131] M. C. Bernini, N. Snejko, E. Gutierrez-Puebla, E. V. Brusau, G. E. Narda, and M. Á. Monge, “Structure-directing and template roles of aromatic molecules in the self-assembly formation process of 3D holmium-succinate MOFs,” *Inorg. Chem.*, vol. 50, no. 13, pp. 5958–5968, 2011, doi: 10.1021/ic102472u.

[132] S. Chule, S. Jonnalagadda, and Current, “Synthesis, structure and luminescence property of a 3D coordination polymer based on La(III) and terephthalic acid,” no. November, 2018, doi: 10.20944/preprints201811.0244.v1.

[133] C. Daiguebonne *et al.*, “Structural and luminescent properties of micro- and nanosized particles of lanthanide terephthalate coordination polymers,” *Inorg. Chem.*, vol. 47, no. 9, pp. 3700–3708, May 2008, doi: 10.1021/ic702325m.

[134] R. Decadt *et al.*, “Synthesis, crystal structures, and luminescence properties of carboxylate based rare-earth coordination polymers,” *Inorg. Chem.*, vol. 51, pp. 11623–11634, 2012, doi: 10.1021/ic301544q.

[135] P. Gil-Mateo, X. Wang, and A. J. Jacobson, “Synthesis and structures of novel lanthanide benzenedicarboxylates,” *Mater. Res. Soc. Symp. Proc.*, vol. 1148, pp. 88–93, 2008, doi: 10.1557/proc-1148-pp08-02.

[136] J. Perles, M. Iglesias, C. Ruiz-Valero, and N. Snejko, “Rare-earths as catalytic centres in organo-inorganic polymeric frameworks,” *J. Mater. Chem.*, vol. 14, no. 17, pp. 2683–2689, 2004, doi: 10.1039/b314220e.

[137] W. Nika, I. Pantenburg, and G. Meyer, “Poly[[[triaquaerbium(III)]-μ3-succinato] chloride dihydrate],” *Acta Crystallogr. Sect. E Struct. Reports Online*, vol. 61, no. 1, pp. m138–m140, Jan. 2005, doi: 10.1107/S1600536804032635.

[138] G. H. Cui, J. R. Li, R. H. Zhang, and X. H. Bu, “Hydrothermal synthesis, crystal structures and luminescent properties of two new Ln(III)-succinate (Ln=Eu, Tb) complexes exhibiting three dimensional networks,” *J. Mol. Struct.*, vol. 740, no. 1–3, pp. 187–191, Apr. 2005, doi: 10.1016/j.molstruc.2005.01.049.

[139] A. Seguatni, M. Fakhfakh, M. J. Vauley, and N. Jouini, “Synthesis, structure, and characterization of hybrid materials: [Ce(H 2O)]2[O2C(CH2)2CO 2]3 and [Sm(H2O)]2[O 2C(CH2)2CO2]3·H2O,” *J. Solid State Chem.*, vol. 177, no. 10, pp. 3402–3410, Oct. 2004, doi: 10.1016/j.jssc.2004.05.042.

[140] J. Perles, M. Iglesias, C. Ruiz-Valero, and N. Snejko, “First high thermally stable organo–inorganic 3D polymer scandium derivative as a heterogeneous Lewis acid catalyst,” *Chem.*

Commun., vol. 3, no. 3, pp. 346–347, Jan. 2003, doi: 10.1039/b210034g.

[141] Q. He, J. F. Zi, and F. J. Zhang, "Poly[diaqua-μ6-succinato-di-μ5-succinato-dineodymium(III)]," *Acta Crystallogr. Sect. E Struct. Reports Online*, vol. 62, no. 6, pp. m1266–m1267, Jun. 2006, doi: 10.1107/S1600536806016278.

[142] Y. C. Chen *et al.*, "Gadolinium(III)-hydroxy ladders trapped in succinate frameworks with optimized magnetocaloric effect," *Chem. - A Eur. J.*, vol. 19, no. 40, pp. 13504–13510, Sep. 2013, doi: 10.1002/chem.201301221.

[143] N. A. Ashashi, M. Kumar, Z. ul Nisa, A. Frontera, S. C. Sahoo, and H. N. Sheikh, "Solvothermal self assembly of three lanthanide(III)-succinates: Crystal structure, topological analysis and DFT calculations on water channel," *J. Mol. Struct.*, vol. 1245, p. 131094, Dec. 2021, doi: 10.1016/j.molstruc.2021.131094.

[144] N. Scales *et al.*, "Neodymium coordination polymers with propionate, succinate and mixed succinate-oxalate ligands: Synthesis, structures and spectroscopic characterization," *Polyhedron*, vol. 102, pp. 130–136, Dec. 2015, doi: 10.1016/j.poly.2015.07.065.

[145] Z. Amghouz *et al.*, "Yttrium-succinates coordination polymers: Hydrothermal synthesis, crystal structure and thermal decomposition," *J. Solid State Chem.*, vol. 182, no. 12, pp. 3365–3373, Dec. 2009, doi: 10.1016/j.jssc.2009.09.027.

[146] X. J. Zhang, Y. H. Xing, J. Han, X. Q. Zeng, M. F. Ge, and S. Y. Niu, "A series of novel ln-succinate-oxalate coordination polymers: Synthesis, structure, thermal stability, and fluorescent properties," *Cryst. Growth Des.*, vol. 8, no. 10, pp. 3680–3688, Oct. 2008, doi: 10.1021/cg800294c.

[147] M. C. Bernini *et al.*, "The effect of hydrothermal and non-hydrothermal synthesis on the formation of holmium(III) succinate hydrate frameworks," *Eur. J. Inorg. Chem.*, vol. 2007, no. 5, pp. 684–693, Feb. 2007, doi: 10.1002/ejic.200600860.

[148] M. C. Bernini, N. Snejko, E. Gutierrez-Puebla, E. V. Brusau, G. E. Narda, and M. Á. Monge, "Structure-directing and template roles of aromatic molecules in the self-assembly formation process of 3D holmium-succinate MOFs," *Inorg. Chem.*, vol. 50, no. 13, pp. 5958–5968, Jul. 2011, doi: 10.1021/ic102472u.

[149] C. A. F. De Oliveira *et al.*, "Synthesis, characterization, luminescent properties and theoretical study of two new coordination polymers containing lanthanide [Ce(III) or Yb(III)] and succinate ions," *J. Mol. Struct.*, vol. 1041, pp. 61–67, Jun. 2013, doi: 10.1016/j.molstruc.2013.03.001.

[150] Y. X. Chi, T. S. Liu, J. Jin, G. N. Zhang, and S. Y. Niu, "Synthesis, structures and near-infrared luminescence properties of Ho 3+ and Yb3+ coordination complexes," *J. Phys. Chem. Solids*, vol. 74, no. 12, pp. 1745–1750, Dec. 2013, doi: 10.1016/j.jpcs.2013.07.002.

[151] M. C. Bernini *et al.*, "Tapes of water hexamer clusters in the interlayer space of a 2D MOF: Structural, spectroscopic and computational insight of the confined water," *Polyhedron*, vol. 31, no. 1, pp. 729–737, 2012, doi: 10.1016/j.poly.2011.10.030.

[152] S. C. Manna, E. Zangrando, A. Bencini, C. Benelli, and N. R. Chaudhuri, "Syntheses, crystal structures, and magnetic properties of [Ln^{III}2(succinate)3(H2O)2]0.5H2O [Ln = Pr,

Nd, Sm, Eu, Gd, and Dy] polymeric networks: Unusual ferromagnetic coupling in Gd derivative," *Inorg. Chem.*, vol. 45, no. 22, pp. 9114–9122, 2006, doi: 10.1021/ic060807d.

[153] Y. F. Zhou, F. L. Jiang, D. Q. Yuan, B. L. Wu, and M. C. Hong, "Blue-greenish photoluminescent Gd(III) complexes with flexible succinate ligand," *J. Mol. Struct.*, vol. 743, no. 1–3, pp. 21–27, 2005, doi: 10.1016/j.molstruc.2005.02.016.

[154] M. C. Bernini, J. C. Garro, E. V. Brusau, G. E. Narda, and E. L. Varetti, "Experimental and theoretical vibrational study of tetraaquatris(succinate)diholmium(III) hexahydrate, a bidimensional hybrid coordination polymer," *J. Mol. Struct.*, vol. 888, no. 1–3, pp. 113–123, 2008, doi: 10.1016/j.molstruc.2007.11.036.

[155] N. Rahahlia, B. Benmerad, A. Guehria-Laïdoudi, S. Dahaoui, and C. Lecomte, "Three-dimensional ionic frameworks built up from La (III) and Ce (III) succinates," *J. Mol. Struct.*, vol. 833, no. 1–3, pp. 42–48, 2007, doi: 10.1016/j.molstruc.2006.08.029.

[156] N. Rahahlia, K. Alioune, A. Guehria-Laidoudi, S. Dahaoui, and C. Lecomte, "Poly[[tetraaquadi-μ4-succinato-μ5-succinato- diytterbium(III)] hexahydrate]," *Acta Crystallogr. Sect. E Struct. Reports Online*, vol. 62, no. 10, pp. m2543–m2545, 2006, doi: 10.1107/S1600536806036002.

[157] G. Y. Dong, G. H. Cui, and J. Lin, "Poly[diaquadi-μ6-succinato-μ5-succinato-dierbium(III)]," *Acta Crystallogr. Sect. E Struct. Reports Online*, vol. 62, no. 4, pp. m738–m740, Apr. 2006, doi: 10.1107/S1600536806007938.

[158] C. X. Wang, Y. Li, Q. H. Zhang, D. J. Cai, and X. B. Xie, "Poly[diaquadi-μ5-succinato-μ6-succinato- didysprosium(III)]," *Acta Crystallogr. Sect. E Struct. Reports Online*, vol. 62, no. 3, pp. m545–m547, Mar. 2006, doi: 10.1107/S1600536806002868.

[159] M. C. Bernini *et al.*, "Reversible breaking and forming of Metal-Ligand coordination bonds: Temperature-Triggered Single-Crystal to Single-Crystal transformation in a Metal-Organic framework," *Chem. - A Eur. J.*, vol. 15, no. 19, pp. 4896–4905, May 2009, doi: 10.1002/chem.200802385.

[160] B. Yu, C. Z. Xie, X. Q. Wang, R. J. Wang, G. Q. Shen, and D. Z. Shen, "Synthesis, crystal structures and luminescent properties of two new Ln(III)-dicarboxylate (Ln=Eu, Tb) complexes exhibiting three dimensional networks," *J. Coord. Chem.*, vol. 60, no. 17, pp. 1817–1825, Sep. 2007, doi: 10.1080/00958970701194074.

[161] W. L. Soon, "Two-Dimensional Lanthanum-BDC Coordination Polymer," *J. Korean Chem. Soc.*, vol. 45, no. 6, pp. 507–512, 2001.

[162] V. Kiritsis, A. Michaelides, S. Skoulika, S. Golhen, and L. Ouahab, "Assembly of a Porous Three-Dimensional Coordination Polymer: Crystal Structure of {[La2(adipate)3(H2O)4]6H2O} n," *Inorg. Chem.*, vol. 37, no. 13, pp. 3407–3410, Jun. 1998, doi: 10.1021/ic980014u.

[163] Kim, M. Suh, and D.-Y. Jung, "Crystal Structure and Spectroscopic Study of Novel Two- and Three-Dimensional Photoluminescent Eu(III)−Adipate Compounds," *Inorg. Chem.*, vol. 43, no. 1, pp. 245–250, Jan. 2004, doi: 10.1021/ic034418k.

[164] D. T. de Lill, N. S. Gunning, and C. L. Cahill, "Toward Templated Metal−Organic

Frameworks: Synthesis, Structures, Thermal Properties, and Luminescence of Three Novel Lanthanide−Adipate Frameworks," *Inorg. Chem.*, vol. 44, no. 2, pp. 258–266, Jan. 2005, doi: 10.1021/ic048755k.

[165] G. Punte *et al.*, "Magnetic and structural properties of two open-frameworks Nd(III) adipates," *Comptes Rendus. Chim.*, vol. 8, no. 9–10, pp. 1469–1476, Apr. 2005, doi: 10.1016/j.crci.2004.07.003.

[166] X.-F. Tan *et al.*, "Synthesis, Crystal Structures and Properties of a Series of Lanthanide Adipates [Ln 2(ad)3(H2O)4] (Ln = Y3+, Ho3+, Er3+, Tm3+)," *J. Clust. Sci.*, vol. 27, no. 6, pp. 2025–2033, Nov. 2016, doi: 10.1007/s10876-016-1066-z.

[167] A. Michaelides and S. Skoulika, "Anion-Induced Formation of Lanthanide-Organic Chains From 3D Framework Solids. Anion Exchange in a Crystal-to-Crystal Manner," *Cryst. Growth Des.*, vol. 9, no. 5, pp. 2039–2042, May 2009, doi: 10.1021/cg801138e.

[168] L.-M. Duan, J.-Q. Xu, F.-T. Xie, Y.-B. Liu, and H. Ding, "A novel three-dimensional open framework constructed from infinite chains of edge-sharing CeO8(H2O) polyhedron: [Ce2(ad)3(H2O)2]n," *Inorg. Chem. Commun.*, vol. 7, no. 2, pp. 216–219, Feb. 2004, doi: 10.1016/j.inoche.2003.11.004.

[169] F.-F. Li, H.-J. Zhang, and L.-N. Zhang, "Poly[[tetraaquatris(μ 3 -hexane-1,6-dicarboxylato)diterbium(III)] 0.25-hydrate]," *Acta Crystallogr. Sect. E Struct. Reports Online*, vol. 67, no. 4, pp. m412–m412, Apr. 2011, doi: 10.1107/S1600536811007719.

[170] Y.-B. Ding, X.-H. Shi, Y. Cheng, J. Zhang, Y.-G. Yin, and W.-H. Gao, "Polycatenated (4,4) lanthanide(III) coordination networks based on apidate: Synthesis, structure and properties," *Inorg. Chem. Commun.*, vol. 12, no. 7, pp. 695–697, Jul. 2009, doi: 10.1016/j.inoche.2009.05.032.

[171] C. Bromant, H. Flemig, W. Nika, I. Pantenburg, and G. Meyer, "Selten-Erd-Metall-Koordinationspolymere: Synthese und Kristallstrukturen von fünf neuen Adipinaten, [M2 (Adi)3(H2O)4](AdiH2)(H2O)4 (M = La, Nd), [Er(Adi)(H2O)5]Cl(H2O) und [M(Adi)(H2O)5](NO3)(H2O) (M = Gd, Er)," *Zeitschrift für Anorg. und Allg. Chemie*, vol. 632, no. 5, pp. 851–858, Apr. 2006, doi: 10.1002/zaac.200500464.

[172] D. S. Chowdhuri, S. Kumar Jana, D. Hazari, E. Zangrando, and S. Dalai, "Topological aspects of lanthanide–adipate–aqua compounds: Close packed and open framework structures," *J. Solid State Chem.*, vol. 203, pp. 128–133, Jul. 2013, doi: 10.1016/j.jssc.2013.04.025.

[173] M. Kariem, M. Kumar, M. Yawer, and H. N. Sheikh, "Solvothermal synthesis and structure of coordination polymers of Nd(III) and Dy(III) with rigid isophthalic acid derivatives and flexible adipic acid," *J. Mol. Struct.*, vol. 1150, no. Iii, pp. 438–446, Dec. 2017, doi: 10.1016/j.molstruc.2017.08.111.

[174] M. Kumar *et al.*, "Magnetic, luminescence, topological and theoretical studies of structurally diverse supramolecular lanthanide coordination polymers with flexible glutaric acid as a linker," *New J. Chem.*, vol. 43, no. 36, pp. 14546–14564, 2019, doi: 10.1039/c9nj03664d.

[175] R. A. Zehnder, N. C. Fontaine, M. Zeller, and R. A. Renn, "Poly[[tetraaquadi-μ4-glutarato-μ2- terephthalato-dineodymium(III)] heptadecahydrate]," *Acta Crystallogr. Sect. C Cryst. Struct. Commun.*, vol. 66, no. 12, pp. m371–m374, Dec. 2010, doi: 10.1107/S0108270110044872.

[176] S. Yimklan *et al.*, "Base-Directed Formation of Isostructural Lanthanide-Sulfate-Glutarate Coordination Polymers with Photoluminescence," *ACS Omega*, Jan. 2023, doi: 10.1021/acsomega.3c08506.

[177] R. M. Nair, M. R. Sudarsanakumar, S. Suma, M. R. Prathapachandra Kurup, and P. K. Sudhadevi Antharjanam, "Poly[tetraaquatriglutaratodicerium(III) decahydrate], a novel luminescent metal-organic framework possessing hydrophilic hexagonal channels," *J. Chem. Sci.*, vol. 128, no. 9, pp. 1385–1393, Sep. 2016, doi: 10.1007/s12039-016-1137-6.

[178] B. Benmerad, A. Guehria-Laïdoudi, S. Dahaoui, and C. Lecomte, "A polynuclear coordination glutarate of lanthanum(III) with an uncommon cage feature," *Acta Crystallogr. Sect. C Cryst. Struct. Commun.*, vol. 60, no. 3, pp. m119–m122, Mar. 2004, doi: 10.1107/S0108270104000848.

[179] R. Vaidhyanathan, S. Natarajan, and C. N. R. Rao, "A chiral mixed carboxylate, [Nd4(H2O) 2(OOC(CH2)3COO)4(C2O 4)2], exhibiting NLO properties," *J. Solid State Chem.*, vol. 177, no. 4–5, pp. 1444–1448, 2004, doi: 10.1016/j.jssc.2003.11.026.

[180] F. Serpaggi and G. Férey, "Synthesis and characterization of a new three-dimensional praseodymium glutarate with perforated layers [Pr4(H2O)2] [O2C(CH2)3CO2]8· 4H2O[MIL-75]," *J. Mol. Struct.*, vol. 656, no. 1–3, pp. 201–206, 2003, doi: 10.1016/S0022-2860(03)00338-7.

[181] R. A. Zehnder *et al.*, "Conversion of lanthanide glutarate chlorides with interstitial THF into lanthanide glutarates with unprecedented topologies," *Inorganica Chim. Acta*, vol. 471, pp. 502–512, 2018, doi: 10.1016/j.ica.2017.11.050.

[182] T. Głowiak, Dao-Cong Ngoan, and J. Legendziewicz, "Structure of diaquatriglutaratodineodymium(III) dihydrate," *Acta Crystallogr. Sect. C Cryst. Struct. Commun.*, vol. 42, no. 11, pp. 1494–1496, 1986, doi: 10.1107/s0108270186091710.

[183] T. Glowiak and al., "Crystal Structure and Spectroscopy of Lanthanide Complexes with Glutaric Acid [Ln(C5H604)(H20)3] ClO4," vol. 34, pp. 153–168, 1987.

[184] X. F. Tan, J. Zhou, H. H. Zou, L. Fu, Q. Tang, and P. Wang, "A series of lanthanide glutarates: lanthanide contraction effect on crystal frameworks of lanthanide glutarates," *RSC Adv.*, vol. 7, no. 29, pp. 17934–17940, 2017, doi: 10.1039/c7ra01552f.

[185] S. Yimklan, Y. Chimupala, S. Wongngam, and N. Kaeosamut, "Crystal structure of a three-dimensional neodymium(III) coordination polymer, [Nd2(H2O)6(glutarato)(SO4)2]n," *Acta Crystallogr. Sect. E Crystallogr. Commun.*, vol. 78, no. 2, pp. 159–163, Feb. 2022, doi: 10.1107/S2056989022000159.

[186] D. Wei, S. Huang, J. Sun, and Y. Zheng, "Crystal structure of diaquadidysprosium triglutarate tetrahydrate , Dy2(H2O)2[O2C(CH2)3CO2]3 4H2O," *Z. Krist. NCS*, vol. 221, pp. 7–8, 2006.

[187] F. Serpaggi, and G. Férey, “Synthesis and crystal structure of MIL-8, a series of lanthanide glutarate with an open framework, [Ln(H2O)]2[O2C(CH2)3CO2]3.4H2O,” *J. Mater. Chem.*, vol. 8, pp. 2737–2741, 1998.

[188] F. Serpaggi, T. Luxbacher, A. K. Cheetham, and G. Férey, “Dehydration and rehydration processes in microporous rare-earth dicarboxylates: A study by thermogravimetry, thermodiffractometry and optical spectroscopy,” *J. Solid State Chem.*, vol. 145, no. 2, pp. 580–586, 1999, doi: 10.1006/jssc.1999.8305.

[189] Y.J. Kim, Y.J. Park, and D.Y. Jung, “Two-dimensional carboxylate bridged network of europium(III)-transition metal (II) glutarate compounds,” *Dalton Trans.* pp. 2603–2609, 2005.

[190] B. Benmerad *et al.*, “Polymeric aqua (glutarato)(hydrogen glutarato)lanthanum (III) monohydrate,” C56, pp. 789–792, 2000.

[191] S. Hussain, I. U. Khan, W. T. A. Harrison, and M. N. Tahir, “Crystal structures and characterization of two rare-earth-glutarate coordination networks: One-dimensional [Nd(C5H6O4)(H2O)4]•Cl and three-dimensional [Pr(C5H6O4)(C5H7O4)(H2O)]•H2O,” *J. Struct. Chem.*, vol. 56, no. 5, pp. 934–941, 2015, doi: 10.1134/S0022476615050169.

[192] J. Legendziewicz, B. Keller, I. Turowska-Tyrk, and W. Wojciechowski, “Synthesis, optical and magnetic properties of homo- and heteronuclear systems and glasses containing them,” *New J. Chem.*, vol. 23, no. 11, pp. 1097–1103, 1999, doi: 10.1039/a905284d.

[193] C. Bromant, W. Nika, I. Pantenburg, and G. Meyer, “Selten-erd-metall-koordinationspolymere: Synthesen und kristallstrukturen von drei neuen glutaraten, [Pr2(Glu)3(H2O)4]·10,5H2O, [Pr(Glu)(H2O)2]Cl und [Er(Glu)(GluH)(H2O)2],” *Zeitschrift fur Anorg. und Allg. Chemie*, vol. 631, no. 12, pp. 2416–2422, 2005, doi: 10.1002/zaac.200500253.

[194] P. Thomas and J. C. Trombe, “Synthesis and crystal structure of [Tb4(H2O)2](C2O4)2(C5H6O4)4,” *J. of Chemical Crystallograohy*, vol. 30, no. 10, pp. 633–639, 2001.

Abstract

This research focuses on the synthesis and characterization of coordination polymers based on rare earth elements, particularly lanthanum(III). Various rigid (aromatic) and flexible (aliphatic) dicarboxylic acid ligands were used in both single- and mixed-ligand systems. The compounds were synthesized using hydrothermal, reflux, and ambient temperature methods and characterised by FT-IR, PXRD, and TGA. The results revealed diverse structural features, coordination modes, and thermal behaviors, influenced by ligand type and reaction conditions. Some compounds showed potential novelty based on diffractogram comparisons. This work enhances understanding of structure–property relationships in rare earth coordination polymers.

Keywords: Coordination polymers, rare earth elements, dicarboxylic acid, hydrothermal synthesis, structural characterization

Résumé

Cette recherche porte sur la synthèse et la caractérisation de polymères de coordination à base d'éléments des terres rares, en particulier le lanthane(III). Divers ligands d'acides dicarboxyliques rigides (aromatiques) et flexibles (aliphatiques) ont été utilisés dans des systèmes à ligand unique et mixtes. Les composés ont été synthétisés par des méthodes hydrothermales, par reflux et à température ambiante, puis caractérisés par FT-IR, DRX sur poudre (PXRD) et analyse thermogravimétrique (TGA). Les résultats ont révélé une diversité de structures, de modes de coordination et de comportements thermiques, influencés par le type de ligand et les conditions de réaction. Certains composés présentent un caractère potentiellement nouveau selon les diffractogrammes. Ce travail contribue à une meilleure compréhension des relations structure–propriétés dans les polymères de coordination à base de terres rares.

Mots clés : polymères de coordination, terres rares, acides dicarboxyliques, hydrothermal, caractérisation structurale.